DEPARTMENT OF TRANSPORTATION

# Estimation of Metro Freeway System Reliability and Resilience

**Eil Kwon, Principal Investigator**
Department of Civil Engineering
University of Minnesota Duluth

**FEBRUARY 2022**

Research Report
Final Report 2022-01

To request this document in an alternative format, such as braille or large print, call 651-366-4718 or 1-800-657-3774 (Greater Minnesota) or email your request to ADArequest.dot@state.mn.us. Please request at least one week in advance.

## Technical Report Documentation Page

| 1. Report No. | 2. | 3. Recipients Accession No. |
| --- | --- | --- |
| MN 2022-01 | | |

| 4. Title and Subtitle | 5. Report Date |
| --- | --- |
| Estimation of Metro Freeway System Reliability and Resilience | February 2022 |
| | 6. |

| 7. Author(s) | 8. Performing Organization Report No. |
| --- | --- |
| Eil Kwon, Chet Jurrens, Cole Wright, Asif Mahmud | |

| 9. Performing Organization Name and Address | 10. Project/Task/Work Unit No. |
| --- | --- |
| Department of Civil Engineering<br>University of Minnesota Duluth<br>252 SCiv, 1405 University Dr.<br>Duluth, MN 55812 | CTS #2020002<br>11. Contract (C) or Grant (G) No.<br>(c) 1003325 (wo) 102 |

| 12. Sponsoring Organization Name and Address | 13. Type of Report and Period Covered |
| --- | --- |
| Minnesota Department of Transportation<br>Office of Research & Innovation<br>395 John Ireland Boulevard, MS 330<br>St. Paul, Minnesota 55155-1899 | Final Report<br>14. Sponsoring Agency Code |

15. Supplementary Notes

https://www.mndot.gov/research/reports/2022/202201.pdf

https://www.mndot.gov/research/reports/2022/202201A.pdf

16. Abstract (Limit: 250 words)

This study has estimated and analyzed the travel-time reliability and traffic-flow performance trends of the freeway corridors in the Twin Cities metro area of Minnesota. First, TeTRES (Travel-Time Reliability Estimation System), developed in the previous study, was enhanced by adding the estimation module of the traffic-flow performance measures for selected routes. Next, the TeTRES database was populated with the external-operating condition data collected from 2010 to 2020. The enhanced TeTRES was then applied to a total of 48 directional corridors in the metro freeway network and the travel-time reliability for each corridor under different operating conditions was estimated and analyzed along with the traffic-flow performance measures for 2016 – 2020 period. In particular, a newly developed vulnerability index, which combines 95$^{th}$ percentile buffer index and 95$^{th}$ percentile travel rate of each route, was applied to determine yearly-reliability trends under different operating conditions for each corridor. The vulnerability index was also applied to identify the most vulnerable bottleneck section within each directional corridor using the 2019 data under all conditions. Finally, a preliminary study to assess the operational resilience of freeway corridors was conducted in this study by formulating the corridor-wide operational resilience with data from a total of six directional corridor routes in the metro freeway network.

| 17. Document Analysis/Descriptors | 18. Availability Statement |
| --- | --- |
| Travel time reliability, Freeways, Highway corridors, Freeway operations | No restrictions. Document available from: National Technical Information Services, Alexandria, Virginia 22312 |

| 19. Security Class (this report) | 20. Security Class (this page) | 21. No. of Pages | 22. Price |
| --- | --- | --- | --- |
| Unclassified | Unclassified | 108 | |

# ESTIMATION OF METRO FREEWAY SYSTEM RELIABILITY AND RESILIENCE

## FINAL REPORT

*Prepared by:*


Eil Kwon
Chet Jurrens
Cole Wright
Department of Civil Engineering
University of Minnesota Duluth

Asif Mahmud
Department of Computer Science
University of Minnesota Duluth


## FEBRUARY 2022


*Published by:*

Minnesota Department of Transportation
Office of Research & Innovation
395 John Ireland Boulevard, MS 336
St. Paul, Minnesota 55155-1899

## ACKNOWLEDGEMENTS

This research was financially supported by the Minnesota Department of Transportation. The authors greatly appreciate the technical guidance and data support from the staff at the Regional Traffic Management Center, especially, Brian Kary and Doug Lau. Also, the administrative support from Thomas Johnson-Kaiser and David Glyer is very much appreciated.

# TABLE OF CONTENTS

## LIST OF FIGURES

# LIST OF TABLES

# EXECUTIVE SUMMARY

A key element in developing and maintaining a reliable freeway system is the capability to monitor and assess corridor-wide travel-time reliability on an ongoing basis. The previous phase of this research developed a comprehensive computer system, TeTRES (Travel-time Reliability Estimation System), which can be used to efficiently collect and integrate a large volume of data from multiple sources, such as traffic, weather, and incident databases, and estimate a set of reliability measures for given corridors and time periods under specified operating conditions.

This report summarized the results from the current research effort to apply TeTRES for analyzing the travel-time reliability trends at the major corridors in the Twin Cities metro freeway network. First, a new module to calculate the traffic-flow measures of effectiveness (MOEs) has been added to TeTRES, so that an integrated analysis using both travel-time reliability and traffic-flow MOEs can be performed in an efficient way for selected corridors and periods. Next, various sets of historical data for the metro freeway network, including non-traffic external condition data, such as weather, incidents, special events, and work zones, were collected from 2012 until 2020. The collected data were processed and loaded into the TeTRES database. Furthermore, a total of 116 directional routes were identified in cooperation with the Regional Transportation Management Center, MnDOT, and for each route, the travel times were calculated for every five-minute interval from 2012 to 2020 and saved in the travel-time database in TeTRES. The calculated travel times were linked to external operating conditions, e.g., weather and incident conditions, and stored in the TeTRES database. The expanded database of TeTRES was then applied to estimate a set of monthly and yearly travel-time reliability measures for 48 directional routes in 23 corridors in the metro network under different operating conditions from 2016 until 2020. These estimation results were then analyzed and the effects of different operating conditions, sch as weather, incidents, and work zones, on travel-time reliability were identified for each route. In particularly, a newly developed vulnerability index, which combines 95th percentile buffer index and 95th percentile travel rate of each route, was applied to determine yearly reliability trends under different operating conditions for each route. The vulnerability index was also applied to identify the most vulnerable bottleneck section within each directional route using the 2019 data under all conditions.

Finally, a preliminary study to assess the operational resilience of freeway corridors was conducted in this study using the data from a total of six directional corridor routes in the metro freeway network. Using the collected traffic and incident data, the congestion start/recovery process of each route was analyzed and a model to quantify the corridor-wide operational resilience (CORI) of a given corridor was formulated and applied to the sample directional routes for the weekday-peak periods under dry-weather conditions. The resulting CORI estimates of the sample directional routes indicated that the southbound routes show consistently stronger resilience with more stable day-to-day variations than those of the northbound route in a same corridor. Furthermore, the average resilience values of all the sample routes were significantly different from each other at a 95% confidence level. Finally, the potential relationship between the operational resilience and the geometric structure of each sample route was analyzed by quantifying the level of potential geometric-friction in each directional route in terms of handling corridor-wide, through-traffic flows. The quantification of the geometric friction was based on the geometry data easily measurable from the field. The resulting geometric-friction levels showed clear correlation with the operational resilience measures of each sample route. For example, the southbound routes in the sample corridors used in this study showed less geometric-friction levels with stronger operational resilience than the northbound routes in the same corridors. This indicates the promising possibilities of the proposed corridor-wide operational resilience measures for accurately understanding the main sources of reliability issues and improving operational effectiveness of given corridors.

# CHAPTER 1: INTRODUCTION

## 1.1 BACKGROUND AND RESEARCH OBJECTIVES

A reliable and resilient freeway network, which can absorb, recover and adapt to various operating conditions, is of critical importance in sustaining the way of life and economic vitality of the Twin Cities metro area. A key element in developing and maintaining such a reliable freeway system is the capability to monitor and assess corridor-wide travel-time reliability, a major performance measure for quantifying the operational effectiveness of a freeway network.

The previous phase of this research developed a comprehensive computer system, Travel-time Reliability Estimation System (TeTRES), which can efficiently process a large amount of data from multiple sources, such as MnDOT traffic-data archives, Computer Aided Dispatch (CAD)-incident database, and the National Oceanic and Atmospheric Administration (NOAA) weather-data storage, and estimate a set of travel-time reliability measures for given corridors and time periods under user-specified operating conditions. This research expands TeTRES by adding the capability to calculate traffic-flow measures of effectiveness (MOEs) for given routes. Furthermore, the enhanced TeTRES is applied to analyze the reliability trends and/or issues of individual corridors in the metro freeway network. The specific objectives of this study include:

- Expansion of TeTRES with the addition of the traffic-flow module of the Traffic Information and Condition Analysis System (TICAS), for an integrated analysis of travel-time reliability and traffic-flow measures of effectiveness for given routes.
- Population of TeTRES database with various types of historical data for the 2012 - 2020 period from multiple sources relevant to the estimation of travel-time reliability measures for selected corridors under given operating conditions.
- Estimation of travel-time reliability measures for the major corridors in the metro freeway network for the selected periods and identification of bottleneck sections in each corridor using the travel-time reliability measures.
- Preliminary study for assessing operational resilience of sample freeway corridors.

## 1.2 REPORT ORGANIZATION

Chapter 2 describes the internal structure of the enhanced TeTRES with the newly added traffic-flow MOE module. The enhancements of administrative and user clients to facilitate the extraction of MOEs are also explained in this chapter. The collection and processing of the historical data, both traffic and non-traffic data, needed to estimate travel-time reliability measures under various operating conditions are explained in Chapter 3. The populated database of TeTRES is used in Chapter 4 to estimate the monthly and yearly values of the travel-time reliability and traffic-flow measures for the major corridors in the metro freeway network. The identification and prioritization of the bottleneck sections in each corridor are also described in Chapter 4. The preliminary study to model and assess the operational resilience of sample freeway corridors is reported in Chapter 5. Finally, Chapter 6 summarizes the benefits of the current research, implementation steps. and conclusions.

# CHAPTER 2: INTEGRATION OF TETRES AND TRAFFIC-FLOW MOE CALCULATION PROCESS

## 2.1 INTRODUCTION

In this chapter, TeTRES is enhanced with the addition of the traffic-flow Measures of Effectiveness (MOEs) calculation functions of TICAS, *Traffic Information, and Condition Analysis System*, developed at the University of Minnesota Duluth, so that an integrated analysis of travel-time reliability and traffic-flow performance measures can be conducted for given corridors. Specifically, the existing travel-time estimation module of TeTRES is modified to incorporate the additional calculations of various traffic-flow MOEs, which are then stored in the TeTRES database, which is also expanded in this study. In the enhanced TeTRES, the calculation of traffic-flow MOEs is performed on a need basis, i.e., users can choose the MOE calculation option for selected routes and time periods. To facilitate the MOE calculation and extraction process, the admin client is revised to allow the administrator to calculate the MOE values for predefined routes for a specific time range with the option of modifying parameter values needed for MOE calculation. The user client is also enhanced with the functions necessary for the traffic-flow MOE calculation/extraction processes. In particular, the MOE-output module, developed and inserted into the User client in this study, extracts the MOE values for selected corridors from the database for user-specified operating conditions and generates a set of the output files in a spreadsheet format. The rest of this chapter summarizes the architecture of the enhanced TeTRES, the processes to calculate, store and extract the traffic-flow MOE values for given routes.

## 2.2 INCORPORATION OF TRAFFIC-FLOW MOE CALCULATION PROCESS INTO TETRES

### 2.2.1 OVERVIEW OF THE ENHANCED TETRES ARCHITECTURE

Figure 2.1 shows the architecture of the enhanced TeTRES, whose highlighted modules incorporated the new processes and functions, developed in this chapter, to calculate, store, and extract the MOE values for pre-defined routes. Specifically, the following modules have been updated with the new MOE-related processes and functions:

- *Travel-Time Database, which is expanded to store a set of MOEs calculated for each route.*
- *Travel-Time and Reliability Calculation Module, where the traffic-flow MOE calculation functions are called and MOEs for each route are calculated.*
- *Admin-Client, where the admin users calculate the MOE values for the predefined routes for a specific time range with the option of modifying different parameters of MOE calculation.*
- *User-Client, where the new MOE output module extracts the MOE values for user-specified operating conditions and generates a set of the output files in a spreadsheet format.*

### 2.2.2 TYPES OF TRAFFIC-FLOW MEASURS OF EFFECTIVENESS

This section summarizes the types of the traffic-flow MOEs incorporated into TeTRES in this study. Figure 2.2 shows the space-discretization scheme adopted in TeTRES, where a freeway corridor is divided into 0.1-mile segments and a set of MOEs are estimated for each segment with the macroscopic flow parameters, i.e., flow rate (q), density (k) and speed (u), for every time interval. In particular, the values of q, k, and u for each 0.1-mile segment are determined by interpolating the measurements from the field detectors installed at fixed locations on freeway corridors. Currently, q, k, and u values for each 0.1-mile segment are estimated for every 5-minute interval for the entire freeway network in Twin Cities, Minnesota. Those q, k, and u values for each segment are used to determine the various types of traffic-flow MOEs for a given route and period. The specific types of traffic-flow MOEs, coded into the MOE module, and their definitions used in this study are as follows:

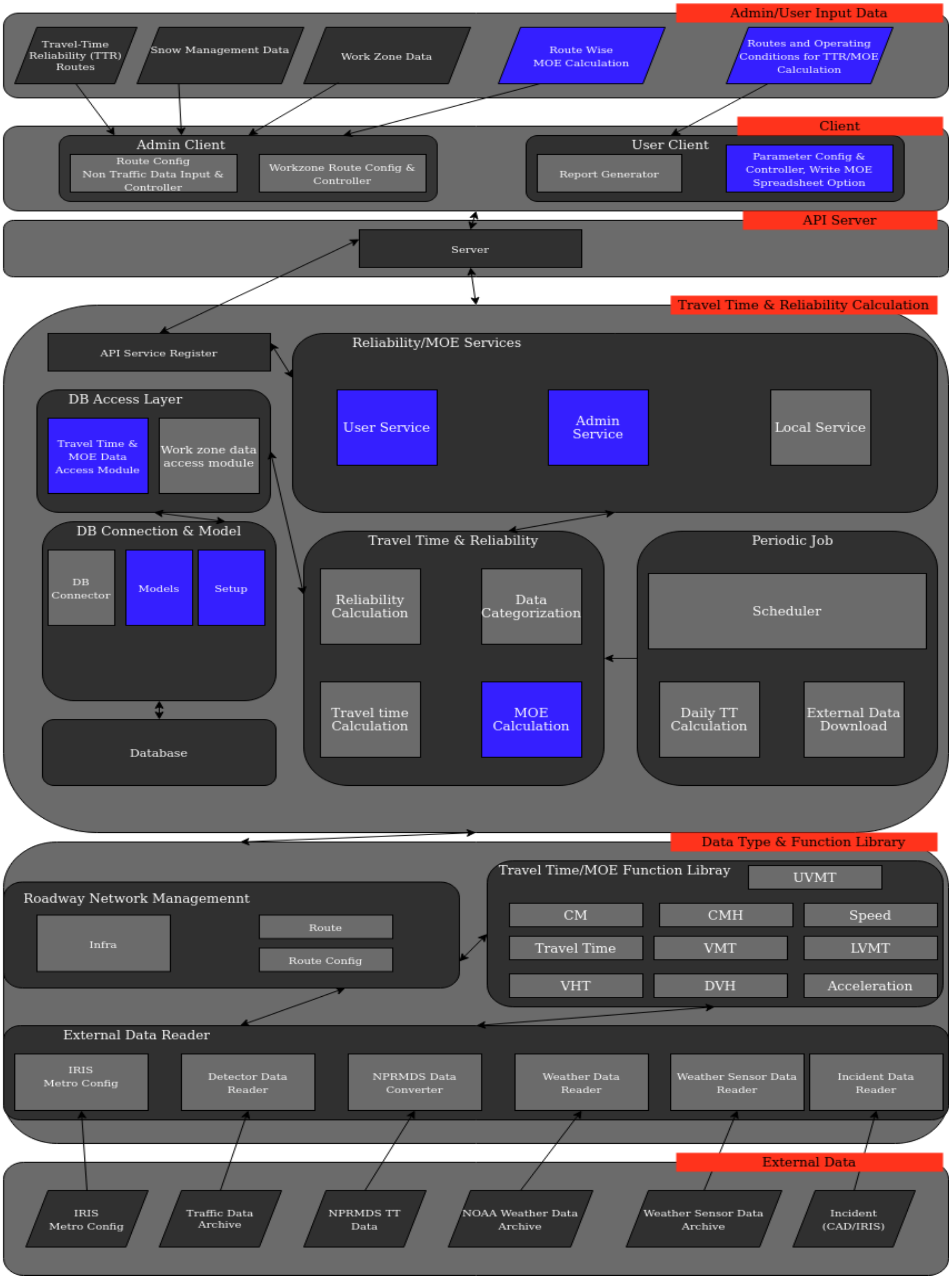


**Figure 2.1: Architecture of Enhanced TeTRES with Traffic-Flow MOE Calculation**

### 2.2.3 Vehicle-Miles Traveled (VMT)

VMT measures the amount of travel for all vehicles in a given roadway during a given time period. In TeTRES, the VMT for a given route is calculated every time interval, t, e.g., 5 minutes in the current version, by adding up all '0.1-mile segment VMTs' in a given route as follows:

***VMT for segment i during t***

***= [density (k)]$_{i,t}$ * segment length (= 0.1 mile) * [speed (u)]$_{i,t}$ * time-interval (=5/60 hr)***

***VMT for a Route during t = Sum of VMTs for all the segments in a route during t***

### 2.2.4 Vehicle-Hours Traveled (VHT)

VHT measures the total amount of time spent by all vehicles in a given roadway over a given period of time. It's a measure of the quality of traffic performance of a given route and estimated for each time interval as follows:

***VHT for segment i during t =[density (k)]$_{i,t}$ * segment length (=0.1) * time-interval (=5/60 hr)***

***VHT for a route during t = Sum of VHTs for all segments in a route during t***

### 2.2.5 Delayed-Vehicle Hours (DVH)

DVH measures the total delay experienced by all the vehicles in a given route over a given period of time and estimated as follows:

***DVH for Segment i during t = [(Estimated Actual-Travel Time)$_{i,t}$ – (Free-flow travel Time)$_{i}$] ****

***[flow rate (q)]$_{I,t}$ * time interval (=5/60 hr)***

***DVH for a route per time interval = Sum of DVHs for All Segments in a Route per time interval***

### 2.2.6 Lost VMT for congestion (LVMT)

LVMT is a measure of the lost capacity, because of congestion, of a given route over a given time period. It measures the inefficiencies of a given roadway traffic system and estimated by converting the lost capacity into VMT for each segment every time interval as follows:

***If (density of segment i per time interval) > critical density,***

***Then***

***LVMT$_{i}$ = (capacity * number of lanes – Total flow rate)I,t * time interval * segment length (=0.1 mile)***

***Else, $LVMT_i$= 0***

***LVMT for a route per time interval = Sum of LVMTs for all segments in a route during t***

### 2.2.7 Unused VMT (UVMT)

UVMT measures the level of unused capacity of a given route for a given time period. UVMT can happen because of the lack of traffic demand or upstream bottlenecks and estimated for each segment by converting the unused capacity into VMT as follows:

***If Density of segment i during t <= Critical Density,***

***Then UVMT for Segment i during t = [capacity * (number of lanes)i – (Total flow rate)i,t] * time interval***

***(=5/60hr) * segment length (=0.1 mile),***

***Else, UVMT i = 0***

***UVMT for a Route during t = Sum of UVMT for All Segments in a Route during t***

### 2.2.8 Congested Miles (CM)

CM measures the amount of congested roadways of a given roadway for a given time period. A segment i is defined as congested when its speed during t is less than a pre-specified congestion-speed vale and the CM for a given route during t is calculated as the sum of all the congested segments during t as follows:

***If speed of segment i during t < congestion _threshold speed,***

***then $CM_i$ = Segment length (=0.1mile), Else $CM_i$ = 0***

***CM for a given route during t = ∑ $CM_i$ for all segments in a given route during t***

### 2.2.9 Congested-Mile Hours (CMH)

CMH measures the extent of congestion for a given roadway during a given time period by adding congested-time duration to CM. The specific formula for CMH for a given route is as follows:

***If speed of segment i during t < congestion_ threshold speed,***

***then $CMH_i$ = Segment length (=0.1mile) * time interval (=5/60 hr), Else CMHi = 0***

***CMH for a given route during t = ∑ $CM_i$ for all segments in a given route during t***

### 2.2.10 Speed Variations (SV)

SV measures the variance of the speed of a given route for a given time period. It's estimated with the speed values of all segments during t for a given route during t, i.e.,

***SV for a route during t = Var[Speed values of all segments for a given route during t]***

In the enhanced TeTRES, average speed, maximum speed, minimum speed, speed difference (maximum speed - minimum speed) and acceleration are also calculated along with speed variance.

### 2.2.11 Number of Vehicles Entered and Exited

*TVE (j): Total number of Vehicles Entered a given corridor during time (j)*

***= Sum [Upstream Boundary Flow Rate(j), $q_r(i,j)$]*** *for all ramp (i), where $q_r(i,j)$ = flow rate of ramp i during j*

*TVE: Total number of Vehicles Entered during a given period*

***= Sum [TVE(j)] for all (j)***

*TVX (j): Total # of Vehicles exited during (j)*

***= Sum [$q_x(i,j)$, Downstream Boundary Flow (j)]*** *for all exit ramp i, where $q_r(i,j)$ = flow rate of ramp I during j*

*TVX**:** Total number of vehicles Exited from during a given period*

***= Sum [TVX(j)] for all (j)***

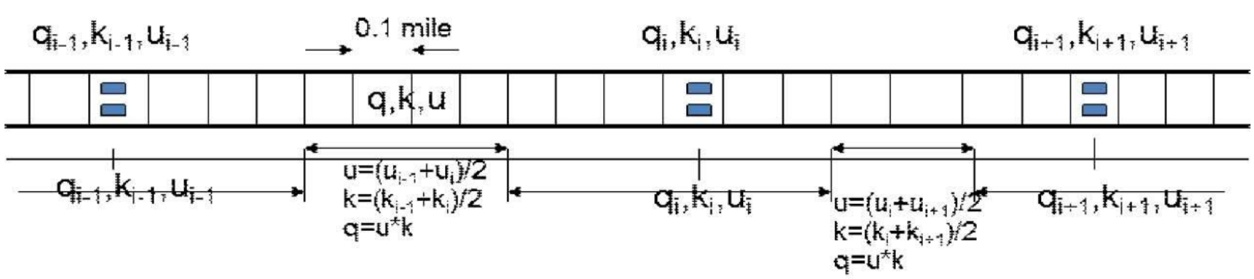


**Figure 2.2: Current space-discretization and flow-parameter estimation scheme in TeTRES**

Field Detector

### 2.2.12 Parameters for Traffic-Flow MOE calculation

The following three parameters need to be predefined to calculate the MOEs defined above:

***Congestion Threshold Speed***

For calculating Congested Miles (CM) and Congested-Mile Hours (CMH) the value of this parameter needs to be defined. The default value used by TeTRES for this parameter is 45 mph.

***Lane Capacity***

For calculating Lost VMT for congestion (LVMT) and Unused VMT (UVMT) the value of this parameter needs to be defined. The default value used by TeTRES for this parameter is 2200 veh/hr/lane.

***Critical Density***

For calculating Lost VMT for congestion (LVMT) and Unused VMT (UVMT) the value of this parameter needs to be defined. The default value used by TeTRES for this parameter is 40 veh/mile/lane.

## 2.3 EXPANSION OF TETRES DATABASE TO STORE TRAFFIC-FLOW MOE VALUES

The first step to incorporate MOE values into TeTRES is to expand the existing database to store those values. The TeTRES database has a specific structure for storing travel-time data for each route for every five minutes. For each year, a separate travel-time table is generated automatically by the system with the following name format: “tt_<year>”. For instance, for 2020, the name of the travel-time table is “tt_2020” in the TeTRES database. Figure 2.3 shows the structure of the expanded, yearly travel-time table to store the MOE values.

```python
class TravelTime(object):

    id = Column(Integer, primary_key=True, unique=True, autoincrement=True)
    route_id = Column(Integer, ForeignKey('route.id'), nullable=False)
    route = relationship("TTRoute")
    time = Column(DateTime, nullable=False)
    tt = Column(Float, nullable=False)
    vmt = Column(Float, nullable=True)
    vht = Column(Float, nullable=True)
    dvh = Column(Float, nullable=True)
    lvmt = Column(Float, nullable=True)
    uvmt = Column(Float, nullable=True)
    cm = Column(Float, nullable=True)
    cmh = Column(Float, nullable=True)
    acceleration = Column(Float, nullable=True)
    meta_data = Column(UnicodeText, nullable=True)
```

**Figure 2.3: Expanded Yearly Travel-Time Table**

The description of each column of the above table is provided below:

- ***id:*** This is the primary key of the table which is a unique auto-incrementing integer.
- ***route_id:*** This column stores the reference route id.
- ***time:*** This column keeps track of the exact date time.
- ***tt:*** The travel time in minutes is stored in this column.
- ***vmt:*** The MOE, Vehicle-Miles Traveled (VMT), is stored in this column.
- ***vht:*** The MOE, Vehicle-Hours Traveled (VHT), is stored in this column.
- ***dvh:*** The MOE, Delayed-Vehicle Hours (DVH), is stored in this column.
- ***lvmt:*** The MOE, Lost VMT due to congestion (LVMT), is stored in this column.
- ***uvmt:*** The MOE, Unused VMT (UVMT), is stored in this column.
- ***cm:*** The MOE, Congested-Miles (CM), is stored in this column.
- ***cmh:*** The MOE, Congested-Mile Hours (CMH), is stored in this column.
- ***acceleration:*** The MOE, acceleration, is stored in this column.
- ***meta_data:*** This column stores a JSON string having a key-value pair structure that stores the following meta-information for the specific route and time:

- Flow
- Speed
- Density
- Lanes
- Speed Limit
- Speed Average
- Speed Variance
- Speed Max
- Speed Min
- Speed Difference
- Number of Vehicles Entered
- Number of Vehicles Exited
- MOE Lane Capacity
- MOE Critical Density
- MOE Congestion Threshold Speed

To facilitate the need-based MOE calculation process by users, a table named "RouteWiseMOEParameters" was created to track the status of MOE calculations for different routes and for different time ranges. This table allows users to choose the MOE calculation option for the selected routes and time ranges. Figure 2.4 shows the structure of this table.

```python
class RouteWiseMOEParameters(Base):
    __tablename__ = 'route_wise_moe_parameters'
    id = Column(Integer, primary_key=True, unique=True, autoincrement=True)
    reference_tt_route_id = Column(Integer, ForeignKey('route.id', ondelete='CASCADE'), nullable=False, index=True)
    reference_tt_route = relationship(TTRoute)
    moe_lane_capacity = Column(Float, nullable=False)
    moe_critical_density = Column(Float, nullable=False)
    moe_congestion_threshold_speed = Column(Float, nullable=False)
    start_time = Column(DateTime, nullable=True)
    end_time = Column(DateTime, nullable=True)
    update_time = Column(DateTime, nullable=False)
    status = Column(VARCHAR(255), nullable=True)
    reason = Column(VARCHAR(255), nullable=True)
```

**Figure 2.4: Route-Wise MOE-Parameters Table**

The definition of each column in the above table is described below:

- ***id:*** This is the primary key of the table which is a unique auto-incrementing integer.
- ***reference_tt_route_id:*** This column stores the reference route id.
- ***moe_lane_capacity:*** Lane capacity value used for the current MOE calculation
- ***moe_critical_density:*** Critical density value used for the current MOE calculation
- ***moe_congestion_threshold_speed:*** Congestion Threshold Speed value used for the current MOE calculation
- ***start_time:*** MOE calculation is performed for a specific route for a specific time range. This column keeps track of the exact starting date-time of the time range.
- ***end_time:*** MOE calculation is performed for a specific route for a specific time range. This column keeps track of the exact ending date-time of the time range.
- ***update_time:*** This column keeps track of the time when the MOE calculation is triggered for the specific route for the specific time range.
- ***status:*** This column keeps track of the current status of the calculation.
- ***reason:*** This column stores the reason for the failure in case the current MOE calculation is failed for some reason.

Further, the above table also keeps track of the values of the key parameters for the MOE calculation, e.g., lane capacity and critical density, so that it can be clear which parameter values were used for which route-MOE calculations, while the specific values of those parameters can be set in the admin client.

## 2.4 ENHANCEMENT OF ADMIN CLIENT TO INCORPORATE MOE CALCULATION PROCESS

In this study, the admin client of TeTRES is enhanced to handle the traffic-flow MOE calculation process, including the specification of the key parameter values, such as lane capacity and critical density, for computing the MOEs, for selected routes and time periods. Specifically, two sub-tabs were developed and inserted into the main window of the admin client. They include:

- 'Default Parameter' sub-tab, which enables user to enter/change the default values of the MOE parameters,
- 'Route Wise MOE Parameters', where users can enter specific values of the MOE parameter values for selected routes and time periods.

Figure 2.5 shows a new sub-tab, "Default Parameters", which can be accessed through System Configuration → Categorization Parameter Settings → MOE Parameters tab in the main window of the admin client. As shown in this figure, the default values of the key MOE parameters can be updated in this sub-tab, while changing the default values of these parameters do not have any impact on the existing MOE values calculated with previous default-parameter values.

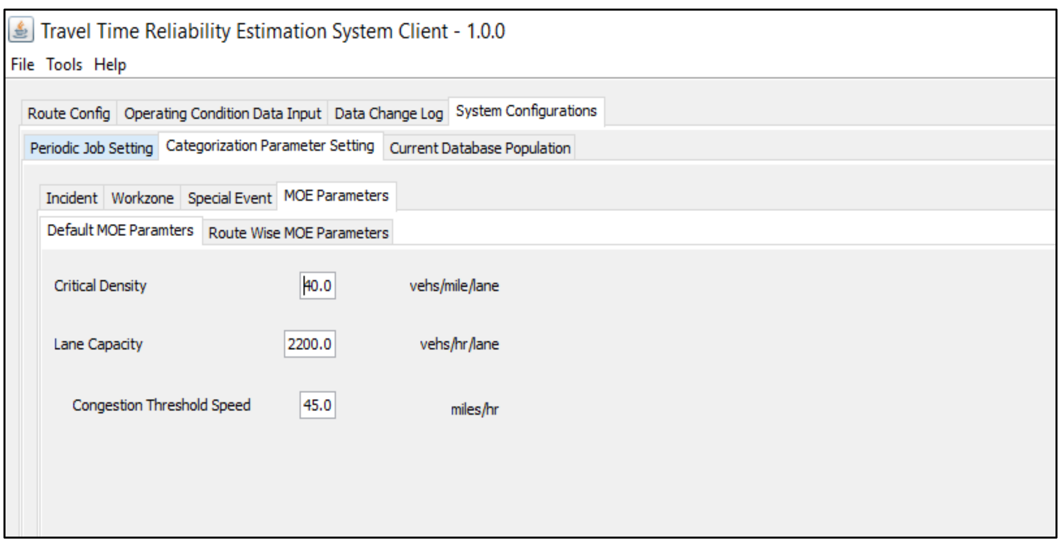


**Figure 2.5: Default Parameters Tab**

Figure 2.6 shows the screenshot of the 'Route Wise MOE Parameters' sub-tab, where an admin-client user can start calculating the MOE values for a specific route for a specified time interval.

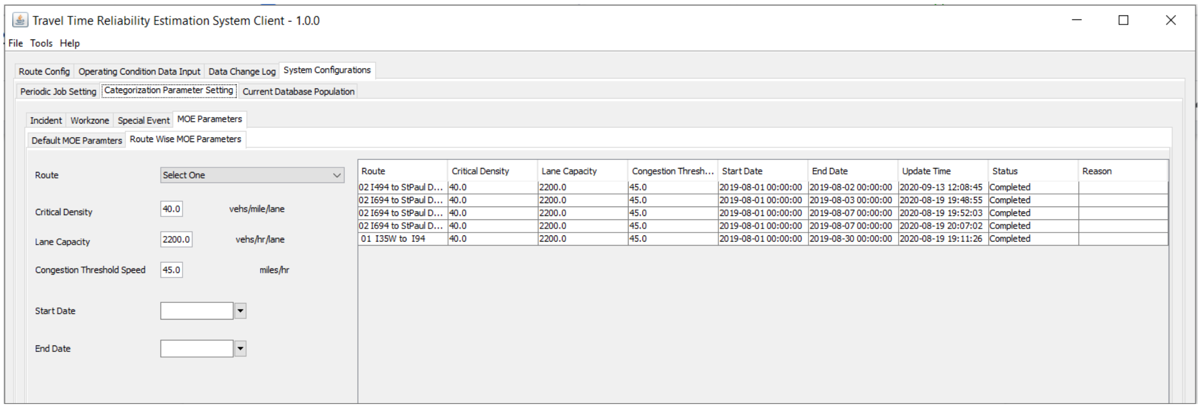

**Figure 2.6: Route Wise MOE Parameters Tab**

As shown above, there are six fields that need to be filled in this tab, while the 3 MOE parameters, i.e., critical density, lane capacity and congestion threshold speed, automatically show the default values specified in the 'Default Parameters' tab:

- *Route*
- *Critical Density*
- *Lane Capacity*
- *Congestion Threshold Speed*
- *Start Date*
- *End Date*

First, the user needs to choose a route from a set of existing defined routes. The user also can change the values of those 3 MOE parameters in this tab if necessary. The newly updated parameter values will only be effective for those selected route and time periods. Then the user needs to select the start and end date. Based on these values, the server will start calculating MOE values for a selected route and the status of the MOE calculation process can also be shown in the 'status' column of the same tab. Figures 2.7 and 2.8 show some of the codes developed for enhancing the admin client and tracking route-wise MOE parameters. Figure 2.7 shows the first function that's invoked by the admin client to calculate the MOE values for a specific route and period, while the major functions in the server to process the 'Route-wise MOE calculation' are listed in Figure 2.8.

```python
def register_api(app):
    @app.route(api_urls_admin.SYSCFG_GET, methods=['GET', 'POST'])
    @requires_auth
    def tetres_syscfg_get():
        syscfg = systemconfig.get_system_config_info()
        return prot.response_success(obj=syscfg)

    @app.route(api_urls_admin.SYSCFG_UPDATE, methods=['POST'])
    @requires_auth
    def tetres_syscfg_update():
        cfginfo_json = request.form.get('cfg', None)
        if not cfginfo_json:
            return prot.response_invalid_request()

        cfginfo = json.loads(cfginfo_json, SystemConfigInfo)

        if not cfginfo or not isinstance(cfginfo, SystemConfigInfo):
            return prot.response_invalid_request()

        for k, v in cfginfo.__dict__.items():
            if k.startswith('_'):
                continue
            if v is None:
                return prot.response_invalid_request()

        prev_syscfg = systemconfig.set_system_config_info(cfginfo)
        if not prev_syscfg:
            return prot.response_fail('fail to update configuration')

        put_task_to_actionlog(prev_syscfg)
        t1 = threading.Thread(target=handle_route_wise_moe_parameters, args=(cfginfo_json,))
        t1.start()
        return prot.response_success()
```

**Figure 2.7: First Function Called in TeTRES Server for MOE Calculation**

```python
def handle_route_wise_moe_parameters(config_json_string):
    import json
    config_json = json.loads(config_json_string)
    route_id = config_json.get("reference_tt_route_id")
    if route_id:
        rw_moe_critical_density = config_json.get("rw_moe_critical_density")
        rw_moe_lane_capacity = config_json.get("rw_moe_lane_capacity")
        rw_moe_congestion_threshold_speed = config_json.get("rw_moe_congestion_threshold_speed")
        rw_moe_start_date = config_json.get("rw_moe_start_date")
        rw_moe_end_date = config_json.get("rw_moe_end_date")
        rw_moe_param_info = create_rw_moe_param_object(route_id, rw_moe_critical_density, rw_moe_lane_capacity,
                                                        rw_moe_congestion_threshold_speed, rw_moe_start_date,
                                                        rw_moe_end_date)

        rw_moe_object_id = save_rw_param_object(rw_moe_param_info)
        if has_traffic_files(rw_moe_start_date, rw_moe_end_date):
            try:
                update_moe_values(config_json)
                update_rw_moe_status(rw_moe_object_id, status="Completed")
            except Exception as e:
                print(e)
                update_rw_moe_status(rw_moe_object_id, status="Failed", reason=str(e))
        else:
            update_rw_moe_status(rw_moe_object_id, status="Failed", reason="Missing traffic files for the given time range.")


def create_rw_moe_param_object(route_id, rw_moe_critical_density, rw_moe_lane_capacity,
                               rw_moe_congestion_threshold_speed, rw_moe_start_date, rw_moe_end_date, status='Running'):
    rw_moe_param_info = RouteWiseMOEParametersInfo()
    rw_moe_param_info.reference_tt_route_id = route_id
    rw_moe_param_info.moe_critical_density = rw_moe_critical_density
    rw_moe_param_info.moe_lane_capacity = rw_moe_lane_capacity
    rw_moe_param_info.moe_congestion_threshold_speed = rw_moe_congestion_threshold_speed
    rw_moe_param_info.start_time = rw_moe_start_date if rw_moe_start_date else None
    rw_moe_param_info.end_time = rw_moe_end_date if rw_moe_end_date else None
    rw_moe_param_info.status = status
    return rw_moe_param_info


def save_rw_param_object(rw_moe_param_info):
    rw_moe_param_info.update_time = datetime.datetime.now().strftime("%Y-%m-%d %H:%M:%S")
    rw_da = RouteWiseMOEParametersDataAccess()
    rw_moe_object = rw_da.insert(rw_moe_param_info)
    rw_da.commit()
    _id = rw_moe_object.id
    rw_da.close_session()
    return _id

def update_rw_moe_status(rw_moe_object_id, status="Completed", reason=None):
    rw_da = RouteWiseMOEParametersDataAccess()
    rw_da.update(rw_moe_object_id, {
        "status": status,
        "reason": reason,
        "update_time": datetime.datetime.now().strftime("%Y-%m-%d %H:%M:%S"),
    })
    rw_da.commit()
    rw_da.close_session()
```

**Figure 2.8: Major Server Functions for Processing Route-specific MOE Calculation**

## 2.5 ENHANCEMENT OF THE TRAVEL-TIME AND RELIABILITY CALCULATION MODULE

To calculate and store the traffic-flow MOE values for selected routes, in this study, a set of new functions have been developed and inserted into the TeTRES server. After the admin client initiates the MOE calculation for specific routes and periods, the server starts calculating the MOE values and stores them in the expanded TeTRES database in the background. Figure 2.9 shows the functions initiating the MOE calculation module. The main function that handles all the MOE calculations is named "calculate_tt_moe_a_route", whose code snippet is listed in the Appendix. The code snippets of the individual functions used to calculate specific MOE values are also included in the Appendix B.

```python
def update_moe_values(rw_moe_param_json, db_info=None, *args, **kwargs):
    rw_moe_param_json['rw_moe_start_date'] = datetime.datetime.strptime(rw_moe_param_json['rw_moe_start_date'],
                                                                        '%Y-%m-%d %H:%M:%S').date()
    rw_moe_param_json['rw_moe_end_date'] = datetime.datetime.strptime(rw_moe_param_json['rw_moe_end_date'],
                                                                      '%Y-%m-%d %H:%M:%S').date()

    _update_moe_values(rw_moe_param_json, db_info=db_info, *args, **kwargs)


def _update_moe_values(rw_moe_param_json,
                       db_info=None, *args, **kwargs):
    logger = getLogger(__name__)
    logger.debug('>> Updating MOE Values')
    _worker_process_to_update_moe_values(rw_moe_param_json['rw_moe_start_date'], rw_moe_param_json['rw_moe_end_date'],
                                         db_info, rw_moe_param_json=rw_moe_param_json)
    logger.debug('<< End of Updating MOE Values')


def _worker_process_to_update_moe_values(start_date, end_date, db_info, **kwargs):
    from pyticas_tetres.db.tetres import conn
    from pyticas.tool import tb
    logger = getLogger(__name__)
    stime = datetime.time(0, 0, 0, 0)
    etime = datetime.time(23, 55, 0, 0)
    daily_periods = period.create_periods(start_date, end_date, stime, etime, cfg.TT_DATA_INTERVAL, target_days=[0, 1, 2, 3, 4, 5, 6], remove_holiday=False)
    logger.debug('>>> Starting Multi Processing (duration= %s to %s)' % (start_date, end_date))
    rw_moe_param_json = kwargs.get("rw_moe_param_json")
    reference_tt_route_id = rw_moe_param_json.get('reference_tt_route_id')
    if db_info:
        conn.connect(db_info)
    da_route = TTRouteDataAccess()
    ttri = da_route.get_by_id(reference_tt_route_id)
    if not ttri:
        logger.debug('route is not found (%s)' % (reference_tt_route_id))
        return
    for pidx, prd in enumerate(daily_periods):
        if prd is None:
            da_route.close_session()
            exit(1)
        try:
            da_route.close_session()
            traveltime.calculate_tt_moe_a_route(prd, ttri, dbsession=da_route.get_session(),
                                                create_or_update=True,
                                                rw_moe_param_json=rw_moe_param_json)
            gc.collect()
        except Exception as ex:
            tb.traceback(ex)
            continue
```

**Figure 2.9: Functions for Facilitating MOE calculation**

## 2.6 ENHANCEMENT OF USER CLIENT TO EXTRACT MOE VALUES

Figure 2.10 shows the data-flow process between the TeTRES server and the user-client, which has been modified in this task to allow the user to specify if the calculated and stored MOE values for selected routes would be extracted from the database and written to a separate spreadsheet file. This action is invoked in the main window of the user client by clicking the Estimate button with the '*Include MOE Spreadsheet'* checkbox selected, as shown in Figure 2.11. By clicking the checkbox, the user client sends a signal to the server, which creates and populates the spreadsheet file, “traveltime-moe-data.xlsx”, where all the MOE values calculated for selected routes are contained.

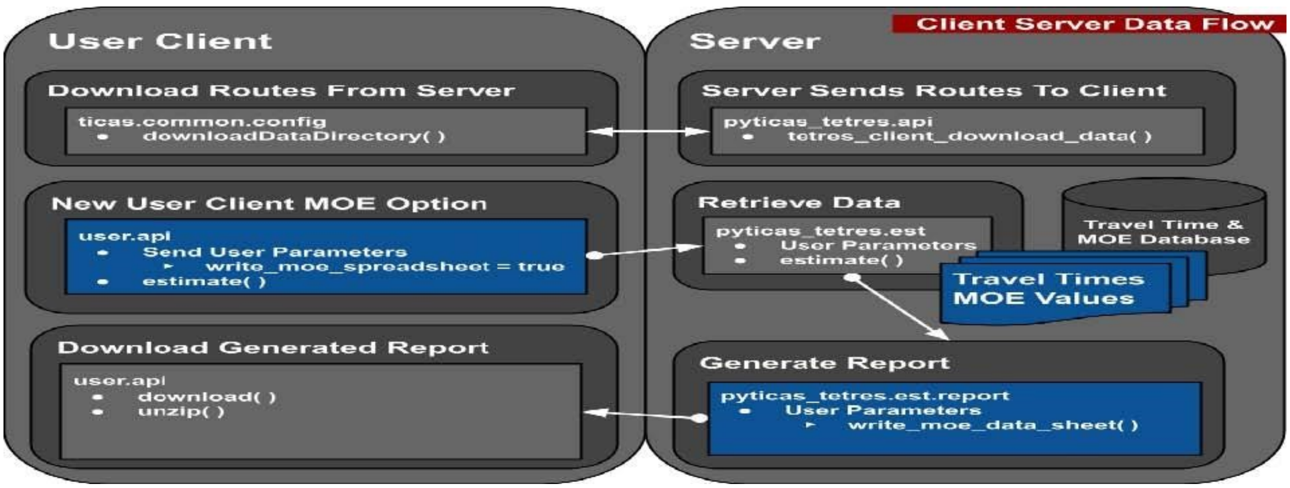


Figure 2.10: Data-Flow Process Between User-Client and Server for MOE Extraction and Writing

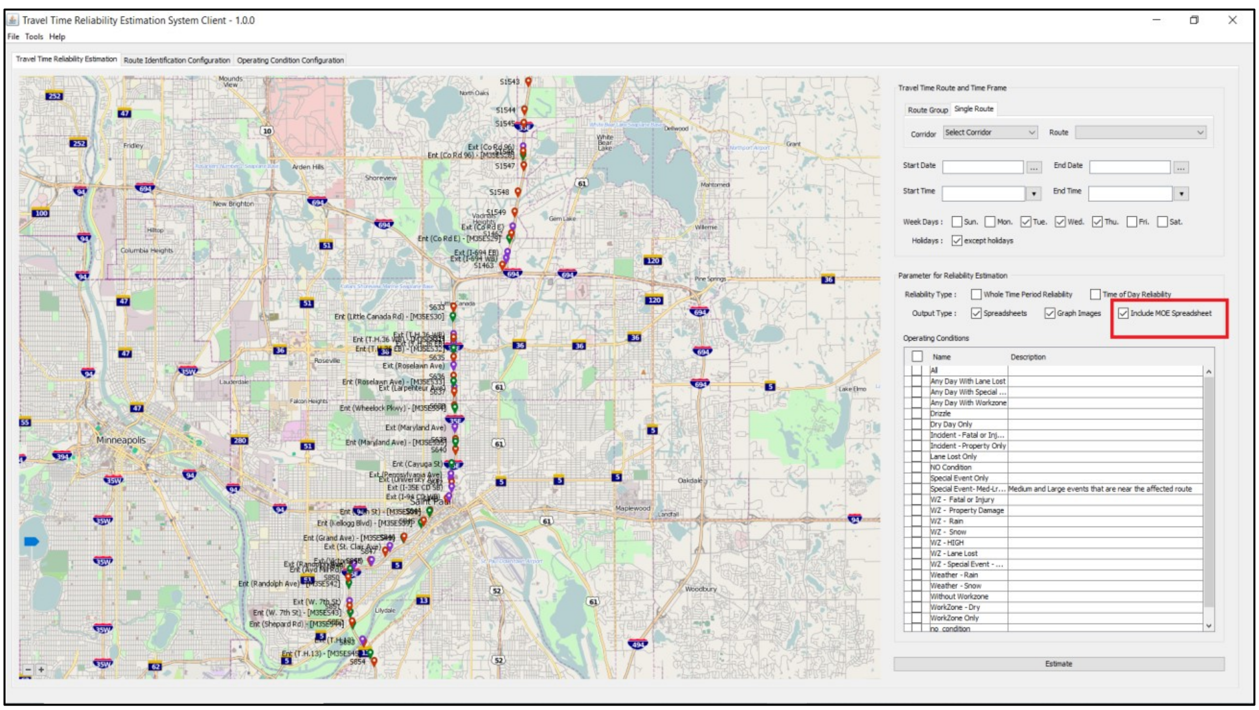


Figure 2.11: Screenshot of User-Client with Added Checkbox for Extracting MOE values

Currently, the following traffic-flow MOE measures are stored every 5 min-interval in the Excel spreadsheet file for each selected route and period:

- *Travel Time*
- *Speed*
- *VMT*
- *VHT*
- *DVH*
- *UVMT*
- *CM*
- *CMH*
- *Acceleration*
- *Number of Vehicles Entered*
- *Number of Vehicles Exited*
- *Speed Average*
- *Speed Variance*
- *Max Speed*
- *Min Speed*
- *Speed Difference*

Figures 2.12 - 2.14 include some of the codes developed for extracting MOE values and writing them to a spreadsheet file.

**Package / File: user.panels.estimation.PanelEstimation.java**
**Class:** PanelEstimation
- `private JCheckBox chkWriteMoeSpreadsheet;`

**Class:** PanelEstimation
**Method:** initComponents *{building Checkbox}*
- `chkWriteMoeSpreadsheet = new JCheckBox();`
- `chkWriteMoeSpreadsheet.setSelected(false);`
- `chkWriteMoeSpreadsheet.setText("Include MOE Spreadsheet");`
- `.addComponent(chkWriteMoeSpreadsheet)`

**Class:** PanelEstimation
**Method:** getRequestOption
- `eri.write_moe_spreadsheet = this.chkWriteMoeSpreadsheet.isSelected();`

**Class:** PanelEstimation
**Method:** loadRequestedInfo
- `this.chkWriteMoeSpreadsheet.setSelected(prevEri.write_moe_spreadsheet);`

**Figure 2.12: Code Snippets of PanelEstimation Class Managing MOE Extraction Request**

**Package / File: user.types.EstimationRequestInfo.java**
**Class:** EstimationRequestInfo
- `public Boolean write_moe_spreadsheet = false;`

**Package / File: pyticas_tetres.est.report.__init__.py**
**Function:** "write"
- `if eparam.write_moe_spreadsheet:`
- `    proc_start_time = time.time()`
- `    logger.debug('>> Writing MOE spread sheet')`
- `    tt_moe_data_writer.write(uid, eparam, operating_conditions)`
- `    logger.debug('<< End of writing MOE spread sheet (elapsed time=%s)' %`
- `        (timeutil.human_time(seconds=(time.time() - proc_start_time))))`

**Figure 2.13: Snippets of Codes for Requesting and Receiving MOE values from Server**

```
def write_moe_data_sheet(eparam, ext_filter_groups, wb):
    #   Created function to write moe data to spreadsheet
    """
    :type eparam: pyticas_tetres.ttypes.EstimationRequestInfo
    :type ext_filter_groups: list[pyticas_tetres.rengine.filter.ftypes.ExtFilterGroup]
    :type wb:xlsxwriter.Workbook
    """

    def clean(v):
        return v if v != math.inf and v and v > 0 else ''

    def cleanMOE(v):
        return v if v != math.inf and v and v >= 0 else ''

    for idx, ef in enumerate(ext_filter_groups):
        ws = wb.add_worksheet('MOE Data (OC=%d)' % idx)
        ws.write_row(0, 0, ['Operating Condition:', eparam.operating_conditions[idx].name])
        ws.write_row(1, 0, [
            '', '', '', '',
            'moe-values', '', '', '',
            '', '', '', '', '',
            'Speed Variation', '', '', '', '',
            'MOE Parameters', '', '',
            'weather', '', '', '', '',
            'incident', '', '', '', '', '', '',
            'workzone', '', '', '', '',
            'special-event', '', '', '',
            'snow-management'

        ])

        ws.write_row(2, 0, [
            'time', 'tt', 'speed', 'vmt',
            'vht', 'dvh', 'lvmt', 'uvmt',
            'cm', 'cmh', 'acceleration', 'number_of_vehicles_entered', 'number_of_vehicles_exited',
            'speed_average', 'speed_variance', 'speed_max_u', 'speed_min_u', 'speed_difference',
            'moe_lane_capacity', 'moe_critical_density', 'moe_congestion_threshold_speed',
            'usaf', 'wban', 'precip_type', 'precip', 'precip_intensity',  # weather
            'type', 'impact', 'cdts', 'udts', 'xdts', 'distance', 'off_distance',  # incident
            'name', 'lane_config', 'closed_length', 'location', 'off_distance',  # workzone
            'name', 'distance', 'attendance', 'type',  # special event
            'truck_route', 'road_status', 'location', 'off_distance'

        ])

        for idx, extdata in enumerate(ef.whole_data):
            x = extdata.tti
            dts = x.time.strftime('%Y-%m-%d %H:%M')
            try:
                meta_data = json.loads(x.meta_data)
            except Exception as e:
                print(e)
                meta_data = {}
            moe_lane_capacity = cleanMOE(meta_data.get("moe_lane_capacity", 0))
            moe_critical_density = cleanMOE(meta_data.get("moe_critical_density", 0))
            moe_congestion_threshold_speed = cleanMOE(meta_data.get("moe_congestion_threshold_speed", 0))
            speed_average = cleanMOE(meta_data.get("speed_average", 0))
            speed_variance = cleanMOE(meta_data.get("speed_variance", 0))
            speed_max_u = cleanMOE(meta_data.get("speed_max_u", 0))
            speed_min_u = cleanMOE(meta_data.get("speed_min_u", 0))
            speed_difference = cleanMOE(meta_data.get("speed_difference", 0))
            number_of_vehicles_entered = cleanMOE(meta_data.get("number_of_vehicles_entered", 0))
            number_of_vehicles_exited = cleanMOE(meta_data.get("number_of_vehicles_exited", 0))
            ws.write_row(idx + 3, 0, [
                dts, clean(x.tt), clean(x.speed), clean(x.vmt),
                cleanMOE(x.vht), cleanMOE(x.dvh), cleanMOE(x.lvmt), cleanMOE(x.uvmt),
                cleanMOE(x.cm), cleanMOE(x.cmh), cleanMOE(x.acceleration), number_of_vehicles_entered,
                number_of_vehicles_exited,
                speed_average, speed_variance, speed_max_u, speed_min_u, speed_difference,
                moe_lane_capacity, moe_critical_density, moe_congestion_threshold_speed,
            ]
                         + get_weather_values(extdata)
                         + get_incident_values(extdata)
                         + get_workzone_values(extdata)
                         + get_specialevent_values(extdata)
                         + get_snowmangement_values(extdata)
                         )
```

Figure 2.14: Code Snippets for Writing MOE values in a Spreadsheet file

# CHAPTER 3: POPULATION OF TETRES DATABASE FOR METRO FREEWAY NETWORK

## 3.1 INTRODUCTION

In this chapter, the database of TeTRES is populated with the historical data, also collected in this study for estimating the travel-time reliability measures for the metro freeway network. The specific types and sources of the data collected and processed in this chapter are as follows:

1) *Freeway traffic-detector data from RTMC, MnDOT*
2) *Weather data from NOAA (National Oceanic and Atmospheric Administration)*
3) *Incident data from CAD (Computer-Aided-Dispatch system, Department of Public Safety) and IRIS (Intelligent Roadway Information System, MnDOT)*
4) *Special-event data from the venues located in the metro area*
5) *Metro freeway Work-Zone data from Metro District, MnDOT*
6) *Winter road-surface data from Metro District, MnDOT*

In the above list, the traffic-detector data are stored in a local hard disk in a structured format, while all other types of data are processed and stored in the TeTRES database (T-database), whose schema and table formats were explained in the previous phase of this research [1]. Further, the weather data from NOAA has been automatically downloaded and stored in the database by the weather-data processing module in TeTRES. For the incident data, the CAD/IRIS incident databases of the past periods were provided off-line by RTMC, MnDOT, and the incident-data loading module of TeTRES was applied to load them into the T-database. It can be noted that the incident-data loading module in TeTRES is also designed to directly load the incident data from those databases if they can be directly accessed by TeTRES in an integrated operating environment. The other types of data, i.e., special event, work zone and winter-road surface data, have been collected manually and organized in a set of Excel-formatted files for each data type. Those Excel files are then batch-processed by a set of the scripts, developed in this task, for an efficient population of the T-database. The rest of this chapter summarizes the types of the data collected and the process to populate the T-database.

## 3.2 COLLECTION AND PROCESSING OF SPECIAL EVENT DATA

First, the data for the metro-area special events, defined as those with large attendance big enough to affect the traffic conditions on the freeways linked to event locations, are collected manually using the publicly available data sources, such as fan-based websites, for the period of 1/2012- 3/2020. The collected data for each event includes event name, date/start/end times, attendance, and coordinates of event location. The following list shows the names of the special event locations and the sources of the event data collected for each location:

### 3.2.1 Mall of America Stadium

- Main events: National Football League games
- Data Sources:
    - https://www.pro-football-reference.com/boxscores/
    - https://www.espn.com/nfl/team/schedule/_/name/min/

### 3.2.2 Target Center

- Main Events: National Basketball Association Games
- Data Sources:
    - https://www.basketball-reference.com/teams/MIN/

### 3.2.3 Target Field

- Main events: Major League Baseball games
- Data Sources:
    - https://www.baseball-reference.com/teams/MIN/
    - https://www.espn.com/mlb/team/schedule/_/name/min/

### 3.2.4 US Bank Stadium

- Main Events: National Football League Games
- Data Sources:
    - https://www.pro-football-reference.com/boxscores/
    - https://www.espn.com/nfl/team/schedule/_/name/min/

### 3.2.5 TCF Bank Stadium

- Main Events: College Football Games
- Data Sources:
    - https://www.espn.com/nfl/team/schedule/_/name/min/

### 3.2.6 Xcel Energy Center

- Main Events: National Hockey League Games
- Data Sources:
    - https://www.hockey-reference.com/leagues/
    - https://www.nhl.com/gamecenter/

- https://www.arcticicehockey.com/2012/5/15/3001213/nhl-average-length-of-regular-season-ot-by-year

All the collected data from the above sources have been organized in an Excel spreadsheet format for each year. Table 3.1 shows a portion of the sample spreadsheet-formatted, special-event data file, collected for the 2012-2013 season, at the Mall of America Stadium in Minneapolis, Minnesota, before its name was changed to US Bank Stadium.

**Table 3.1: Sample Organized Data for Special Events at Mall of America Stadium in 2012-13**

| DATE | START | END | TITLE | TYPE | ATTEND | LAT | LON |
|---|---|---|---|---|---|---|---|
| 2012-09-09 | 12:00:00 | 15:15:00 | MN Vikings Vs Jacksonville Jaguars | Football | 56607 | 44.9738927 | -93.2602443 |
| 2012-09-23 | 12:00:00 | 15:15:00 | MN Vikings Vs San Francisco 49ers | Football | 57288 | 44.9738927 | -93.2602443 |
| 2012-10-07 | 15:15:00 | 18:35:00 | MN Vikings Vs Tennessee Titans | Football | 57652 | 44.9738927 | -93.2602443 |
| 2012-10-21 | 12:00:00 | 15:00:00 | MN Vikings Vs Arizona Cardinals | Football | 61068 | 44.9738927 | -93.2602443 |
| 2012-10-25 | 19:30:00 | 22:50:00 | MN Vikings Vs Tampa Bay Buccaneers | Football | 60860 | 44.9738927 | -93.2602443 |
| 2012-11-11 | 12:00:00 | 15:00:00 | MN Vikings Vs Detroit Lions | Football | 64059 | 44.9738927 | -93.2602443 |
| 2012-12-09 | 12:00:00 | 15:15:00 | MN Vikings Vs Chicago Bears | Football | 64134 | 44.9738927 | -93.2602443 |
| 2012-12-30 | 15:20:00 | 18:40:00 | MN Vikings Vs Green Bay Packers | Football | 64134 | 44.9738927 | -93.2602443 |
| 2012-08-17 | 19:00:00 | 22:15:00 | MN Vikings Vs Buffalo Bills | Football | 64121 | 44.9738927 | -93.2602443 |
| 2012-08-24 | 19:00:00 | 22:15:00 | MN Vikings Vs San Diego Chargers | Football | 64121 | 44.9738927 | -93.2602443 |
| 2013-09-22 | 12:00:00 | 15:30:00 | MN Vikings Vs Cleveland Browns | Football | 63672 | 44.9738927 | -93.2602443 |
| 2013-10-13 | 12:00:00 | 15:00:00 | MN Vikings Vs Carolina Panthers | Football | 63963 | 44.9738927 | -93.2602443 |
| 2013-10-27 | 19:30:00 | 22:30:00 | MN Vikings Vs Green Bay Packers | Football | 64134 | 44.9738927 | -93.2602443 |
| 2013-11-07 | 19:35:00 | 22:35:00 | MN Vikings Vs Washington Redskins | Football | 64011 | 44.9738927 | -93.2602443 |
| 2013-12-01 | 12:00:00 | 15:50:00 | MN Vikings Vs Chicago Bears | Football | 64134 | 44.9738927 | -93.2602443 |
| 2013-12-15 | 12:00:00 | 15:30:00 | MN Vikings Vs Philadelphia Eagles | Football | 64087 | 44.9738927 | -93.2602443 |
| 2013-12-29 | 12:00:00 | 14:55:00 | MN Vikings Vs Detroit Lions | Football | 64134 | 44.9738927 | -93.2602443 |
| 2013-08-09 | 19:00:00 | 15:15:00 | MN Vikings Vs Houston Texas | Football | 64121 | 44.9738927 | -93.2602443 |
| 2013-08-29 | 19:00:00 | 15:15:00 | MN Vikings Vs Tennessee Titans | Football | 64121 | 44.9738927 | -93.2602443 |

## 3.3 DATABASE POPULATION FOR SPECIAL EVENT DATA WITH BATCH-LOADING PROCESS

Figure 3.1 shows the special-event data input module of the TeTRES Admin Client, where an administrator can enter manually each event data while the location of an event place can be directly located on the map. In this study, a batch-loading process was developed for an efficient population of the T-database with all the special-event data collected and organized in a set of Excel-formatted files as shown in the previous section. Figure 3.2 shows a screenshot of the main module of the Python script, which was designed to read the Excel-formatted special-event data files and load them to the T-database. The resulting T-database contains the special-event data at the metro area from 1/2012 until 3/2020.

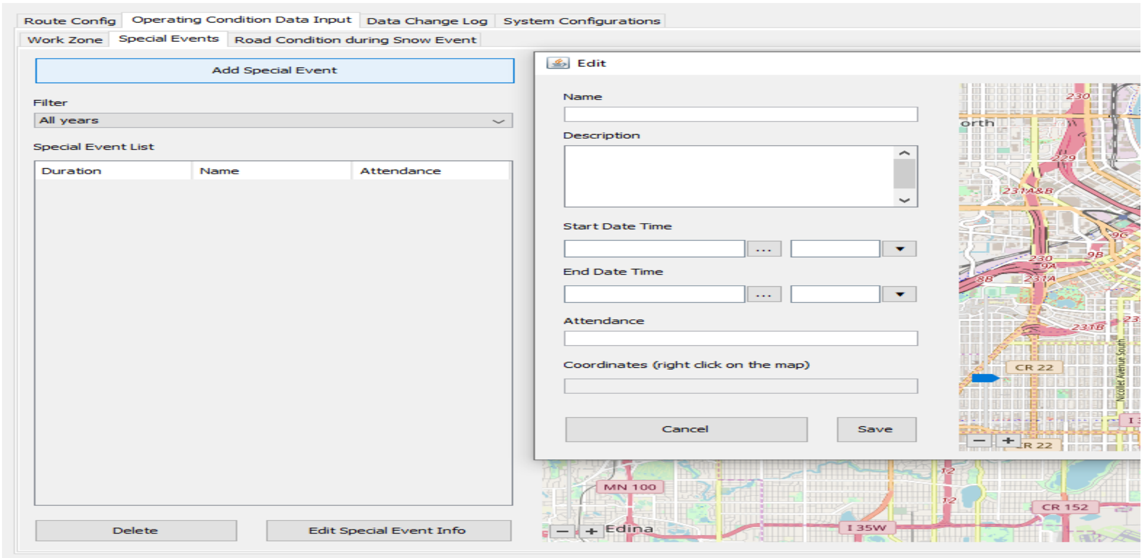


**Figure 3.1: Special-Event Data Input Screen of TeTRES Admin Client**

```python
from special_event_api_writer import SpecialEventAPIWriter
from special_event_excel_reader import SpecialEventExcelReader

base_url = "http://localhost:5000"
special_event_add_route = "/tetres/adm/sevent/add"
special_event_list_route = "/tetres/adm/sevent/list"
filename = "./data/special_event_updated_05_26_2020.xlsx"

if __name__ == "__main__":
    special_event_excel_reader = SpecialEventExcelReader(filename=filename)
    special_event_api_writer = SpecialEventAPIWriter(base_url=base_url, add_url=special_event_add_route,
                                                     list_url=special_event_list_route)
    special_event_api_writer.post_special_event_data(special_event_excel_reader)
```

**Figure 3.2: Snippets of the Python Script for Uploading Special-Event Data to TeTRES Database**

## 3.4 COLLECTION AND PROCESSING OF WORK-ZONE DATA

The work-zone data for TeTRES were collected from the construction-project maps provided by the Metro District, MnDOT, for the 2012-2020 period. Figure 3.3 shows the 2017 construction-project map, showing the information of each work zone, i.e., start/end locations and period, of all the roadway-construction projects implemented in the metro district in 2017. In this task, the information for each construction project on the freeways of the metro area were manually converted from the construction-project maps to a set of the Excel-formatted files, which were then used to populate the TeTRES database with the newly developed Python script. In particular, the detector station IDs corresponding to the start/end locations of each project were identified for each direction by comparing each year's project map with the MnDOT detector-station map. Table 3.2 shows a sample Excel-formatted work-zone data file containing the information for all the freeway work zones in 2017. Figure 3.4 also shows the Python script developed in this task to populate the T-database with those Excel-formatted work-zone data files organized for each year.  The resulting T-database contains the data for all the freeway-work zones in the metro network from 4/2012 to 9/2020.

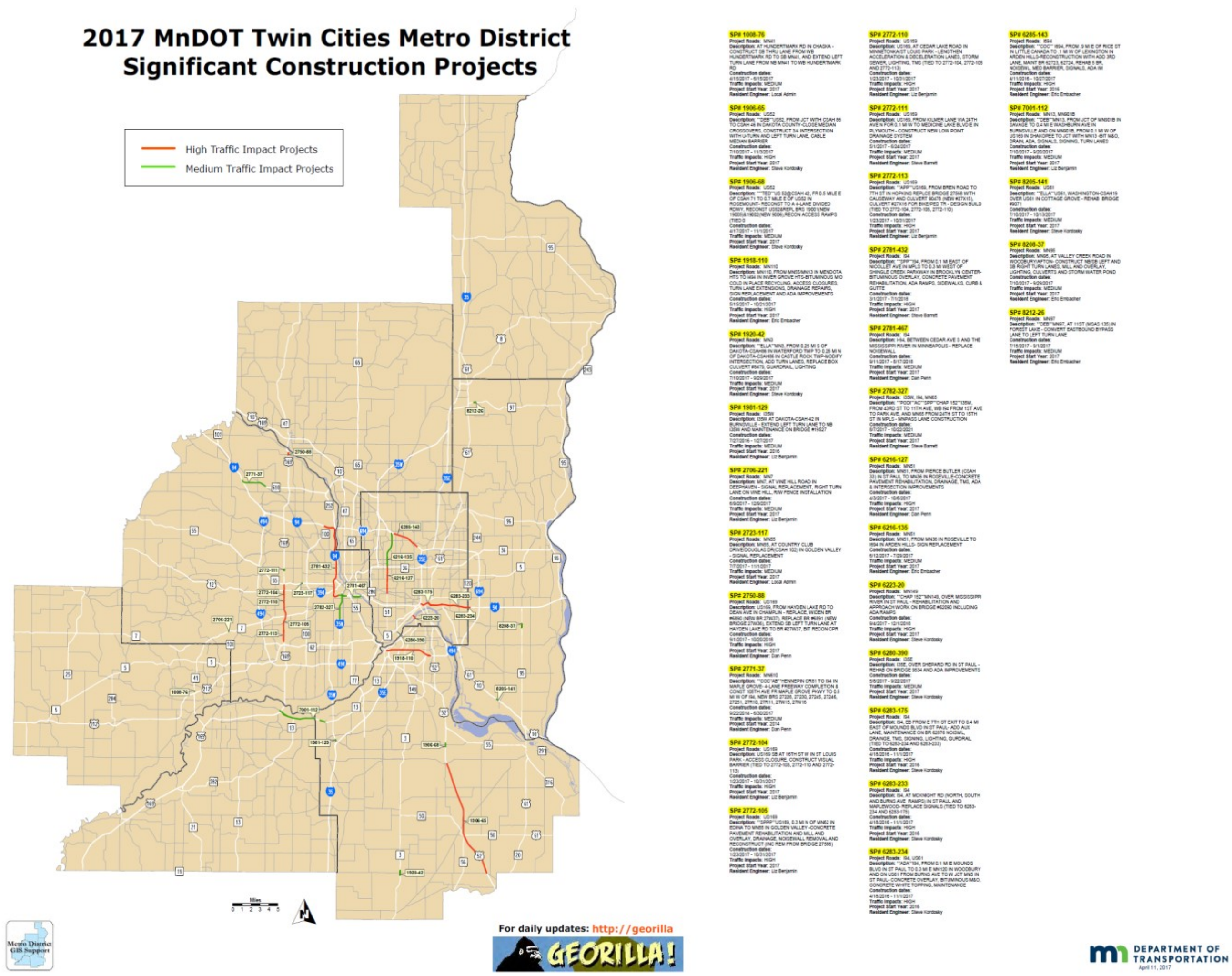


**Figure 3.3: Construction Project Map for 2017**

### Table 3.2: Sample Excel-formatted File for 2017 Work-Zone Data

| Rote ID # | Memo | Start | End | Begin Station | End Station | IMPACT |
|---|---|---|---|---|---|---|
| SP# 1981-129 | No Lane Config Available | 07/27/2016 | 1/27/2017 | S71 | S71 | MED |
| SP# 2771-37 | No Lane Config Available | 09/22/2014 | 06/30/2017 | S1958 | S1961 | MED |
| SP# 2772-105 | No Lane Config Available | 01/23/2017 | 10/31/2017 | S430 | S442 | HI |
| SP# 2772-110 | No Lane Config Available | 01/23/2017 | 10/31/2017 | S438 | S438 | HI |
| SP# 2772-113 | No Lane Config Available | 01/23/2017 | 10/31/2017 | S430 | S431 | HI |
| SP# 2781-432 | No Lane Config Available | 03/01/2017 | 07/01/2018 | S86 | S128 | HI |
| SP# 2781-467 | No Lane Config Available | 09/11/2017 | 08/17/2018 | S1813 | S466 | MED |
| SP# 2782-327 | No Lane Config Available | 08/07/2017 | 10/22/2021 | S57 | S565 | MED |
| | | | | S76 | S76 | |
| | | | | S64 | S64 | |
| SP# 6280-390 | No Lane Config Available | 05/08/2017 | 09/22/2017 | S832 | S832 | MED |
| SP# 6283-175 | No Lane Config Available | 04/18/2016 | 11/01/2017 | S779 | S780 | HI |
| SP# 6283-233 | No Lane Config Available | 04/18/2016 | 11/01/2017 | S1045 | S1045 | HI |
| SP# 6283-234 | No Lane Config Available | 04/18/2016 | 11/01/2017 | S780 | S1047 | HI |
| SP# 6285-143 | No Lane Config Available | 04/11/2016 | 10/27/2017 | S1461 | S1086 | HI |
| SP# 8205-141 | No Lane Config Available | 07/10/2017 | 10/13/2017 | S1923 | S1923 | MED |

```python
import sys

sys.path.append("server")
import common
from pyticas import ticas
from pyticas.infra import Infra
from pyticas_tetres import api_urls_admin

from tetres_data_populator.work_zone_data.work_zone_api_reader import WorkZoneAPIReader
from tetres_data_populator.work_zone_data.work_zone_api_writer import WorkZoneAPIWriter
from tetres_data_populator.work_zone_data.work_zone_excel_reader import WorkZoneExcelReader

if __name__ == "__main__":

    ticas.initialize(common.DATA_PATH)
    infra = Infra.get_infra()

    base_url = "http://localhost:5000"
    only_file_names = ["work_zone_2010.xlsx", "work_zone_2011.xlsx", "work_zone_2012.xlsx", "work_zone_2013.xlsx", "work_zone_2014.xlsx"]
    for only_file_name in only_file_names:
        work_zone_filename = "server/data_populator_libs/tetres_data_populator/excel_data/work_zone_data/{}".format(only_file_name)
        work_zone_excel_reader = WorkZoneExcelReader(filename=work_zone_filename)

        # adding work zone group data
        work_zone_api_writer = WorkZoneAPIWriter(infra=infra)
        work_zone_api_writer.post_data(excel_reader=work_zone_excel_reader,
                                       post_url=base_url + api_urls_admin.WZ_GROUP_INSERT,
                                       list_url=base_url + api_urls_admin.WZ_GROUP_LIST,
                                       data_type="work_zone_group",
                                       api_reader_class=WorkZoneAPIReader)

        work_zone_api_writer.post_data(excel_reader=work_zone_excel_reader,
                                       post_url=base_url + api_urls_admin.WZ_INSERT,
                                       list_url=base_url + api_urls_admin.WZ_LIST_ALL,
                                       data_type="work_zone",
                                       api_reader_class=WorkZoneAPIReader)

        work_zone_api_writer.populate_work_zone_years(api_reader=WorkZoneAPIReader())
```

### Figure 3.4: Snippets of the Python script for Processing Work-Zone Data Files

## 3.5 COLLECTION AND PROCESSING OF WINTER ROAD-CONDITION DATA

Tables 3.3 and 3.4 show a portion of the plow-route and snow-event data provided by the Metro District, MnDOT for the 2016-19 period. First, the detector station IDs for the start and end location of each plow route in the metro-freeway network are identified by visually matching the MnDOT detector-station map with the plow-route locations from Table 3.3. The station IDs for each plow route were then organized in an Excel-format. Table 3.5 shows a portion of the Excel-formatted file with the station data for each plow route. Next, the detailed information for each snow event on the metro freeways, i.e., event date/time, route ID and bare-lane lost/regain times, were extracted from the MnDOT snow-event data shown in Table 3.6 and stored in a set of the Excel-formatted files. Table 3.6 includes a converted snow-event data file. Those Excel-formatted files with the converted snow-event data were then used for populating the TeTRES database. Figure 3.5 shows the snippets of the Python script developed in this study to populate the TeTRES database with those Excel-formatted snow-event data.

It can be noted that, according to the MnDOT '*Snow and Ice Event/Bare Lane Training, 2016-2017*' [2], the *'bare lanes'* are defined as those with '*all driving lanes are 95% free of snow and ice between the outer edges of the wheel paths and have less than 1 inch of accumulation on the center of the roadway*'. Using the bare-lane lost/regain time data for each snow-event, TeTRES identifies 'Lost' or 'Normal' freeway segments, which are linked to each travel-time route defined by the TeTRES Admin Client, so that the travel-time reliability for given routes under the 'lane-lost' or 'normal' conditions can be estimated. In this study, the snow-event data from 2012 until 2019 have been collected, processed, and uploaded to the T-Database.

**Table 3.3: Sample Data for Plow-Route Locations from MnDOT**

| Route_NM | Road_Cl | Route_ | Hwy_NM | From_Loc | To_Loc | MP_Begin | True_Mi_ | MP_End | True_Mi_ |
|---|---|---|---|---|---|---|---|---|---|
| TP5A0101 | SC | 2016 | US10 | 3 exit ramp to US 169 NB/MN 101 | S end of BR#2003 BNSF RR | 214.553 | 216 | 230.402 | 232 |
| TP5A0471 | UC | 2016 | MN47 | st Junction US10/East Junction US | Pederson Dr./Cty 81 | 20.662 | 21 | 34.802 | 35 |
| TP5A0651 | SC | 2016 | MN65 | Main St CSAH-14 X-ING/BR# 0205 | Anoka Co. Rd. 24/237th Ave NE in East Bethel | 15.42 | 17 | 29.389 | 31 |
| TP5A1691 | SC | 2016 | US169 | yton Rd, N Jct CSAH-12, LT Miller | unction T.H. 10, Junction MN 47/BR #9713, Ferry St in A | 145.715 | 143 | 146.874 | 144 |
| TP5B0941 | SC | 2016 | I94 | n County line, NW end of Bridge 27 | EB exit loop to CSAH-81 | 205.367 | 206 | 220.541 | 221 |
| TP5B1011 | SC | 2016 | MN101 | on Hennepin Co. Rd. 81 in Rogers J | burne County Line (North end of Bridge 86005 over Mis | 39.64 | 40 | 46.35 | 46 |
| TP5B1691 | SC | 2016 | US169 | Junction T.H. 55 in Plymouth | Dayton Rd N Jct CSAH-12, LT Miller RD | 130.94 | 129 | 145.715 | 143 |
| TP5B4941 | SC | 2016 | I494 | BR #27905 Under Fish Lake Road | Junction I-94 (Fish Lake Interchange) | 27.15 | 27 | 27.973 | 28 |
| TP5B6101 | UC | 2016 | MN610 | WB EXIT RAMP TO WB CSAH 81 | WB exit ramp to West Broadway CSAH 103 | 2.486 | 2 | 6.122 | 6 |
| TP5C0121 | SC | 2016 | US12 | dependence, W Urban boundary N | Junction I-394/I-494 in Minnetonka | 145.522 | 145 | 156+1.014 | 157 |
| TP5C0551 | UC | 2016 | MN55 | 27044; Wright-Hennepin Co/N end | East end BR# 27785 over I94 | 165.336 | 165 | 189.677 | 190 |
| TP5C3941 | SC | 2016 | I394 | Junction I-494 in Minnetonka | Junction T.H. 100 in Golden Valley | 0 | 0 | 5.925 | 6 |
| TP5C4941 | SC | 2016 | I494 | Junction MN 7 - Bridge 27V6O | BR# 27905 Under Fish Lake Road | 16.259 | 16 | 27.15 | 27 |
| TP5E0010 | SC | 2016 | US10 | tween I694EB ent ramp and MN5 | East junction of US10/I694 (EB) | 240.592 | 243 | 240+01.183 | 243 |
| TP5E0941 | SC | 2016 | I94 | EB exit loop to CSAH-81 | Junction MNTH - 252 | 220.541 | 221 | 224.977 | 226 |
| TP5E1001 | SC | 2016 | MN100 | Junction T.H. 62 in Edina | Junction I-694 in Brooklyn Center | 2.139 | 2 | 16.158 | 16 |
| TP5E6941 | SC | 2016 | I694 | Junction I-94 in Brooklyn Center | W end BR# 9209/9210 over Island Lake Channel | 34.197 | 34 | 43.45 | 43 |
| TP5F0101 | SC | 2016 | US10 | E end of BR# 9722 EB over BNSF R | I-35W North Jct. | 230.402 | 232 | 237.035 | 239 |
| TP5F0101 | SC | 2016 | US10 | Junction I35W NB/US910A | Between MN51 and junction with I694 | 238.393 | 240 | 240.592 | 243 |
| TP5F0101 | UC | 2016 | US910A | Cty Rd H Crossing, CSAH 9&10 | Jct I-35W NB, US 10 | 237.906 | 240 | 238.393 | 240 |
| TP5F0471 | UC | 2016 | MN47 | Anoka County Line at Minneapolis | E Junction USTH-10 | 5.37 | 5 | 13.076 | 13 |

### Table 3.4: Sample Snow-Event Data from MnDOT

| Project Id | Project Maintenance Route | Service Level Name | Event Begin Date Time | Event End Date Time | Event Duration Hours | Lane Lost Date Time | Lane Regain Date Time |
|---|---|---|---|---|---|---|---|
| TP5P1691 | MN282/2ND ST-JCT MN 41/CSAH78 | SUPER COMMUTER | 12/4/2016 12:00:00 AM | 12/4/2016 5:30:00 AM | 5.5 | 12/4/2016 1:00:00 AM | 12/4/2016 6:00:00 AM |
| TP5P1691 | MN282/2ND ST-JCT MN 41/CSAH78 | SUPER COMMUTER | 12/10/2016 12:00:00 PM | 12/11/2016 11:00:00 AM | 23.0 | 12/10/2016 5:00:00 PM | 12/11/2016 11:00:00 AM |
| TP5P1691 | MN282/2ND ST-JCT MN 41/CSAH78 | SUPER COMMUTER | 12/15/2016 9:45:00 PM | 12/17/2016 6:30:00 AM | 32.8 | 12/15/2016 10:15:00 PM | 12/19/2016 10:00:00 AM |
| TP5P1691 | MN282/2ND ST-JCT MN 41/CSAH78 | SUPER COMMUTER | 12/23/2016 10:30:00 AM | 12/23/2016 3:45:00 PM | 5.3 | | |
| TP5P1691 | MN282/2ND ST-JCT MN 41/CSAH78 | SUPER COMMUTER | 1/2/2017 2:30:00 PM | 1/3/2017 3:30:00 AM | 13.0 | | |
| TP5P1691 | MN282/2ND ST-JCT MN 41/CSAH78 | SUPER COMMUTER | 1/9/2017 11:30:00 AM | 1/9/2017 4:30:00 PM | 5.0 | 1/9/2017 12:00:00 PM | 1/9/2017 9:30:00 PM |
| TP5P1691 | MN282/2ND ST-JCT MN 41/CSAH78 | SUPER COMMUTER | 1/10/2017 4:00:00 AM | 1/10/2017 2:30:00 PM | 10.5 | 1/10/2017 5:30:00 AM | 1/10/2017 5:15:00 PM |

### Table 3.5: Sample Plow-Route Location Data with Detector Station IDs

| Station name | Plow ID | Starting Station | Ending Station |
|---|---|---|---|
| | TP5H0521 | S1943 | S122 |
| | TP5H0941 | S170 | S2203 |
| | TP5H35W1 | S565 | S573 |
| Camden | TP5H3941 | S281 | S291 |
| | TP5J0051 | S495 | S497 |
| | TP5J0551 | S533 | S818 |
| | TP5J0621 | S301 | S1135 |
| | TP5J0651 | S560 | S1810 |
| | TP5J0771 | S920 | S531 |
| | TP5J1001 | S375 | S378 |
| | TP5J35W1 | ST3501 | S23 |
| Cedar | TP5J4941 | S474 | S494 |
| | TP9F0361 | S590 | S597 |
| | TP9F0521 | S1176 | S1178 |
| | TP9F0611 | S1039 | S1944 |
| | TP9F0941 | S2203 | S1044 |
| | TP9F2801 | S1466 | S1471 |
| | TP9F35E1 | S838 | S1489 |
| Maryland | TP9F6941 | S1078 | S1454 |
| | TP9B0351 | S1591 | S1511 |
| Forest Lake | TP9B35E1 | S1485 | S1504 |
| North Branch | TP9A0351 | S1512 | ST3583 |
| | TP9K0361 | S599 | S1852 |
| | TP9K0941 | S1045 | S1358 |
| | TP9K4941 | S1029 | S1034 |
| Oakdale | TP9K6941 | S1398 | S1028 |

### Table 3.6: Sample Snow-Event Data for Freeway-based Routes

| Event Start | Event End | Affected Routes | Lane Lost Time | Lane Regain Time |
|---|---|---|---|---|
| 11/18/2016 2:30:00 PM | 11/18/2016 10:00:00 PM | TP9K0941 | | |
| | | TP5E1001 | 11/22/2016 10:00:00 PM | 11/23/2016 4:30:00 AM |
| 11/22/2016 7:00:00 AM | 11/23/2016 11:00:00 AM | TP5E6941 | 11/22/2016 10:00:00 PM | 11/23/2016 3:30:00 AM |
| | | TP5B0941 | 11/22/2016 11:00:00 PM | 11/23/2016 5:00:00 AM |
| 11/22/2016 7:30:00 AM | 11/23/2016 5:00:00 AM | TP5B1691 | 11/22/2016 11:00:00 PM | 11/23/2016 5:00:00 AM |
| | | TP5J0551 | 11/22/2016 9:00:00 PM | 11/23/2016 2:30:00 AM |
| 11/22/2016 8:00:00 AM | 11/23/2016 1:00:00 AM | TP5J0771 | 11/22/2016 9:00:00 PM | 11/23/2016 2:30:00 AM |
| 11/22/2016 9:00:00 AM | 11/23/2016 1:00:00 AM | TP9K0941 | 11/22/2016 7:00:00 PM | 11/23/2016 2:30:00 AM |
| 11/22/2016 2:00:00 PM | 11/23/2016 2:00:00 AM | TP9P35E1 | 11/22/2016 9:00:00 PM | 11/23/2016 2:30:00 AM |
| 11/22/2016 2:00:00 PM | 11/23/2016 1:00:00 AM | TP9P35W1 | 11/22/2016 8:00:00 PM | 11/23/2016 1:30:00 AM |
| 11/22/2016 3:00:00 PM | 11/23/2016 1:00:00 AM | TP9M4941 | 11/23/2016 4:00:00 AM | 11/23/2016 9:30:00 AM |
| 11/22/2016 3:00:00 PM | 11/23/2016 2:00:00 AM | TP9F0941 | 11/22/2016 10:00:00 PM | 11/23/2016 1:30:00 AM |
| 11/22/2016 3:00:00 PM | 11/23/2016 3:30:00 AM | TP9F35E1 | 11/22/2016 11:00:00 PM | 11/23/2016 2:00:00 AM |
| 11/22/2016 3:15:00 PM | 11/23/2016 3:30:00 AM | TP9F6941 | 11/22/2016 11:00:00 PM | 11/23/2016 2:00:00 AM |
| 11/22/2016 5:00:00 PM | 11/23/2016 12:00:00 PM | TP9B35E1 | 11/22/2016 6:00:00 PM | 11/23/2016 4:00:00 AM |
| | | TP5M1691 | 11/23/2016 1:00:00 AM | 11/23/2016 4:00:00 AM |
| 11/22/2016 6:00:00 PM | 11/23/2016 2:15:00 AM | TP5M2121 | 11/22/2016 7:00:00 PM | 11/23/2016 2:45:00 AM |
| 11/22/2016 6:30:00 PM | 11/23/2016 10:00:00 AM | TP5P1691 | 11/22/2016 6:00:00 PM | 11/23/2016 5:30:00 AM |
| 11/22/2016 7:30:00 PM | 11/23/2016 11:30:00 AM | TP9N0611 | 11/22/2016 7:30:00 PM | 11/23/2016 2:00:00 AM |

```python
import sys

sys.path.append("server")
import common
from pyticas import ticas
from pyticas.infra import Infra
from pyticas_tetres import api_urls_admin

from tetres_data_populator.snow_event_data.snow_event_api_reader import SnowEventAPIReader
from tetres_data_populator.snow_event_data.snow_event_api_writer import SnowEventAPIWriter
from tetres_data_populator.snow_event_data.snow_event_excel_reader import SnowEventExcelReader

if __name__ == "__main__":
    ticas.initialize(common.DATA_PATH)
    infra = Infra.get_infra()

    base_url = "http://localhost:5000"

    only_file_name = input("Enter the name of the snow event excel file: ")
    snow_event_filename = "server/data_populator_libs/tetres_data_populator/excel_data/snow_event_data/{}".format(only_file_name)
    snow_event_excel_reader = SnowEventExcelReader(filename=snow_event_filename)

    # adding snow route data
    snow_event_api_writer = SnowEventAPIWriter(infra)
    snow_event_api_writer.post_data(excel_reader=snow_event_excel_reader,
                                    post_url=base_url + api_urls_admin.SNR_INSERT,
                                    list_url=base_url + api_urls_admin.SNR_LIST,
                                    data_type="snow_route",
                                    api_reader_class=SnowEventAPIReader)

    # adding snow event data
    snow_event_api_writer.post_data(excel_reader=snow_event_excel_reader,
                                    post_url=base_url + api_urls_admin.SNE_INSERT,
                                    list_url=base_url + api_urls_admin.SNE_LIST,
                                    data_type="snow_event",
                                    api_reader_class=SnowEventAPIReader)

    # adding snow management data
    snow_event_api_writer.post_data(excel_reader=snow_event_excel_reader,
                                    post_url=base_url + api_urls_admin.SNM_INSERT,
                                    list_url=base_url + api_urls_admin.SNM_LIST_ALL,
                                    data_type="snow_management",
                                    api_reader_class=SnowEventAPIReader)
```

**Figure 3.5: Snippets of the Python Script for Populating Snow-Event Data**

## 3.6 DATA CATEGORIZATION FOR DEFINED ROUTES

As described in the previous sections, in this study, various types of historical data needed for TeTRES were collected, processed, and loaded into the TeTRES database, which contains the following data sets:

- Special event data for 1/2012-3/2020
- Work zone data from 4/2012 – 9/2020
- Winter road condition data from 10/2012 – 4/2019
- Weather data from NOAA for 2010 – 9/30/2020
- Incident data from CAD/IRIS database for 2010 – 9/30/2020
- Traffic-detector data (stored separately in a local hard disk): 2010 – 9/2020.

It needs to be noted that the traffic-flow data from the field detector stations have been collected separately and stored in a local hard disk in a structured directory for the period of 2010 – 2020. In this study, the travel times of 116 routes, defined in the previous phase for the travel-time reliability analysis, have also been calculated for every 5-minute interval from 1/1/2010 until 9/30/2020 and stored in the travel-time database, a subset of the TeTRES database. Figure 3.6 shows the screenshots of the TeTRES admin client showing the list of currently defined routes. Finally, the categorization of the non-traffic data, e.g., weather and incident, collected/processed in this chapter, was performed and the categorized external data were linked to each route's travel-time data. Figures 3.7 – 3.9 include the sample database tables showing the links between the travel-time and non-traffic data for the selected routes. The resulting TeRES database, which contains each route's 5-minute travel-time data linked to the non-traffic external condition data during the same 5-minute interval, can be applicable for estimating the reliability measures under different operating conditions for selected routes and periods. The populated TeTRES database can be accessed at the following link: https://drive.google.com/open?id =1iA8_27j_4Htw9oAtrWSnNbjgo_X23W5m

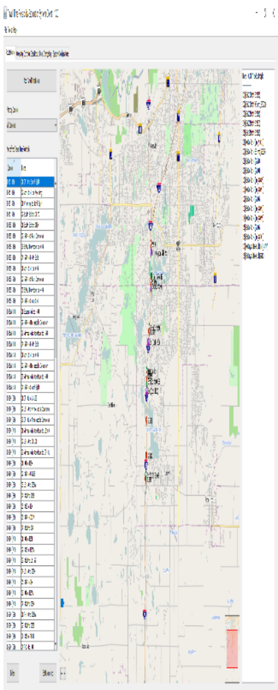

| | |
|---|---|
| I-35 (NB) | 01 CR70 to South Split |
| I-35 (NB) | 02 North Split to Wyoming |
| I-35 (SB) | 01 Wyoming to North Split |
| I-35 (SB) | 02 South Split to CR70 |
| I-35E (NB) | 01 South Split to I494 |
| I-35E (NB) | 02 I494 to StPaul Downtown |
| I-35E (NB) | 03 StPaul Downtown to I694 |
| I-35E (NB) | 04 I694 to North Split |
| I-35E (SB) | 01 North Split to I694 |
| I-35E (SB) | 02 I694 to StPaul Downtown |
| I-35E (SB) | 03 StPaul Downtown to I494 |
| I-35E (SB) | 04 I494 to South Split |
| I-35W (NB) | 01 Sourth Split to I494 |
| I-35W (NB) | 02 I494 to Minneapolis Downtown |
| I-35W (NB) | 03 Minneapolis Downtown to I694 |
| I-35W (NB) | 04 I694 to North Split |
| I-35W (SB) | 01 North Split to I694 |
| I-35W (SB) | 02 I694 to Minneapolis Downtown |
| I-35W (SB) | 03 Minneapolis Downtown to I494 |
| I-35W (SB) | 04 I494 to Sourth Split |
| I-394 (EB) | 01 CR101 to US169 |
| I-394 (EB) | 02 US169 to Minneapolis Downtown |
| I-394 (EB) | 03 CR101 to Minneapolis Downtown |
| I-394 (WB) | 01 Minneapolis Downtown to US169 |
| I-394 (WB) | 02 US169 to CR101 |
| I-394 (WB) | 03 Minneapolis Downtown to CR101 |
| I-494 (EB) | 01 I94 to I394 |
| I-494 (EB) | 02 I394 to US169 |
| I-494 (EB) | 03 US169 to I35W |
| I-494 (EB) | 04 I35W to I35E |
| I-494 (EB) | 05 I35E to I94 |
| I-494 (EB) | 06 I394 to I35W |
| I-494 (EB) | 07 I35W to I94 |
| I-494 (WB) | 01 I94 to I35E |
| I-494 (WB) | 02 I35E to I35W |
| I-494 (WB) | 03 I35W to US169 |
| I-494 (WB) | 04 US169 to I394 |
| I-494 (WB) | 05 I394 to I94 |
| I-494 (WB) | 06 I94 to I35W |
| I-494 (WB) | 07 I35W to I394 |
| I-694 (EB) | 01 TH100 to I35W |
| I-694 (EB) | 02 I35W to I35E |
| I-694 (EB) | 03 I35E to TH36 |

| | |
|---|---|
| I-694 (EB) | 04 TH36 to I94 |
| I-694 (EB) | 05 I35E to I94 |
| I-694 (WB) | 01 I94 to TH36 |
| I-694 (WB) | 02 TH36 to I35E |
| I-694 (WB) | 03 I35E to I35W |
| I-694 (WB) | 04 I35W to TH100 |
| I-694 (WB) | 05 I94 to I35E |
| I-694 (WB) | 06 I35E to I494 |
| I-94 (EB) | 01 TH101 to I494 |
| I-94 (EB) | 02 I494 to TH252 |
| I-94 (EB) | 03 TH252 to I35W |
| I-94 (EB) | 04 I35W to I35E |
| I-94 (EB) | 05 I35E to I694 |
| I-94 (EB) | 06 I694 to TH95 |
| I-94 (EB) | 07 I94 to I35E |
| I-94 (EB) | Opposite Direction of samplei-94v |
| I-94 (EB) | SAMPLE I-94(EB) |
| I-94 (EB) | SAMPLE I-94(EB) 2.0 |
| I-94 (EB) | SAMPLE I-94(EB) 3.0 |
| I-94 (WB) | 01 TH95 to I694 |
| I-94 (WB) | 02 I694 to I35E |
| I-94 (WB) | 03 I35E to I35W |
| I-94 (WB) | 04 I35W to TH252 |
| I-94 (WB) | 05 TH252 to I494 |
| I-94 (WB) | 06 I494 to TH101 |
| I-94 (WB) | Opposite Direction of SAMPLE I-94(EB) ... |
| I-94 (WB) | SAMPLE I-94(EB) *OD* |
| I-94 (WB) | samplei-94v |
| T.H.10 (EB) | 01 US169 to I35W |
| T.H.10 (WB) | 02 I35W to US169 |
| T.H.100 (NB) | 01 I494 to I394 |
| T.H.100 (NB) | 02 I394 to I694 |
| T.H.100 (SB) | 01 I694 to I394 |
| T.H.100 (SB) | 02 I394 to I494 |
| T.H.212 (EB) | 01 TH41 to US169 |
| T.H.212 (WB) | 01 US169 to TH41 |
| T.H.280 (NB) | 01 I94 to I35W |
| T.H.280 (SB) | 01 I35W to I94 |
| T.H.36 (EB) | 01 I35W to I35E |
| T.H.36 (EB) | 02 I35E to TH5 |
| T.H.36 (EB) | 03 I35E to I694 |
| T.H.36 (WB) | 01 TH5 to I35E |
| T.H.36 (WB) | 02 I35E to I35W |

| | |
|---|---|
| T.H.36 (WB) | 03 I694 to I35E |
| T.H.5 (EB) | 01 I494 to TH55 |
| T.H.5 (WB) | 01 TH55 to I494 |
| T.H.52 (NB) | 01 TH55 to I94 |
| T.H.52 (SB) | 01 I94 to TH55 |
| T.H.61 (NB) | 01 Hastings to I494 |
| T.H.61 (NB) | 02 I494 to I94 |
| T.H.61 (SB) | 01 I94 to I494 |
| T.H.61 (SB) | 02 I494 to Hastings |
| T.H.610 (EB) | 01 I94 to US169 |
| T.H.610 (EB) | 02 US169 to TH47 |
| T.H.610 (WB) | 01 TH47 to US169 |
| T.H.610 (WB) | 02 US169 to I94 |
| T.H.62 (EB) | 01 I494 to I35W |
| T.H.62 (EB) | 02 I35W to TH55 |
| T.H.62 (EB) | 03 I494 to TH55 |
| T.H.62 (WB) | 01 TH55 to I35W |
| T.H.62 (WB) | 02 I35W to I494 |
| T.H.62 (WB) | 03 TH55 to I494 |
| T.H.77 (NB) | 01 CR38 to TH62 |
| T.H.77 (SB) | 01 TH62 to CR38 |
| U.S.169 (NB) | 01 Canterbury Rd to I494 |
| U.S.169 (NB) | 02 I494 to I394 |
| U.S.169 (NB) | 03 I394 to I694 |
| U.S.169 (NB) | 04 I694 to TH610 |
| U.S.169 (SB) | 01 TH610 to I694 |
| U.S.169 (SB) | 02 I694 to I394 |
| U.S.169 (SB) | 03 I394 to I494 |
| U.S.169 (SB) | 04 I494 to Canterbury Rd |
| U.S.169 (SB) | 05 I694 to MN62 |

**Figure 3.6: Screenshot of TeTRES Admin Client showing the List of Current Travel-Time Routes**

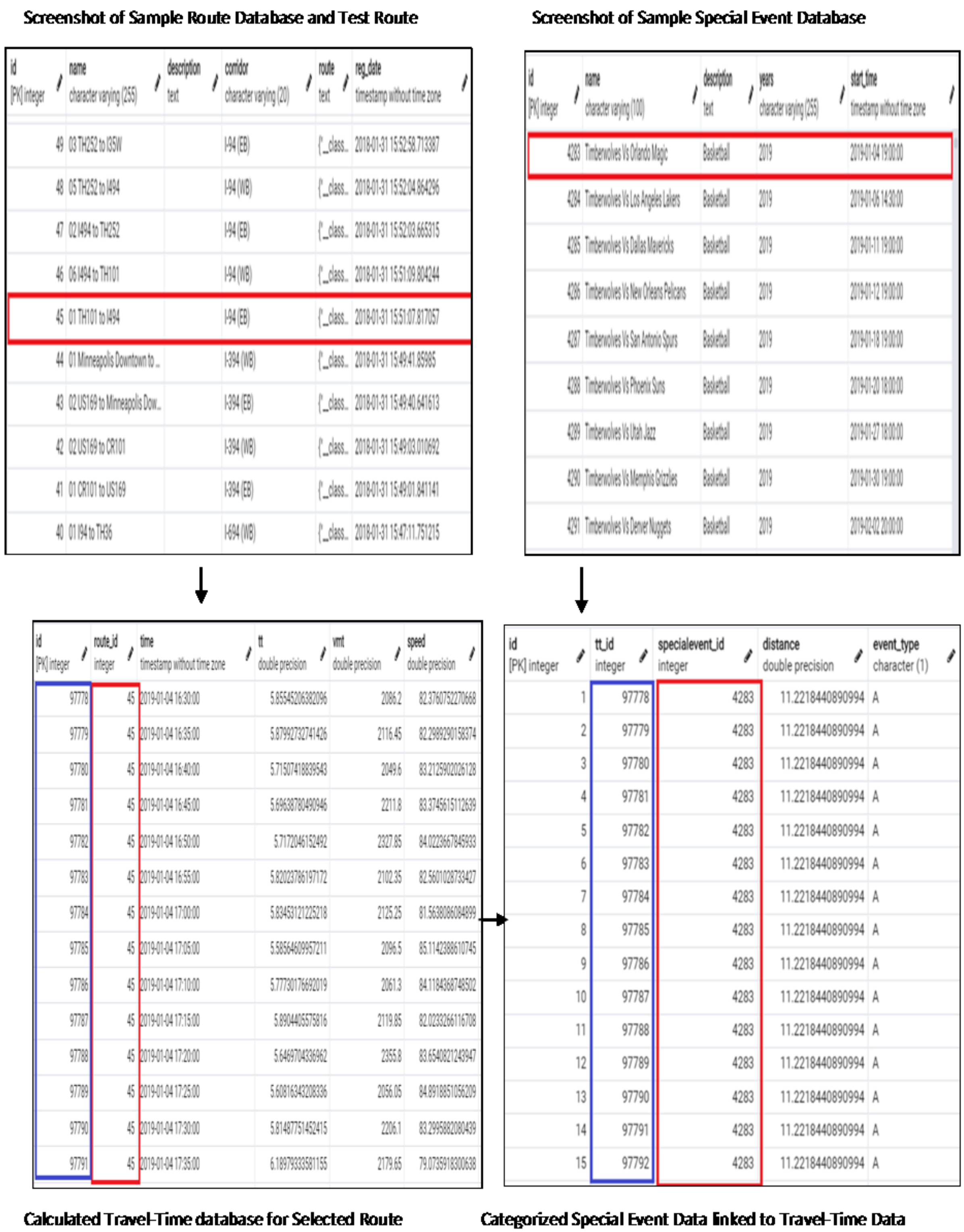

**Screenshot of Sample Route Database and Test Route**

| id [PK] integer | name character varying (255) | description text | corridor character varying (20) | route text | reg_date timestamp without time zone |
|---|---|---|---|---|---|
| 49 | 03 TH252 to I35W | | I-94 (EB) | {"_class... | 2018-01-31 15:52:58.713387 |
| 48 | 05 TH252 to I494 | | I-94 (WB) | {"_class... | 2018-01-31 15:52:04.864296 |
| 47 | 02 I494 to TH252 | | I-94 (EB) | {"_class... | 2018-01-31 15:52:03.665315 |
| 46 | 06 I494 to TH101 | | I-94 (WB) | {"_class... | 2018-01-31 15:51:09.804244 |
| 45 | 01 TH101 to I494 | | I-94 (EB) | {"_class... | 2018-01-31 15:51:07.817057 |
| 44 | 01 Minneapolis Downtown to ... | | I-394 (WB) | {"_class... | 2018-01-31 15:49:41.85985 |
| 43 | 02 US169 to Minneapolis Dow... | | I-394 (EB) | {"_class... | 2018-01-31 15:49:40.641613 |
| 42 | 02 US169 to CR101 | | I-394 (WB) | {"_class... | 2018-01-31 15:49:03.010692 |
| 41 | 01 CR101 to US169 | | I-394 (EB) | {"_class... | 2018-01-31 15:49:01.841141 |
| 40 | 01 I94 to TH36 | | I-694 (WB) | {"_class... | 2018-01-31 15:47:11.751215 |

**Screenshot of Sample Special Event Database**

| id [PK] integer | name character varying (100) | description text | years character varying (255) | start_time timestamp without time zone |
|---|---|---|---|---|
| 4283 | Timberwolves Vs Orlando Magic | Basketball | 2019 | 2019-01-04 19:00:00 |
| 4284 | Timberwolves Vs Los Angeles Lakers | Basketball | 2019 | 2019-01-06 14:30:00 |
| 4285 | Timberwolves Vs Dallas Mavericks | Basketball | 2019 | 2019-01-11 19:00:00 |
| 4286 | Timberwolves Vs New Orleans Pelicans | Basketball | 2019 | 2019-01-12 19:00:00 |
| 4287 | Timberwolves Vs San Antonio Spurs | Basketball | 2019 | 2019-01-18 19:00:00 |
| 4288 | Timberwolves Vs Phoenix Suns | Basketball | 2019 | 2019-01-20 18:00:00 |
| 4289 | Timberwolves Vs Utah Jazz | Basketball | 2019 | 2019-01-27 18:00:00 |
| 4290 | Timberwolves Vs Memphis Grizzlies | Basketball | 2019 | 2019-01-30 19:00:00 |
| 4291 | Timberwolves Vs Denver Nuggets | Basketball | 2019 | 2019-02-02 20:00:00 |

| id [PK] integer | route_id integer | time timestamp without time zone | tt double precision | vmt double precision | speed double precision |
|---|---|---|---|---|---|
| 97778 | 45 | 2019-01-04 16:30:00 | 5.85545206382096 | 2086.2 | 82.3760752270668 |
| 97779 | 45 | 2019-01-04 16:35:00 | 5.87992732741426 | 2116.45 | 82.2989290158374 |
| 97780 | 45 | 2019-01-04 16:40:00 | 5.71507418839543 | 2049.6 | 83.2125902026128 |
| 97781 | 45 | 2019-01-04 16:45:00 | 5.69638780490946 | 2211.8 | 83.3745615112639 |
| 97782 | 45 | 2019-01-04 16:50:00 | 5.7172046152492 | 2327.85 | 84.0223667845933 |
| 97783 | 45 | 2019-01-04 16:55:00 | 5.82023786197172 | 2102.35 | 82.5601028733427 |
| 97784 | 45 | 2019-01-04 17:00:00 | 5.83453121225218 | 2125.25 | 81.5638086084899 |
| 97785 | 45 | 2019-01-04 17:05:00 | 5.58564609957211 | 2096.5 | 85.1142388610745 |
| 97786 | 45 | 2019-01-04 17:10:00 | 5.77730176692019 | 2061.3 | 84.1184368748502 |
| 97787 | 45 | 2019-01-04 17:15:00 | 5.8904405575816 | 2119.85 | 82.0233266116708 |
| 97788 | 45 | 2019-01-04 17:20:00 | 5.6469704336962 | 2355.8 | 83.6540821243947 |
| 97789 | 45 | 2019-01-04 17:25:00 | 5.60816343208336 | 2056.05 | 84.8918851056209 |
| 97790 | 45 | 2019-01-04 17:30:00 | 5.81487751452415 | 2206.1 | 83.2995882080439 |
| 97791 | 45 | 2019-01-04 17:35:00 | 6.18979333581155 | 2179.65 | 79.0735918300638 |

**Calculated Travel-Time database for Selected Route**

| id [PK] integer | tt_id integer | specialevent_id integer | distance double precision | event_type character (1) |
|---|---|---|---|---|
| 1 | 97778 | 4283 | 11.2218440890994 | A |
| 2 | 97779 | 4283 | 11.2218440890994 | A |
| 3 | 97780 | 4283 | 11.2218440890994 | A |
| 4 | 97781 | 4283 | 11.2218440890994 | A |
| 5 | 97782 | 4283 | 11.2218440890994 | A |
| 6 | 97783 | 4283 | 11.2218440890994 | A |
| 7 | 97784 | 4283 | 11.2218440890994 | A |
| 8 | 97785 | 4283 | 11.2218440890994 | A |
| 9 | 97786 | 4283 | 11.2218440890994 | A |
| 10 | 97787 | 4283 | 11.2218440890994 | A |
| 11 | 97788 | 4283 | 11.2218440890994 | A |
| 12 | 97789 | 4283 | 11.2218440890994 | A |
| 13 | 97790 | 4283 | 11.2218440890994 | A |
| 14 | 97791 | 4283 | 11.2218440890994 | A |
| 15 | 97792 | 4283 | 11.2218440890994 | A |

**Categorized Special Event Data linked to Travel-Time Data**

**Figure 3.7: Example Categorized Special Event Data Linked to Travel-Time of Sample Route**

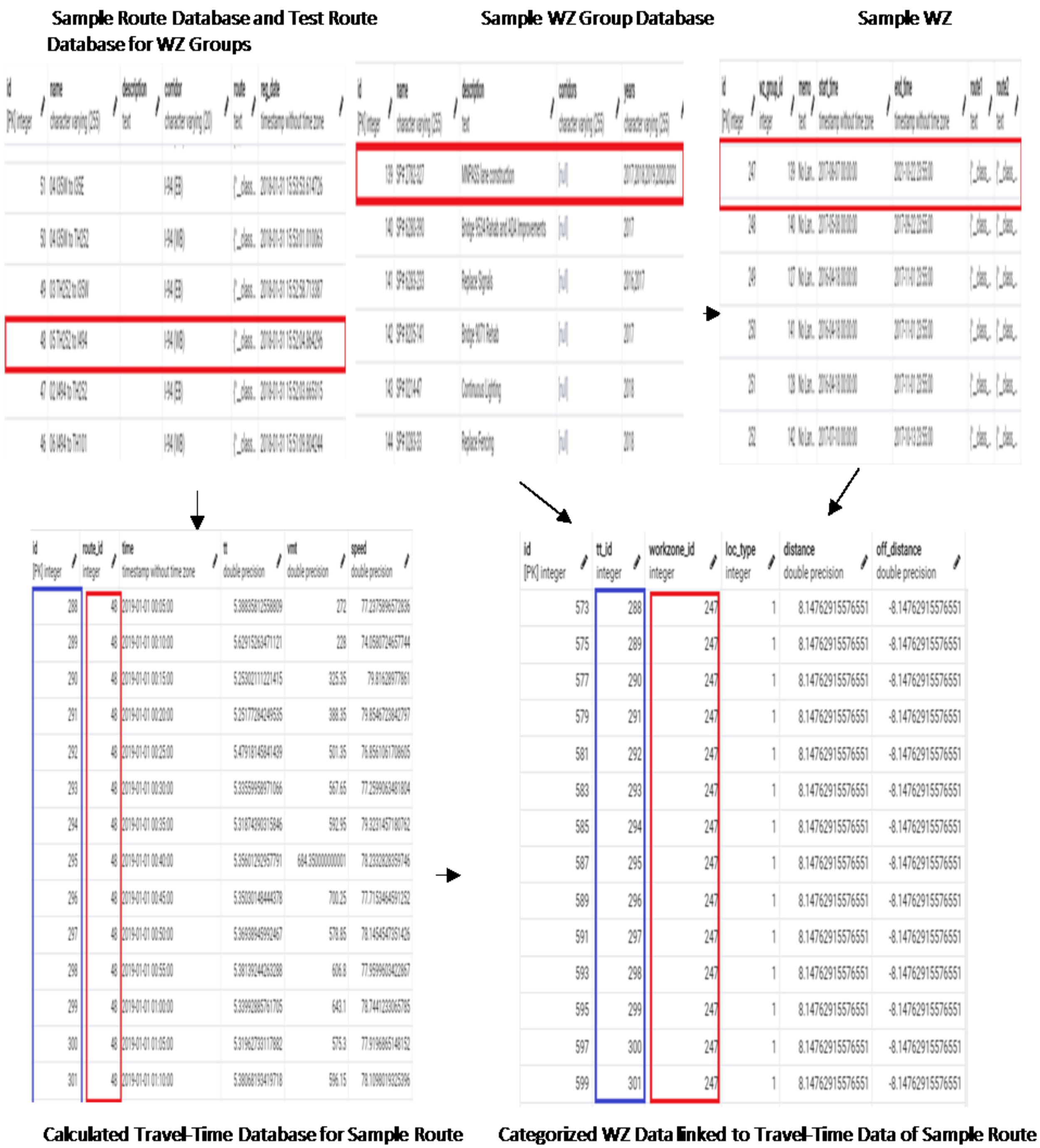


**Figure 3.8: Example Categorized Work-Zone Data Linked to Travel-Time Data of Sample Route**

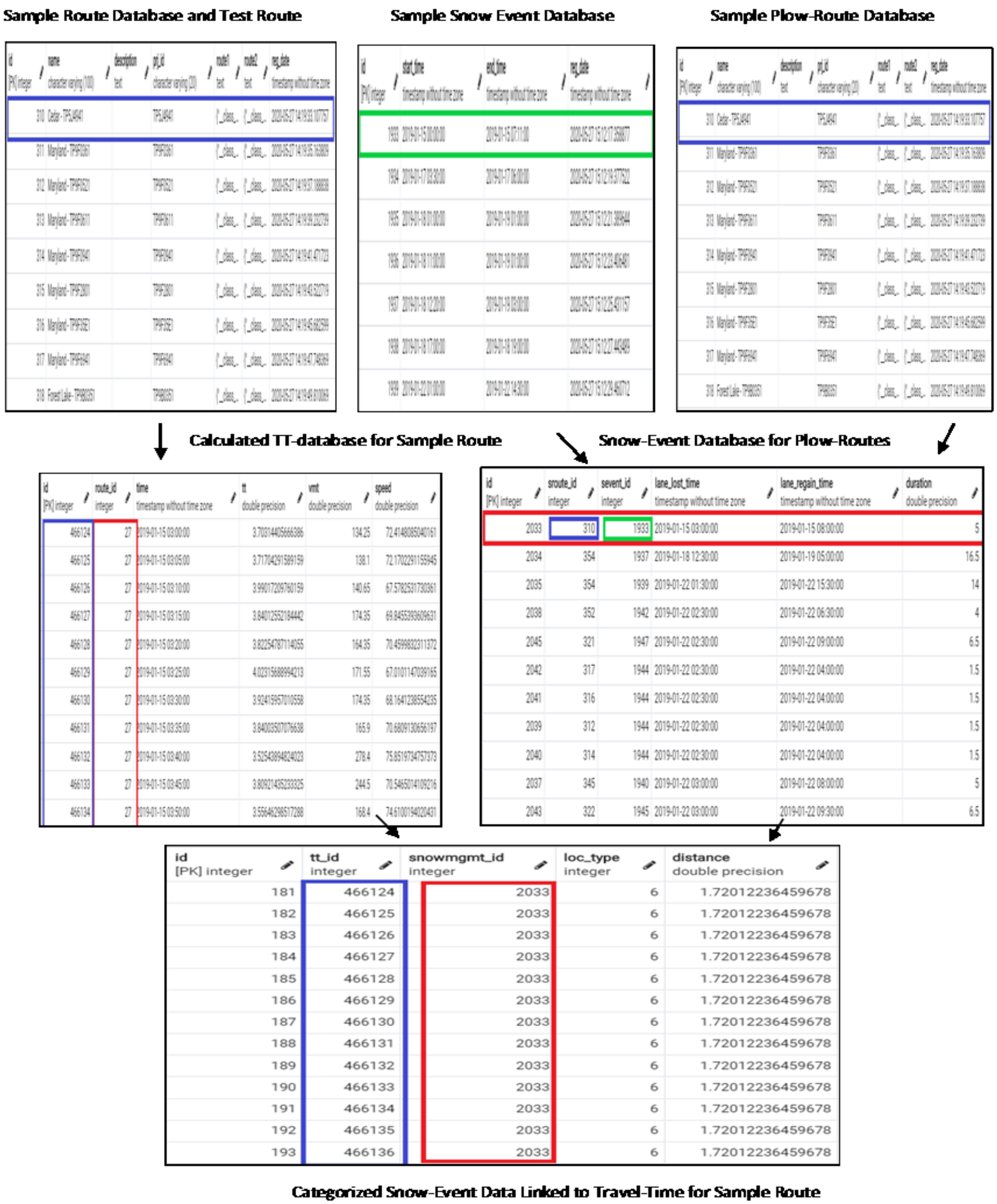


| id [PK] integer | sroute_id integer | sevent_id integer | lane_lost_time timestamp without time zone | lane_regain_time timestamp without time zone | duration double precision |
|---|---|---|---|---|---|
| 2033 | 310 | 1933 | 2019-01-15 03:00:00 | 2019-01-15 08:00:00 | 5 |
| 2034 | 354 | 1937 | 2019-01-18 12:30:00 | 2019-01-19 05:00:00 | 16.5 |
| 2035 | 354 | 1939 | 2019-01-22 01:30:00 | 2019-01-22 15:30:00 | 14 |
| 2038 | 352 | 1942 | 2019-01-22 02:30:00 | 2019-01-22 06:30:00 | 4 |
| 2045 | 321 | 1947 | 2019-01-22 02:30:00 | 2019-01-22 09:00:00 | 6.5 |
| 2042 | 317 | 1944 | 2019-01-22 02:30:00 | 2019-01-22 04:00:00 | 1.5 |
| 2041 | 316 | 1944 | 2019-01-22 02:30:00 | 2019-01-22 04:00:00 | 1.5 |
| 2039 | 312 | 1944 | 2019-01-22 02:30:00 | 2019-01-22 04:00:00 | 1.5 |
| 2040 | 314 | 1944 | 2019-01-22 02:30:00 | 2019-01-22 04:00:00 | 1.5 |
| 2037 | 345 | 1940 | 2019-01-22 03:00:00 | 2019-01-22 08:00:00 | 5 |
| 2043 | 322 | 1945 | 2019-01-22 03:00:00 | 2019-01-22 09:30:00 | 6.5 |

| id [PK] integer | tt_id integer | snowmgmt_id integer | loc_type integer | distance double precision |
|---|---|---|---|---|
| 181 | 466124 | 2033 | 6 | 1.72012236459678 |
| 182 | 466125 | 2033 | 6 | 1.72012236459678 |
| 183 | 466126 | 2033 | 6 | 1.72012236459678 |
| 184 | 466127 | 2033 | 6 | 1.72012236459678 |
| 185 | 466128 | 2033 | 6 | 1.72012236459678 |
| 186 | 466129 | 2033 | 6 | 1.72012236459678 |
| 187 | 466130 | 2033 | 6 | 1.72012236459678 |
| 188 | 466131 | 2033 | 6 | 1.72012236459678 |
| 189 | 466132 | 2033 | 6 | 1.72012236459678 |
| 190 | 466133 | 2033 | 6 | 1.72012236459678 |
| 191 | 466134 | 2033 | 6 | 1.72012236459678 |
| 192 | 466135 | 2033 | 6 | 1.72012236459678 |
| 193 | 466136 | 2033 | 6 | 1.72012236459678 |

**Figure 3.9: Example Categorized Snow-Event Data Linked to Travel-Time Data of Sample Route**

# CHAPTER 4: TRAVEL-TIME RELIABILITY TRENDS AND BOTTLENECK PRIORITIZATION FOR FREEWAY CORRIDORS

## 4.1 INTRODUCTION

In this chapter, the travel-time reliability trends of a total of 23 corridors were analyzed and the bottleneck sections within each directional route were identified. First, using the database populated in the previous chapter, a set of the reliability measures of the individual corridors in the metro freeway network during morning or afternoon peak periods were estimated under different operating conditions from 1/1/2016 until 9/30/2020. Figure 4.1 shows a total of 23 freeway corridors, whose boundaries have been determined in cooperation with the Regional Transportation Management Center, MnDOT. For each corridor, two directional routes, one for morning and the other for afternoon peak-period, were identified depending on the peak-period traffic patterns of each corridor, while the I-94 corridor between St. Paul and Minneapolis have four routes, i.e., two directional routes for both morning and afternoon peak periods. Therefore, there are a total of 48 directional routes, 24 routes for morning and 24 for afternoon peak periods. Table 4.1 includes the IDs of start and end stations of each directional route of each corridor.

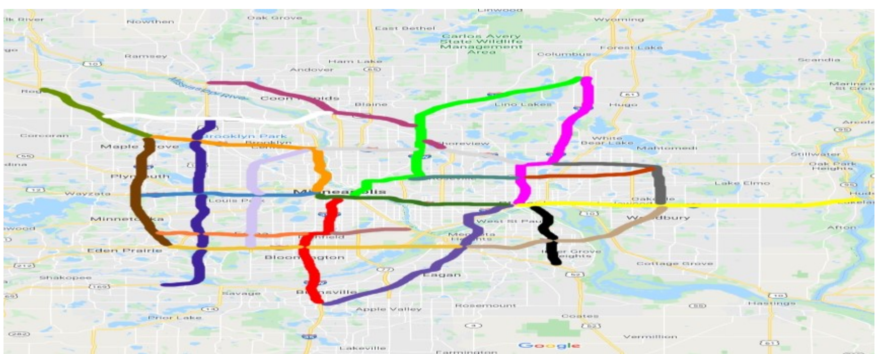


**Figure 4.1: Individual Corridors for Reliability Estimation**

### Table 4.1: Start/End Stations of Each Corridor Directional Route

| Corridor | Description | Start | End |
|---|---|---|---|
| I35W (NB) | South Split to Minneapolis Downtown | S911 | S566 |
| I35W (NB) | Minneapolis Downtown to North Split | S566 | S1557 |
| I35W (SB) | North Split to Minneapolis Downtown | S1567 | S585 |
| I35W (SB) | Minneapolis Downtown to South Split | S585 | S915 |
| I35E (NB) | South Split to Saint Paul Downtown | S870 | S619 |
| I35E (NB) | Saint Paul Downtown to North Split | S619 | S1504 |
| I35E (SB) | North Split to Saint Paul Downtown | S1531 | S644 |
| I35E (SB) | Saint Paul Downtown to South Split | S644 | S905 |
| I394 (EB) | I494 to Minneapolis Downtown | S269 | S291 |
| I394 (WB) | Minneapolis Downtown to I494 | S262 | S345 |
| I94 (EB) | TH101 to I494 | S1115 | S211 |
| I94 (EB) | I494 to Minneapolis Downtown | S211 | S110 |
| I94 (EB) | Minneapolis Downtown to Saint Paul Downtown | S110 | S499 |
| I94 (EB) | Saint Paul Downtown to Wisconsin Border | S499 | S1358 |
| I94 (WB) | Wisconsin Border to Saint Paul Downtown | S1359 | S500 |
| I94 (WB) | Saint Paul Downtown to Minneapolis Downtown | S500 | S1943 |
| I94 (WB) | Minneapolis Downtown to I494 | S1943 | S213 |
| I94 (WB) | I494 to TH101 | S213 | S1112 |
| TH52 (NB) | TH55 to Saint Paul Downtown | S1166 | S1178 |
| TH52 (SB) | Saint Paul Downtown to TH55 | S1151 | S1163 |
| I494 (EB) | I694 to TH212 | S209 | S473 |
| I494 (EB) | TH212 to I35E | S474 | S863 |
| I494 (EB) | I35E to I94 | S863 | S1026 |
| I494 (WB) | I94 to I35E | S1029 | S864 |
| I494 (WB) | I35E to TH212 | S864 | S484 |
| I494 (WB) | TH212 to I694 | S484 | S210 |
| I694 (EB) | TH252 to I35E | S145 | S1452 |
| I694 (EB) | I35E to I94 | S1452 | S1028 |
| I694 (WB) | I94 to I35E | S1027 | S1459 |
| I694 (WB) | I494 to TH100 | S1459 | S144 |
| US169 (NB) | Canterbury Rd to TH610 | S1617 | S1966 |
| US169 (SB) | TH610 to Canterbury Rd | S1795 | S1626 |
| TH100 (NB) | I494 to I94 | S375 | S1614 |
| TH100 (SB) | I94 to I494 | S1100 | S421 |
| TH10 (EB) | US169 to I694 | S940 | S1825 |
| TH10 (WB) | I694 to US169 | S1949 | S992 |
| TH610 (EB) | I94 to TH10 | S1954 | S966 |
| TH610 (WB) | TH10 to I94 | S995 | S1961 |
| TH36 (EB) | TH280 to I35E | S587 | S600 |
| TH36 (EB) | I35E to I694 | S600 | S1426 |
| TH36 (WB) | I694 to I35E | S1425 | S608 |
| TH36 (WB) | I35E to I35W | S608 | S618 |
| TH62 (EB) | I494 to I35W | S301 | S329 |
| TH62 (EB) | I35W to Hiawatha | S329 | S1135 |
| TH62 (WB) | Hiawatha to I35W | S1136 | S133 |
| TH62 (WB) | I35W to I494 | S133 | S369 |

Next, for each directional route of the individual corridors shown in Figure 4.1, the monthly and yearly travel-time reliability measures were estimated under different operating conditions using TeTRES and their trends were analyzed. It needs to be noted that, in this study, only regular non-holiday weekdays, i.e., Tuesdays, Wednesdays, Thursdays, were included for estimating travel-time reliability measures for each route. In addition, a set of the traffic-flow performance measures were also estimated and presented for each route. The specific measures and operating conditions used in this analysis are as follows:

- **Travel-time Reliability Measures:**
  - Buffer Index ($95^{th}$ %ile) = ($95^{th}$ %ile Travel Time – Average Travel Time)/(Average Travel Time)
  - Planning Index ($95^{th}$ %ile) = $95^{th}$ %ile Travel Time / Free-Flow Travel Time
  - Travel Rate ($95^{th}$ %ile), minutes/mile = $95^{th}$ %ile Travel Time / Route Length
- **Operating Conditions**
  - Weather: All, Dry, Rain, Snow
  - Incident: All, No-Incident (N), Property Damage Only (PD), Severe/Fatal (INJ,FA)
  - Work Zone: All, No-WZ (N), Light Impact-WZ (L), Medium-Heavy Effect WZ (M,H)
- **Peak Periods**: Morning: 6:00 – 9:00 a.m. Afternoon: 3:30 – 6:30 p.m.
- **Traffic-Flow Measures**: VMT (Vehicle-Miles Traveled), VHT (Vehicle-Hours Traveled), DVH (Delayed Vehicle-Hours)

Further, to assess the overall reliability condition of a route, in this study, two travel-time reliability measures, i.e., buffer index (BI) and travel rate (TR) , were combined in a BI-TR space as shown in Figure 4.2 and a vulnerability of a given route is quantified as the Euclidian distance between the origin and the data point of each route, i.e.,

$$\textit{Vulnerability Index (VI) of Route } i = sqrt\ [(95^{th} \textit{ percentile BI})_i^2 + (95^{th} \textit{ percentile TR})_i^2]$$

In this study, the above VI is estimated with the yearly measures of both BI and TR of each directional route under all conditions and used for the comparative analysis with other routes. Figure 4.2 also shows 5 levels of vulnerability in terms of BI and TR values of each route. Those vulnerability levels are used to capture the network-wide variation trends of the route vulnerability from 2016 to 2020. Finally, the potential bottleneck sections within each directional route were identified and the VI of each section was estimated with the 2019 data. The VIs of those potential bottleneck sections were then compared and the most vulnerable bottleneck section was determined for each route. The rest of this report summarizes the yearly variation trends of the travel-time reliability at each directional route and the identification of the most vulnerable bottleneck section in each directional route. The detailed estimation and analysis results of individual routes' travel-time reliability trends under different operating conditions are included in the Appendix.

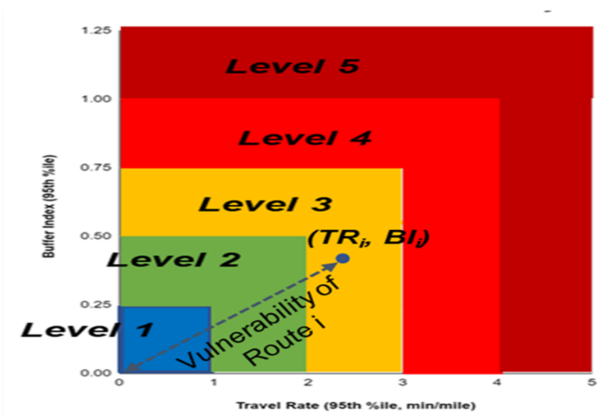


| Level | BI (95th %-ile) | TR (95th %-ile) |
|---|---|---|
| 1 | BI < 0.25 | < 1.0 |
| 2 | 0.25 ≤ BI < 0.5 | 1.0 ≤ TR < 2.0 |
| 3 | 0.5 ≤ BI < 0.75 | 2.0 ≤ TR < 3.0 |
| 4 | 0.75 ≤ BI < 1.0 | 3.0 ≤ TR < 4.0 |
| 5 | 1.0 ≤ BI | 4.0 ≤ TR |

**Figure 4.2: Vulnerability Index and 5 Levels**

## 4.2 TRAVEL-TIME RELIABILITY TRENDS OF INDIVIDUAL DIRECTIONAL ROUTES IN METRO FREEWAY NETWORK

### 4.2.1 COMPARISON OF YEARLY RELIABILITY MEASURES OF INDIVDIDUAL DIRECTIONAL ROUTES

First, the travel-time reliability measures of each directional route were estimated with yearly data under all conditions using TeTRES from 1/1/2016 until 9/30/2020. Further, all the 48 routes were categorized into either morning or afternoon-route groups depending on the peak period of each route.

Figures 4.3 – 4.7 show the 95th percentile buffer index (BI) and the 95th percentile travel rate (TR) of each route from 2016 to 2020 in the BI-TR space for each route group. The vulnerability index (VI) of each route is also calculated and shown in the bar graphs as well.

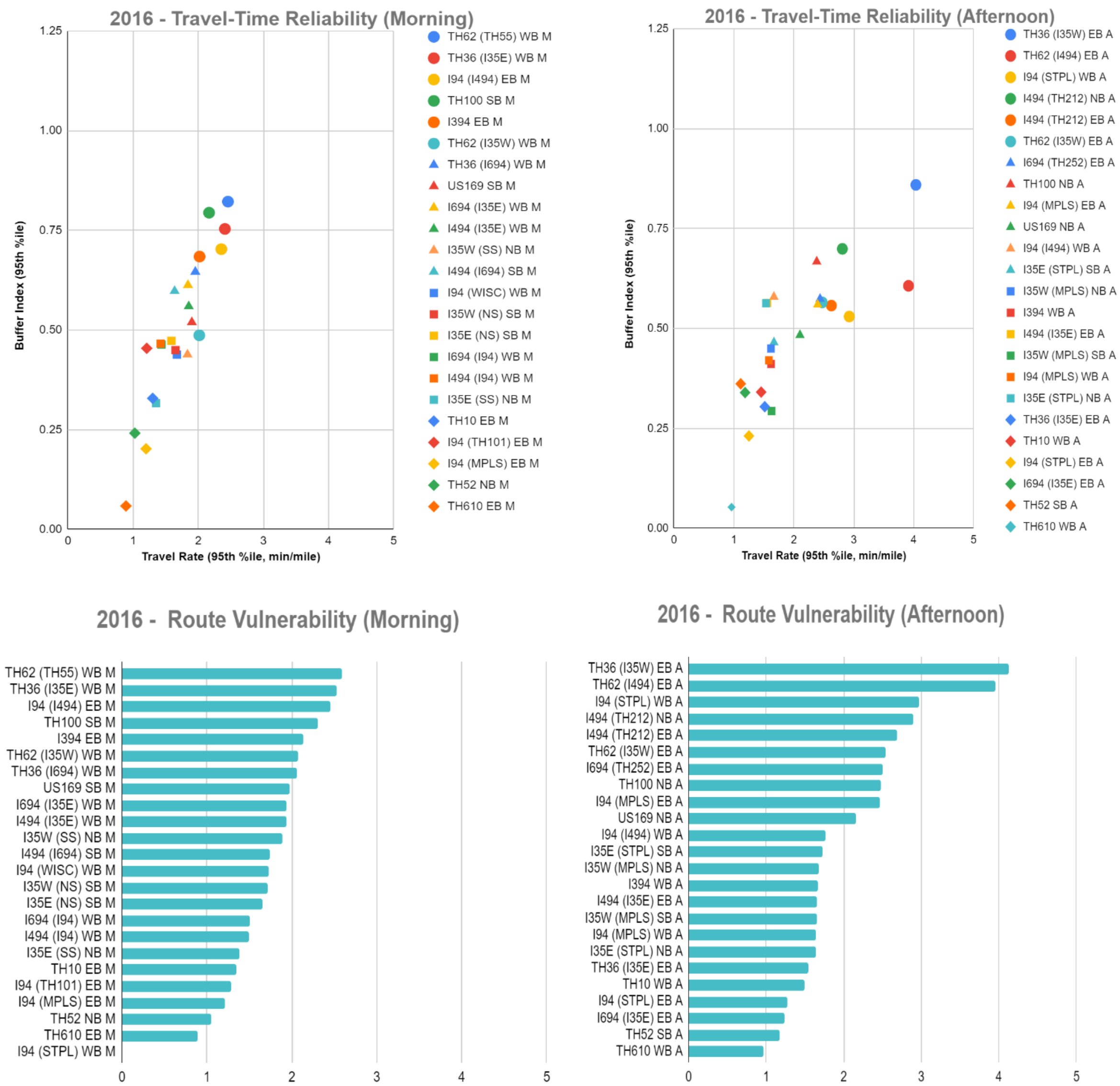


Figure 4.3: Travel-Time Reliability and Vulnerability of Morning and Afternoon Routes (2016)

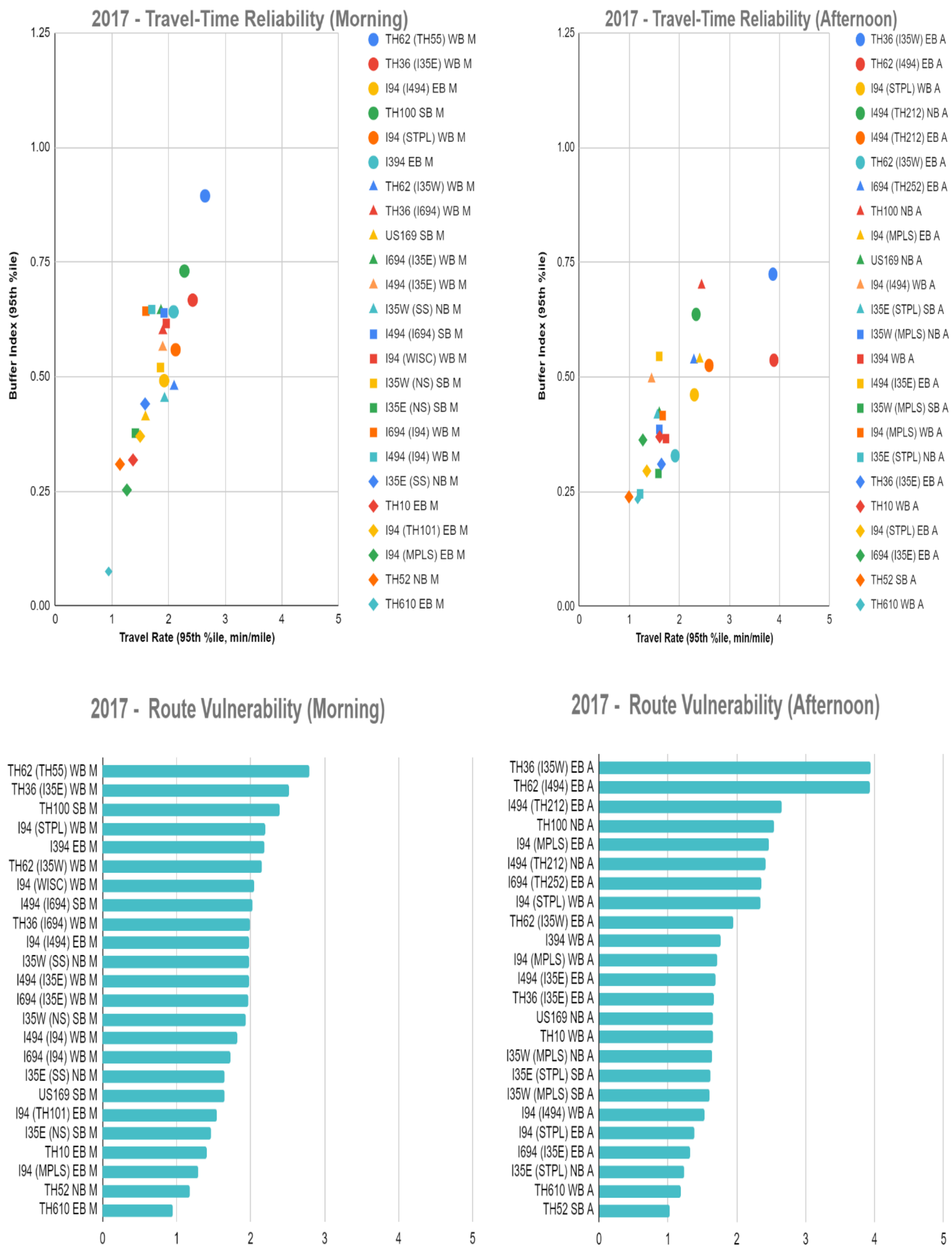


**Figure 4.4: Travel-Time Reliability and Vulnerability of Morning and Afternoon Routes (2017)**

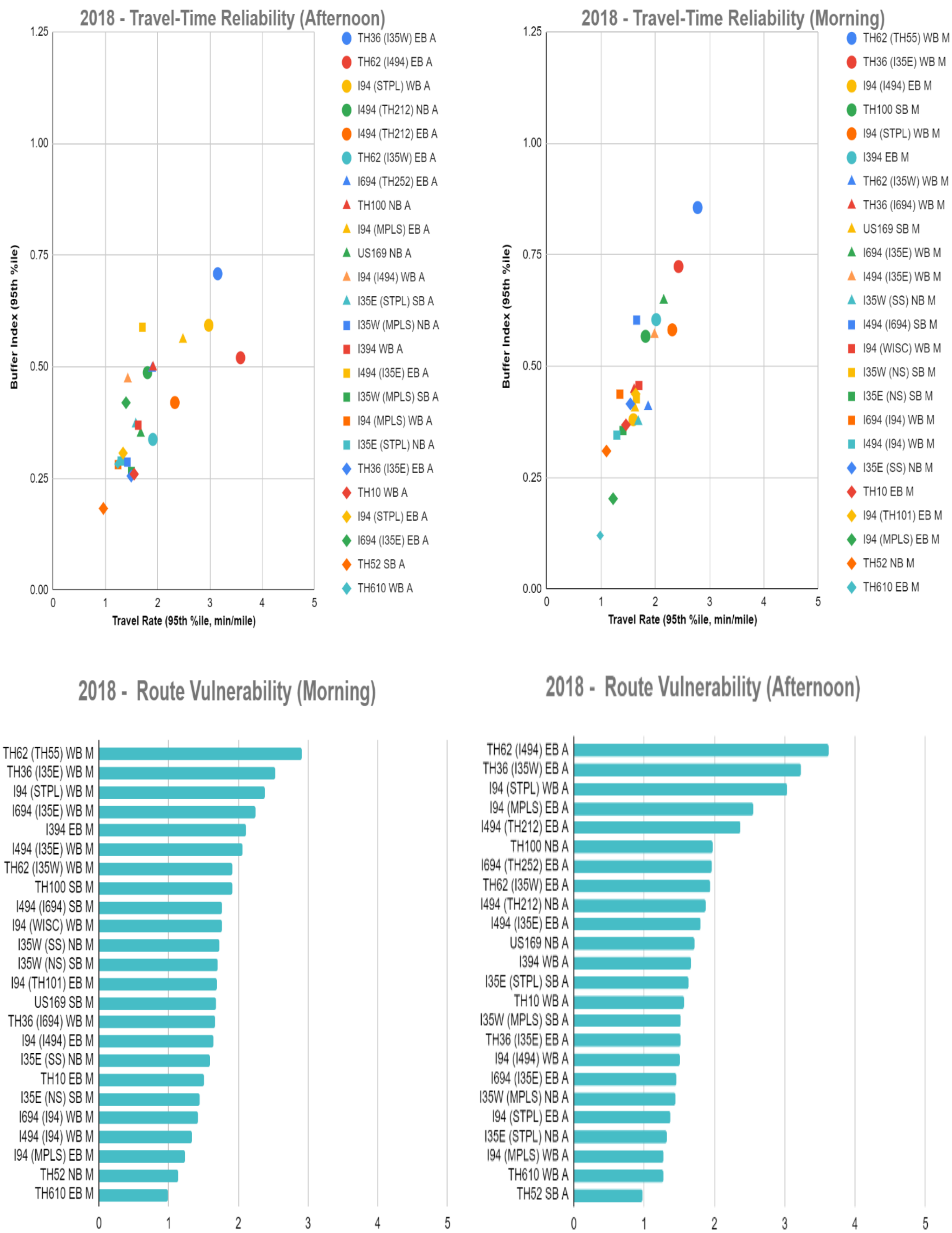


**Figure 4.5: Travel-Time Reliability and Vulnerability of Morning and Afternoon Routes (2018)**

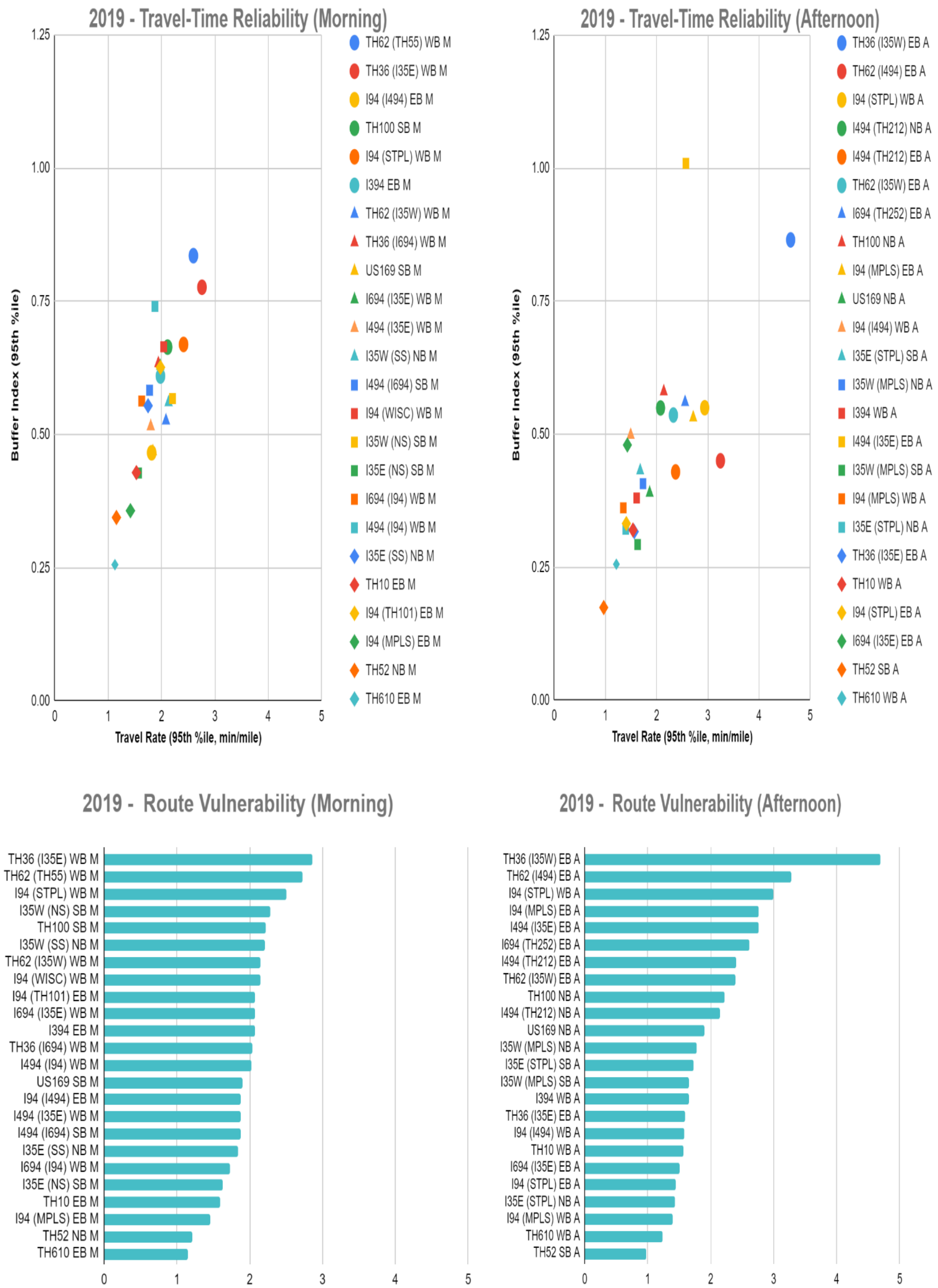


**Figure 4.6: Travel-Time Reliability and Vulnerability of Morning and Afternoon Routes (2019)**

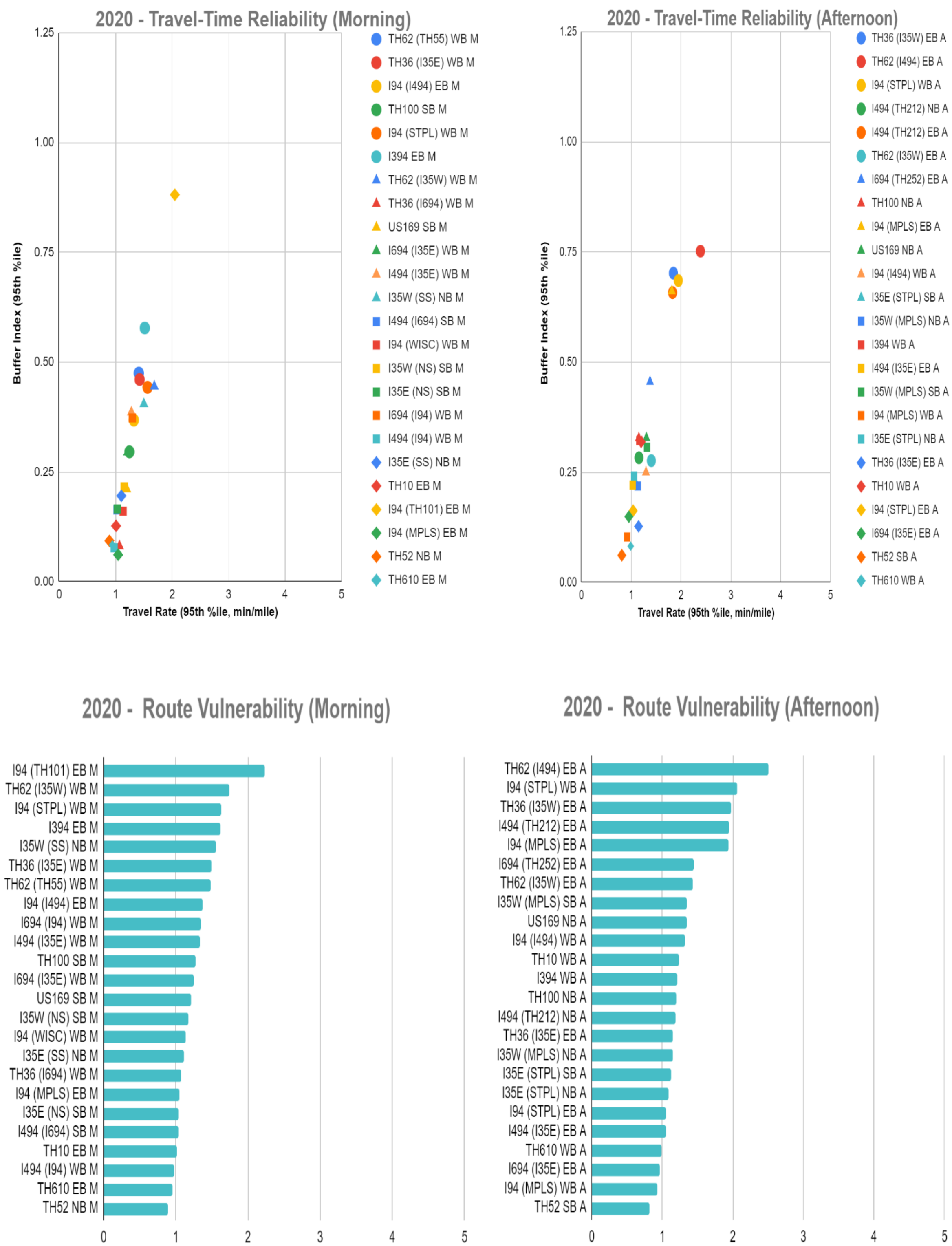


**Figure 4.7: Travel-Time Reliability and Vulnerability of Morning and Afternoon Routes (2020)**

Tables 4.2 and 4.3 include the vulnerability indices for each of the morning and afternoon routes from 2016 to 2020. As indicated in Figures 4.3-4.7 and also in Tables 4.2 and 4.3, the afternoon routes show consistently more vulnerabilities than the morning routes. Further, the afternoon routes generally exhibit higher 95$^{th}$ percentile travel times per mile than the morning routes, while the buffer index, i.e., the travel-time variability, is mostly higher with the morning routes. The yearly variations of the route vulnerability levels for all the routes including both morning and afternoon groups are shown in Figure 4.8, which indicates the overall improving trends of the route vulnerability levels from 2016 to 2018, while in 2019 the number of the routes with higher vulnerability, i.e., above level 3, significantly increased. The same trends were also noticed from the traffic-flow measures, as shown in Figure 4.9, which shows that the total Vehicle-Miles Traveled were substantially decreased in 2019, while the total Delayed-Vehicle Hours increased for both morning and afternoon routes.

### Table 4.2: Route Vulnerability Variation (Morning Routes)

| 2016 | | 2017 | | 2018 | | 2019 | | 2020 | |
|---|---|---|---|---|---|---|---|---|---|
| Route | VI | Route | VI | Route | VI | Route | VI | Route | VI |
| TH62 (TH55) WB M | 2.6 | TH62 (TH55) WB M | 2.8 | TH62 (TH55) WB M | 2.9 | TH36 (I35E) WB M | 2.9 | I94 (TH101) EB M | 2.2 |
| TH36 (I35E) WB M | 2.5 | TH36 (I35E) WB M | 2.5 | TH36 (I35E) WB M | 2.5 | TH62 (TH55) WB M | 2.7 | TH62 (I35W) WB M | 1.7 |
| I94 (I494) EB M | 2.5 | TH100 SB M | 2.4 | I94 (STPL) WB M | 2.4 | I94 (STPL) WB M | 2.5 | I94 (STPL) WB M | 1.6 |
| TH100 SB M | 2.3 | I94 (STPL) WB M | 2.2 | I694 (I35E) WB M | 2.3 | I35W (NS) SB M | 2.3 | I394 EB M | 1.6 |
| I394 EB M | 2.1 | I394 EB M | 2.2 | I394 EB M | 2.1 | TH100 SB M | 2.2 | I35W (SS) NB M | 1.6 |
| TH62 (I35W) WB M | 2.1 | TH62 (I35W) WB M | 2.2 | I494 (I35E) WB M | 2.1 | I35W (SS) NB M | 2.2 | TH36 (I35E) WB M | 1.5 |
| TH36 (I694) WB M | 2.1 | I94 (WISC) WB M | 2.1 | TH62 (I35W) WB M | 1.9 | TH62 (I35W) WB M | 2.1 | TH62 (TH55) WB M | 1.5 |
| US169 SB M | 2.0 | I494 (I694) SB M | 2.0 | TH100 SB M | 1.9 | I94 (WISC) WB M | 2.1 | I94 (I494) EB M | 1.4 |
| I694 (I35E) WB M | 1.9 | TH36 (I694) WB M | 2.0 | I494 (I694) SB M | 1.8 | I94 (TH101) EB M | 2.1 | I694 (I94) WB M | 1.3 |
| I494 (I35E) WB M | 1.9 | I94 (I494) EB M | 2.0 | I94 (WISC) WB M | 1.8 | I694 (I35E) WB M | 2.1 | I494 (I35E) WB M | 1.3 |
| I35W (SS) NB M | 1.9 | I35W (SS) NB M | 2.0 | I35W (SS) NB M | 1.7 | I394 EB M | 2.1 | TH100 SB M | 1.3 |
| I494 (I694) SB M | 1.7 | I494 (I35E) WB M | 2.0 | I35W (NS) SB M | 1.7 | TH36 (I694) WB M | 2.0 | I694 (I35E) WB M | 1.2 |
| I94 (WISC) WB M | 1.7 | I694 (I35E) WB M | 2.0 | I94 (TH101) EB M | 1.7 | I494 (I94) WB M | 2.0 | US169 SB M | 1.2 |
| I35W (NS) SB M | 1.7 | I35W (NS) SB M | 1.9 | US169 SB M | 1.7 | US169 SB M | 1.9 | I35W (NS) SB M | 1.2 |
| I35E (NS) SB M | 1.7 | I494 (I94) WB M | 1.8 | TH36 (I694) WB M | 1.7 | I94 (I494) EB M | 1.9 | I94 (WISC) WB M | 1.1 |
| I694 (I94) WB M | 1.5 | I694 (I94) WB M | 1.7 | I94 (I494) EB M | 1.6 | I494 (I35E) WB M | 1.9 | I35E (SS) NB M | 1.1 |
| I494 (I94) WB M | 1.5 | I35E (SS) NB M | 1.6 | I35E (SS) NB M | 1.6 | I494 (I694) SB M | 1.9 | TH36 (I694) WB M | 1.1 |
| I35E (SS) NB M | 1.4 | US169 SB M | 1.6 | TH10 EB M | 1.5 | I35E (SS) NB M | 1.8 | I94 (MPLS) EB M | 1.0 |
| TH10 EB M | 1.3 | I94 (TH101) EB M | 1.5 | I35E (NS) SB M | 1.4 | I694 (I94) WB M | 1.7 | I35E (NS) SB M | 1.0 |
| I94 (TH101) EB M | 1.3 | I35E (NS) SB M | 1.5 | I694 (I94) WB M | 1.4 | I35E (NS) SB M | 1.6 | I494 (I694) SB M | 1.0 |
| I94 (MPLS) EB M | 1.2 | TH10 EB M | 1.4 | I494 (I94) WB M | 1.3 | TH10 EB M | 1.6 | TH10 EB M | 1.0 |
| TH52 NB M | 1.1 | I94 (MPLS) EB M | 1.3 | I94 (MPLS) EB M | 1.2 | I94 (MPLS) EB M | 1.5 | I494 (I94) WB M | 1.0 |
| TH610 EB M | 0.9 | TH52 NB M | 1.2 | TH52 NB M | 1.1 | TH52 NB M | 1.2 | TH610 EB M | 0.9 |
| I94 (STPL) WB M | 0.0 | TH610 EB M | 0.9 | TH610 EB M | 1.0 | TH610 EB M | 1.2 | TH52 NB M | 0.9 |

## Table 4.3: Route Vulnerability Variation (Afternoon Routes)

| 2016 | | 2017 | | 2018 | | 2019 | | 2020 | |
|---|---|---|---|---|---|---|---|---|---|
| Route | VI | Route | VI | Route | VI | Route | VI | Route | VI |
| ***TH36 (I35W) EB A*** | ***4.1*** | ***TH36 (I35W) EB A*** | ***3.9*** | ***TH62 (I494) EB A*** | ***3.6*** | ***TH36 (I35W) EB A*** | ***4.7*** | ***TH62 (I494) EB A*** | ***2.5*** |
| ***TH62 (I494) EB A*** | ***4.0*** | ***TH62 (I494) EB A*** | ***3.9*** | ***TH36 (I35W) EB A*** | ***3.2*** | ***TH62 (I494) EB A*** | ***3.3*** | ***I94 (STPL) WB A*** | ***2.1*** |
| ***I94 (STPL) WB A*** | ***3.0*** | ***I494 (TH212) EB A*** | ***2.6*** | ***I94 (STPL) WB A*** | ***3.0*** | ***I94 (STPL) WB A*** | ***3.0*** | ***TH36 (I35W) EB A*** | ***2.0*** |
| ***I494 (TH212) NB A*** | ***2.9*** | ***TH100 NB A*** | ***2.5*** | ***I94 (MPLS) EB A*** | ***2.5*** | ***I94 (MPLS) EB A*** | ***2.8*** | I494 (TH212) EB A | 1.9 |
| ***I494 (TH212) EB A*** | ***2.7*** | ***I94 (MPLS) EB A*** | ***2.5*** | ***I494 (TH212) EB A*** | ***2.4*** | ***I494 (I35E) EB A*** | ***2.8*** | I94 (MPLS) EB A | 1.9 |
| ***TH62 (I35W) EB A*** | ***2.5*** | ***I494 (TH212) NB A*** | ***2.4*** | ***TH100 NB A*** | ***2.0*** | ***I694 (TH252) EB A*** | ***2.6*** | I694 (TH252) EB A | 1.5 |
| ***I694 (TH252) EB A*** | ***2.5*** | ***I694 (TH252) EB A*** | ***2.4*** | ***I694 (TH252) EB A*** | ***2.0*** | ***I494 (TH212) EB A*** | ***2.4*** | TH62 (I35W) EB A | 1.4 |
| ***TH100 NB A*** | ***2.5*** | ***I94 (STPL) WB A*** | ***2.3*** | TH62 (I35W) EB A | 1.9 | ***TH62 (I35W) EB A*** | ***2.4*** | I35W (MPLS) SB A | 1.4 |
| ***I94 (MPLS) EB A*** | ***2.5*** | TH62 (I35W) EB A | 1.9 | I494 (TH212) NB A | 1.9 | ***TH100 NB A*** | ***2.2*** | US169 NB A | 1.3 |
| ***US169 NB A*** | ***2.2*** | I394 WB A | 1.8 | I494 (I35E) EB A | 1.8 | ***I494 (TH212) NB A*** | ***2.1*** | I94 (I494) WB A | 1.3 |
| I94 (I494) WB A | 1.8 | I94 (MPLS) WB A | 1.7 | US169 NB A | 1.7 | US169 NB A | 1.9 | TH10 WB A | 1.2 |
| I35E (STPL) SB A | 1.7 | I494 (I35E) EB A | 1.7 | I394 WB A | 1.7 | I35W (MPLS) NB A | 1.8 | I394 WB A | 1.2 |
| I35W (MPLS) NB A | 1.7 | TH36 (I35E) EB A | 1.7 | I35E (STPL) SB A | 1.6 | I35E (STPL) SB A | 1.7 | TH100 NB A | 1.2 |
| I394 WB A | 1.7 | US169 NB A | 1.7 | TH10 WB A | 1.6 | I35W (MPLS) SB A | 1.7 | I494 (TH212) NB A | 1.2 |
| I494 (I35E) EB A | 1.7 | TH10 WB A | 1.6 | I35W (MPLS) SB A | 1.5 | I394 WB A | 1.7 | TH36 (I35E) EB A | 1.2 |
| I35W (MPLS) SB A | 1.7 | I35W (MPLS) NB A | 1.6 | TH36 (I35E) EB A | 1.5 | TH36 (I35E) EB A | 1.6 | I35W (MPLS) NB A | 1.2 |
| I94 (MPLS) WB A | 1.6 | I35E (STPL) SB A | 1.6 | I94 (I494) WB A | 1.5 | I94 (I494) WB A | 1.6 | I35E (STPL) SB A | 1.1 |
| I35E (STPL) NB A | 1.6 | I35W (MPLS) SB A | 1.6 | I694 (I35E) EB A | 1.5 | TH10 WB A | 1.6 | I35E (STPL) NB A | 1.1 |
| TH36 (I35E) EB A | 1.5 | I94 (I494) WB A | 1.5 | I35W (MPLS) NB A | 1.4 | I694 (I35E) EB A | 1.5 | I94 (STPL) EB A | 1.1 |
| TH10 WB A | 1.5 | I94 (STPL) EB A | 1.4 | I94 (STPL) EB A | 1.4 | I94 (STPL) EB A | 1.4 | I494 (I35E) EB A | 1.1 |
| I94 (STPL) EB A | 1.3 | I694 (I35E) EB A | 1.3 | I35E (STPL) NB A | 1.3 | I35E (STPL) NB A | 1.4 | TH610 WB A | 1.0 |
| I694 (I35E) EB A | 1.2 | I35E (STPL) NB A | 1.2 | I94 (MPLS) WB A | 1.3 | I94 (MPLS) WB A | 1.4 | I694 (I35E) EB A | 1.0 |
| TH52 SB A | 1.2 | TH610 WB A | 1.2 | TH610 WB A | 1.3 | TH610 WB A | 1.2 | I94 (MPLS) WB A | 0.9 |
| TH610 WB A | 1.0 | TH52 SB A | 1.0 | TH52 SB A | 1.0 | TH52 SB A | 1.0 | TH52 SB A | 0.81 |

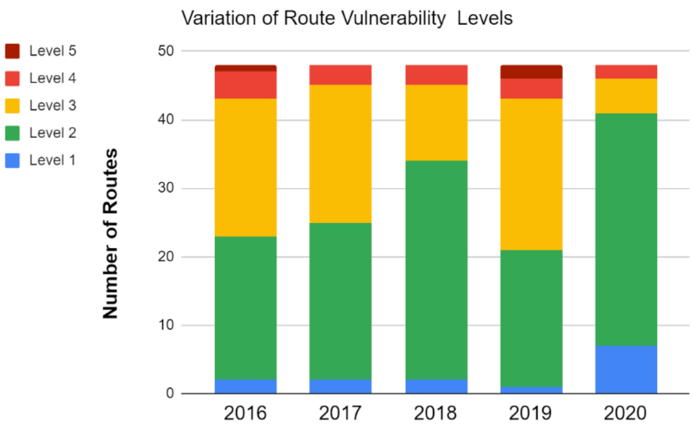


| | 2016 | 2017 | 2018 | 2019 | 2020 |
|---|---|---|---|---|---|
| Level 1 | 2 | 2 | 2 | 1 | 7 |
| Level 2 | 21 | 23 | 32 | 20 | 34 |
| Level 3 | 20 | 20 | 11 | 22 | 5 |
| Level 4 | 4 | 3 | 3 | 3 | 2 |
| Level 5 | 1 | 0 | 0 | 2 | 0 |

**Figure 4.8: Yearly Variations of Route Vulnerability**


**Figure 4.9: Variations in Traffic-Flow Measures (2016-2019)**

### 4.2.2 MONTHLY AND YEARLY RELIABILITY TRENDS OF INDIVIDUAL DIRECTIONAL ROUTES

As described in the previous section, this study also performed a detailed analysis of individual route's reliability trends under various operating conditions. This section presents a sample output from such an individual-route analysis for the 169 northbound (NB) route. The reliability estimation and analysis results of all other individual routes are included in the Appendix A.

#### 4.2.2.1 Monthly Reliability Trends of US-169 NB Corridor for Afternoon Peak Periods

**Figure 4.10: Location of 169 NB Route**

#### 4.2.2.2 Effects of Weather conditions on Travel-Time Reliability

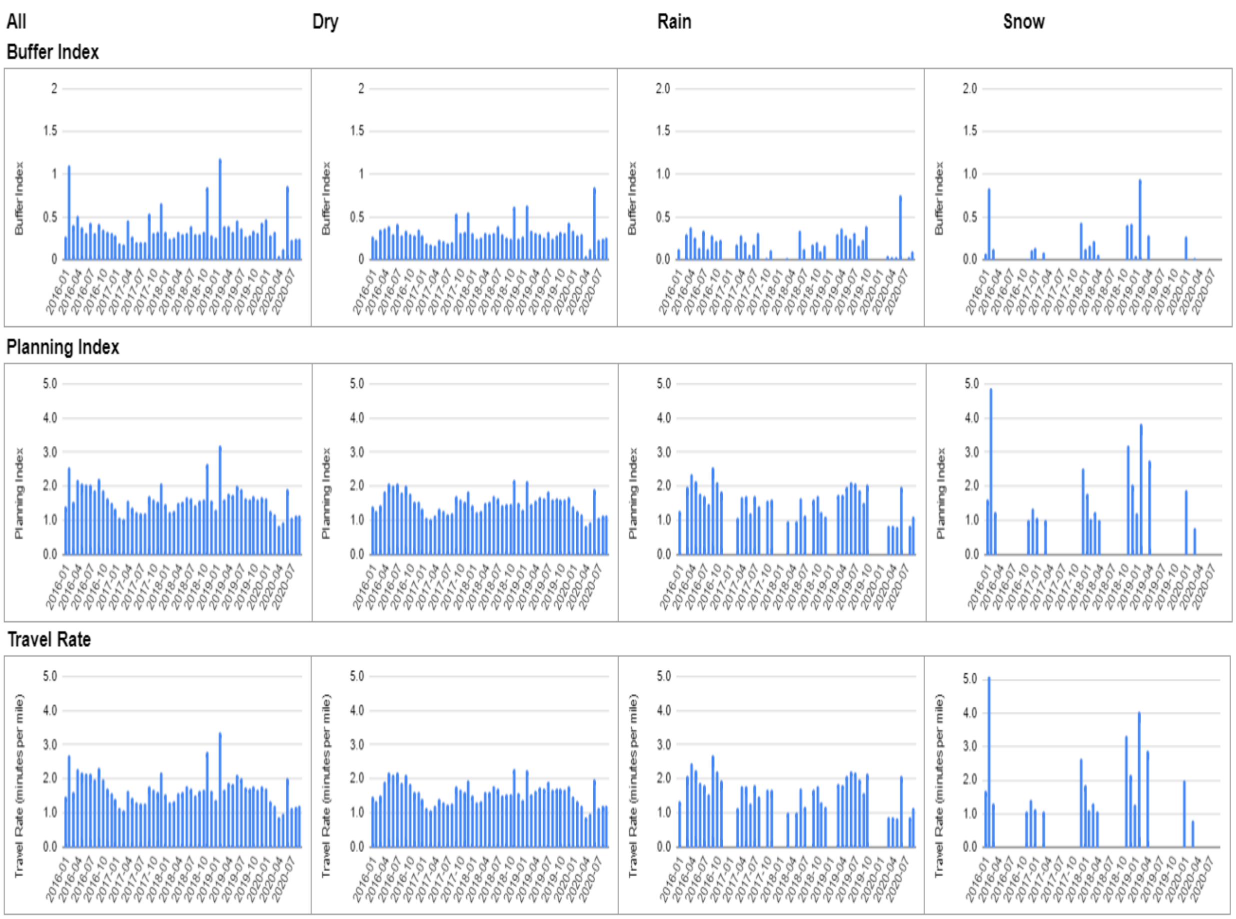


**Figure 4.11: Monthly Variations of Reliability Measures under Different Weather Conditions (169 NB)**

#### 4.2.2.3 Effects of Incidents

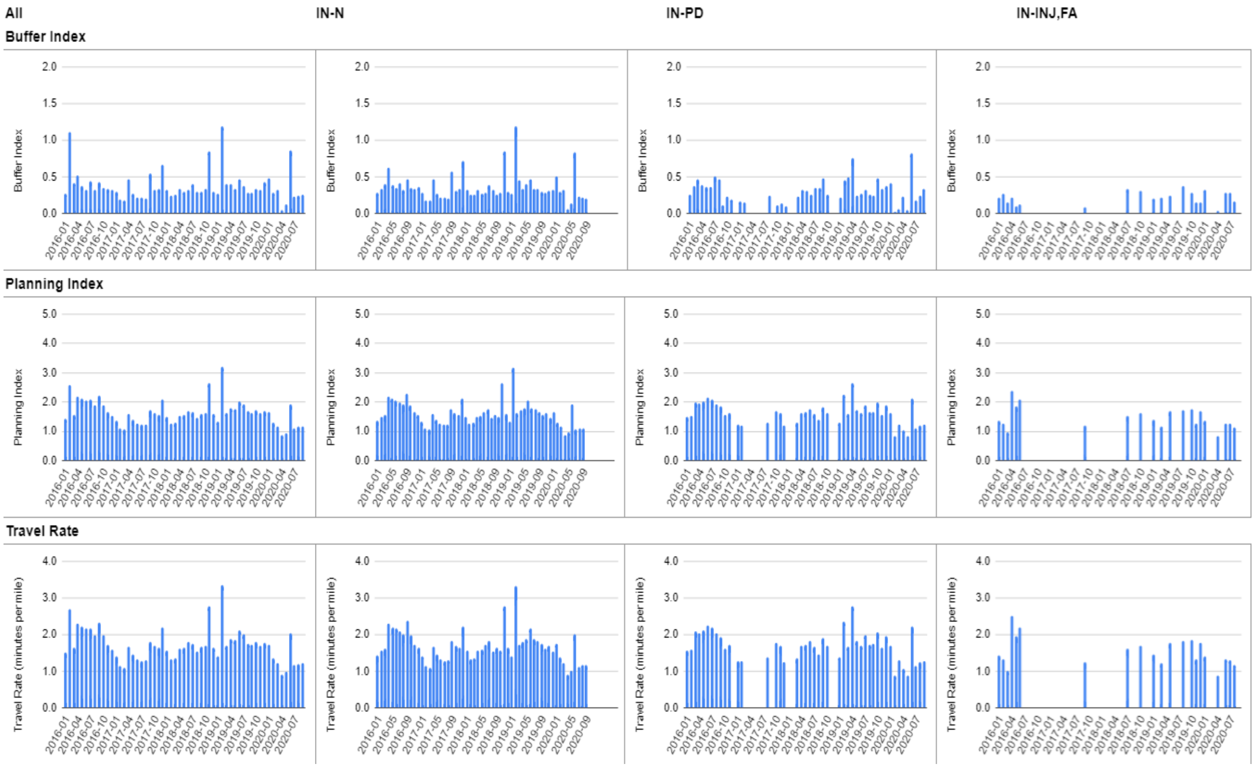


**Figure 4.12: Monthly Variations of Reliability Measures under Different Incident Conditions (169 NB)**

### 4.2.2.4 Effects of Work Zones

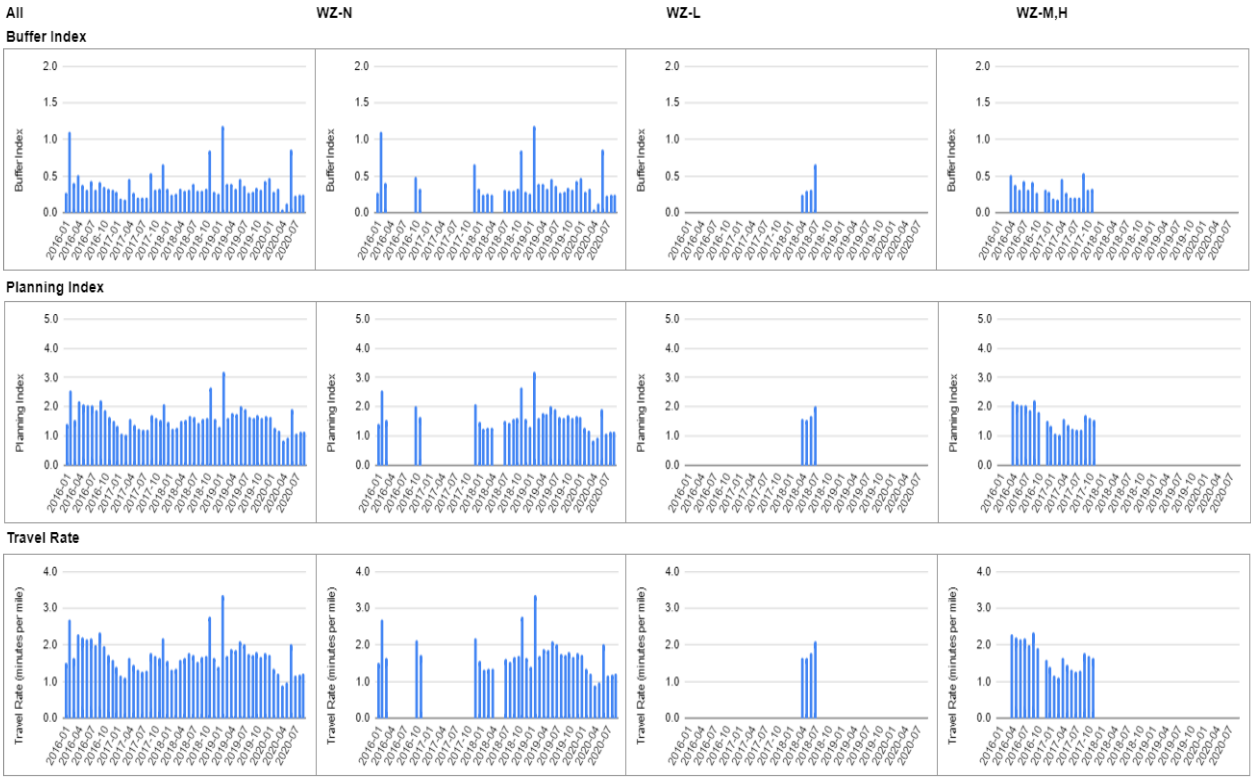


**Figure 4.13: Monthly Variations of Reliability Measures under Different Work-Zone Conditions (169 NB)**

### *4.2.2.5* Yearly Variations - *Weather Effects*


**Figure 4.14: Yearly Variations of Reliability Measures under Different Weather Conditions (169 NB)**

### 4.2.3 Incident Effects

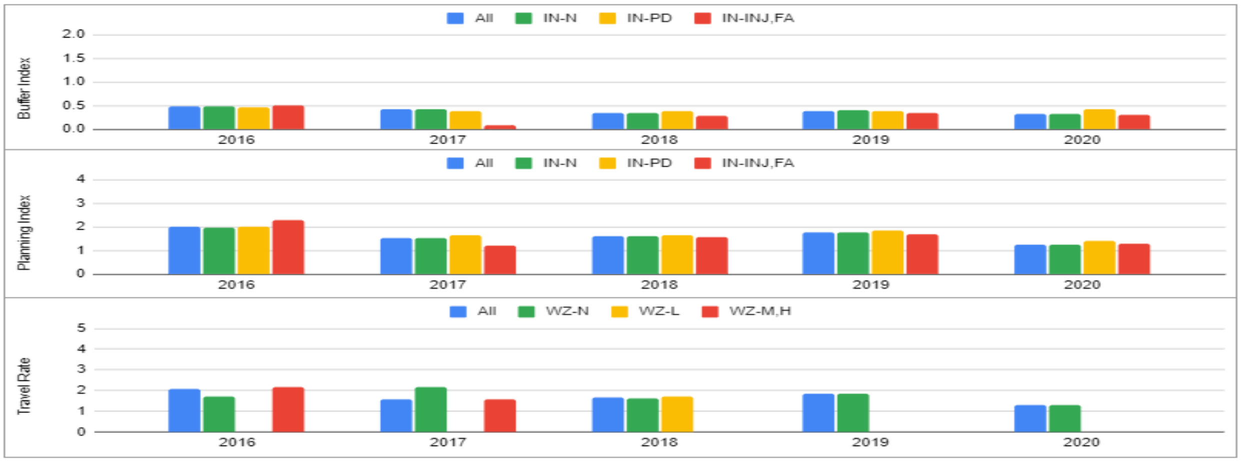


**Figure 4.15: Yearly Variations of Reliability Measures under Different Incident Conditions (169 NB)**

#### 4.2.3.1 Work-Zone Effects

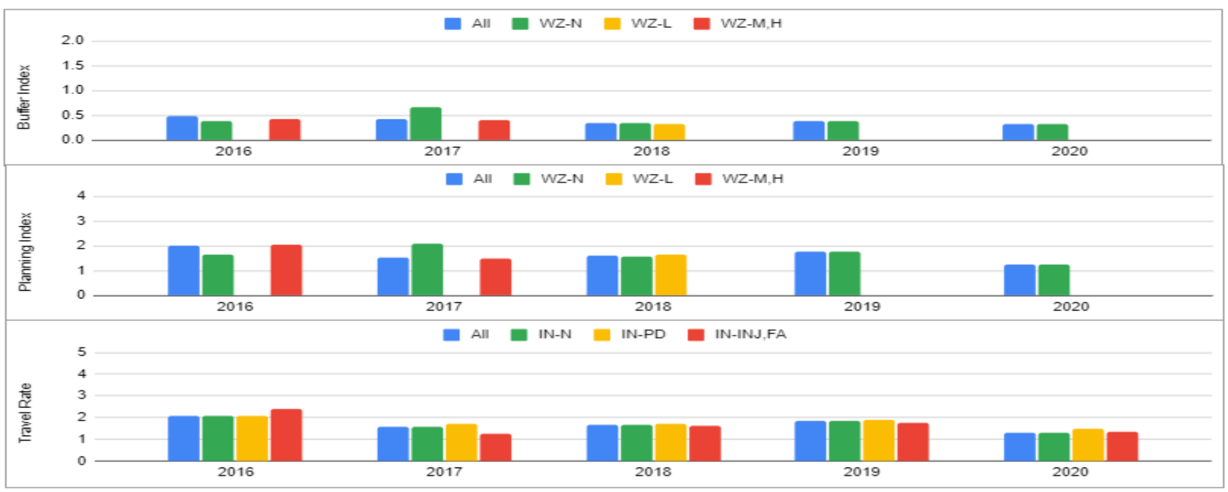


**Figure 4.16: Yearly Variations of Reliability Measures under Different Work-Zone Conditions (169 NB)**

### 4.2.3.2 Yearly Variations of Combined (Vulnerability) Index

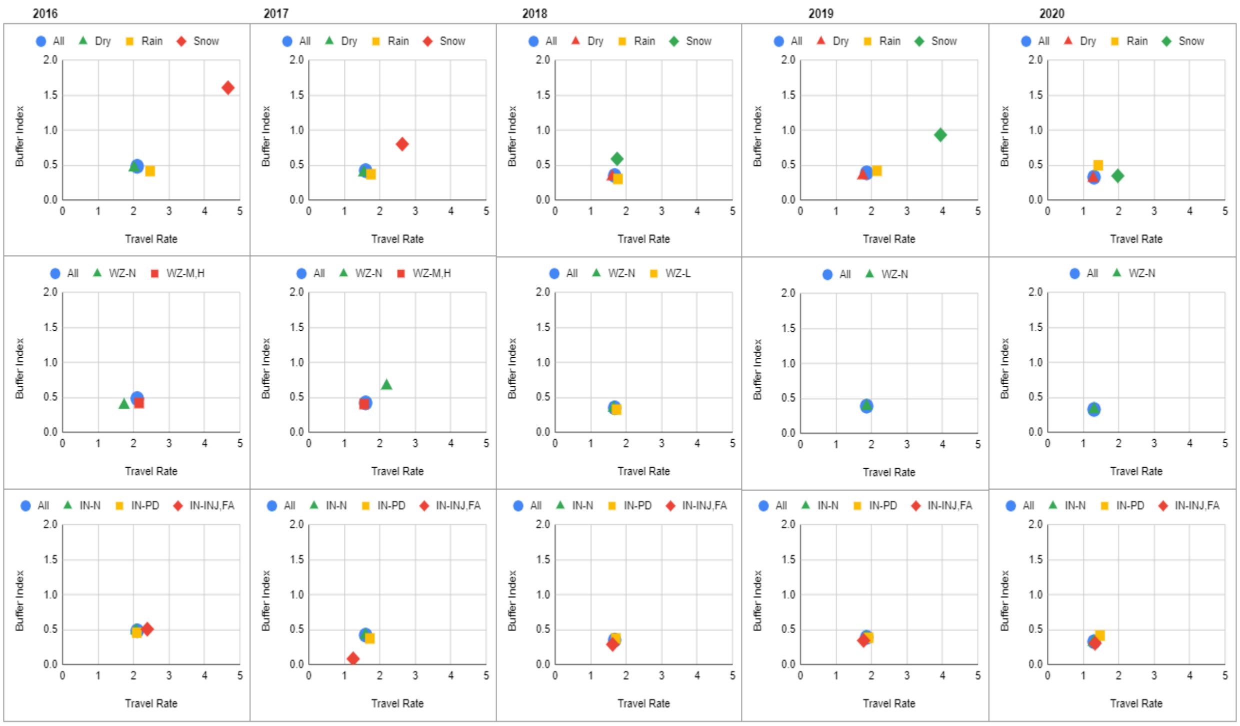


**Figure 4.17: Yearly Variations of Combine Reliability Measures (169 NB)**

### 4.2.3.3 Variations of Traffic-Flow Measures

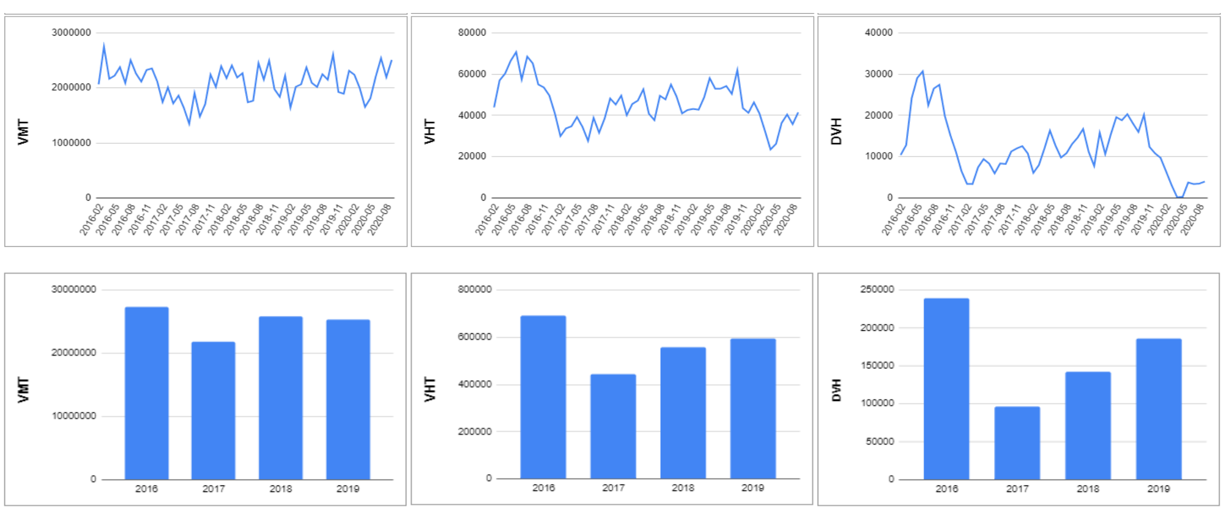


**Figure 4.18: Yearly Variations of Traffic-Flow Measures (169 NB)**

### 4.2.4 Trends Summary for 169 NB corridor

- The planning and travel-rate indices show consistently ascending trend from 2017 until the end of 2019, indicating the congestion level on this route had been rising before the pandemic, as also indicated on the variations on VMT, VHT and DVH.
- The effects of snow were significantly higher than those from rain on this route through years, while incidents had not made much difference on the reliability values.

## 4.3 BOTTLENECK PRIORITIZATION FOR INDIVIDUAL DIRECTIONAL ROUTES

In this section, the severity of the bottleneck sections within each directional route is analyzed with the travel-time reliability measures estimated from the 2019 weekday data. First, the potential bottleneck sections of the corridor routes were identified by examining the traffic speed patterns during normal weekdays and by considering the geometry of each route. Next, a set of the travel-time reliability measures were estimated for each bottleneck section with the 2019 travel-time data under all conditions and the vulnerability index of each bottleneck section was estimated with the $95^{th}$ %-ile buffer index and the $95^{th}$ percentile travel rate of each bottleneck section as described in the previous sections. Finally, the vulnerability index for each bottleneck section was compared with those of other sections in a route and the section with the highest Vulnerability Index value is determined as the most severe bottleneck section for a given route.

The rest of this section presents the vulnerability index estimation results of the potential bottleneck sections in each route along with the geographical locations of each sections. The bottleneck section with the highest vulnerability index value is highlighted as the most vulnerable section in a given route.

### 4.3.1 US169 SB Route (Morning Peak): Section with the highest vulnerability index ⇒ *I394 to TH7*

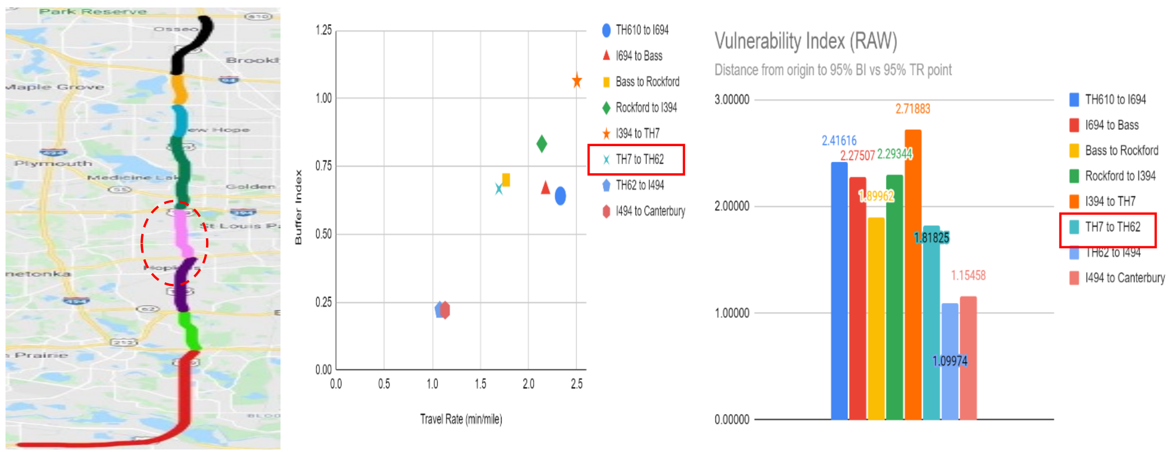


**Figure 4.19: Identification of Bottleneck Sections (169 NB)**

### 4.3.2 US169 NB Route (Afternoon Peak) ⇒ *I494 to TH62*

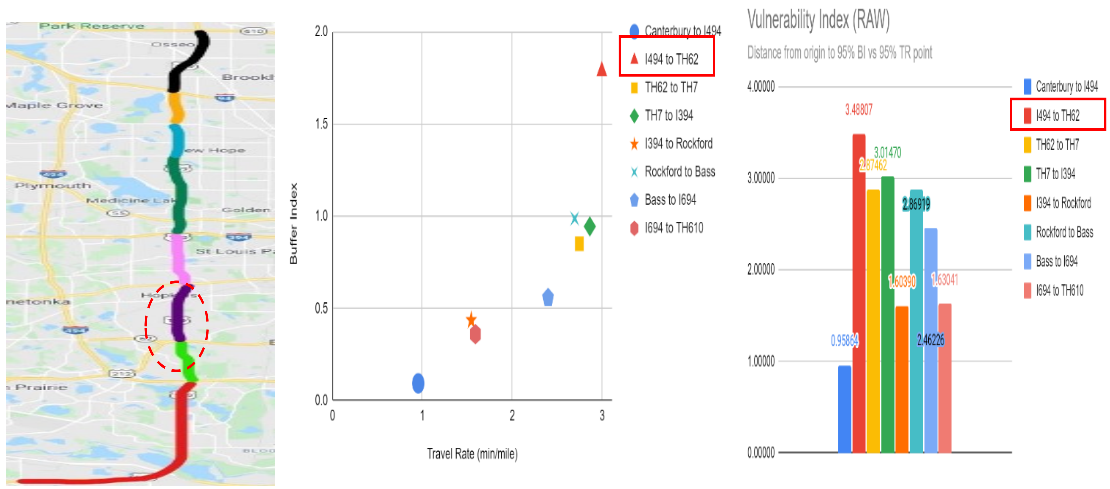


**Figure 4.20: Identification of Bottleneck Sections (169 SB)**

### 4.3.3 TH610 EB Morning ⇒ *US169 to TH47*

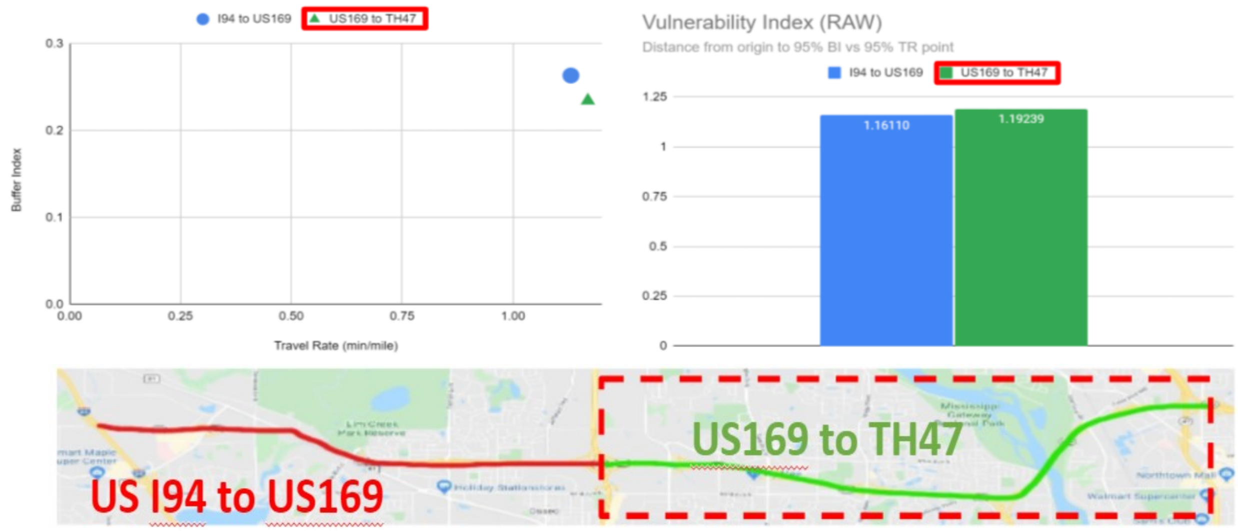


Figure 4.21: Identification of Bottleneck Sections (TH610 EB)

### 4.3.4 TH610 WB Afternoon ⇒ *US169 to I94*

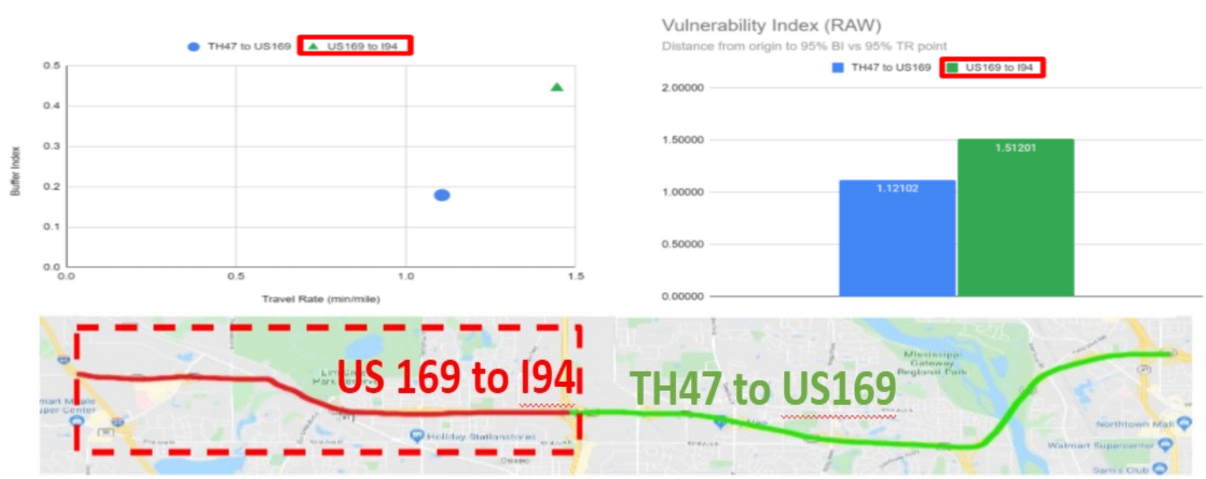


Figure 4.22: Identification of Bottleneck Sections (TH610 WB)

### 4.3.5 TH100 SB Morning ⇒ *I694 to 36th*

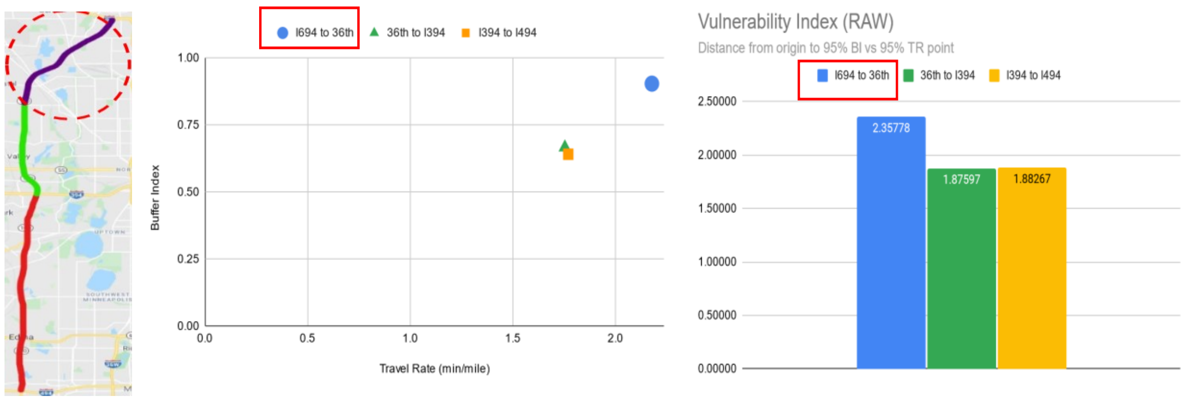


**Figure 4.23: Identification of Bottleneck Sections (TH100 SB)**

### 4.3.6 TH100 NB Afternoon ⇒ *I494 to I394*


**Figure 4.24: Identification of Bottleneck Sections (TH100 NB)**

## 4.3.7 TH62 EB Afternoon ⇒ *TH100 to US169*


Figure 4.25: Identification of Bottleneck Sections (TH62 EB)

## 4.3.8 TH62 WB Morning ⇒ *I35W to TH100*

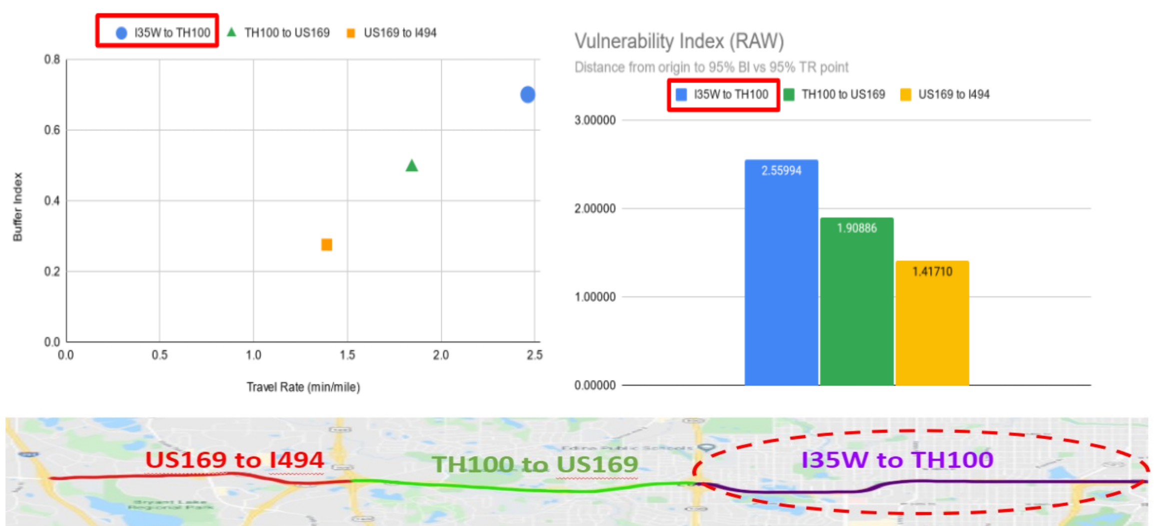


Figure 4.26: Identification of Bottleneck Sections (TH62 WB)

### 4.3.9 TH52 SB Afternoon ⇒ *I94 to I494*

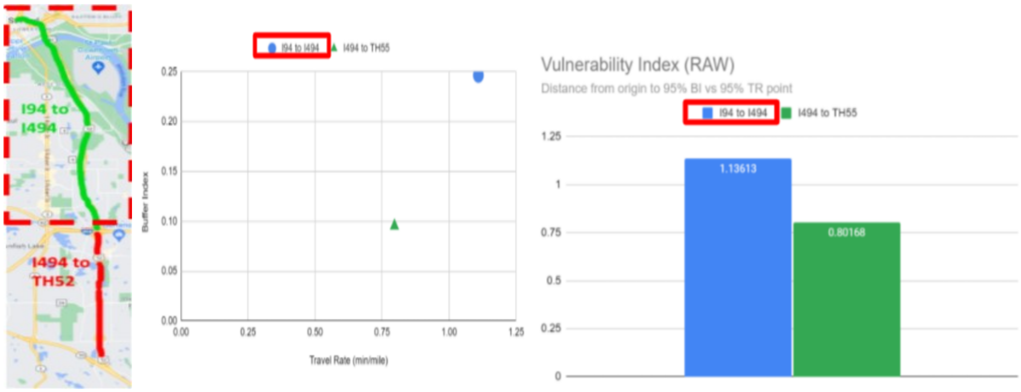


**Figure 4.27: Identification of Bottleneck Sections (TH52 SB)**

### 4.3.10 TH52 NB Morning ⇒ *I494 to I94*

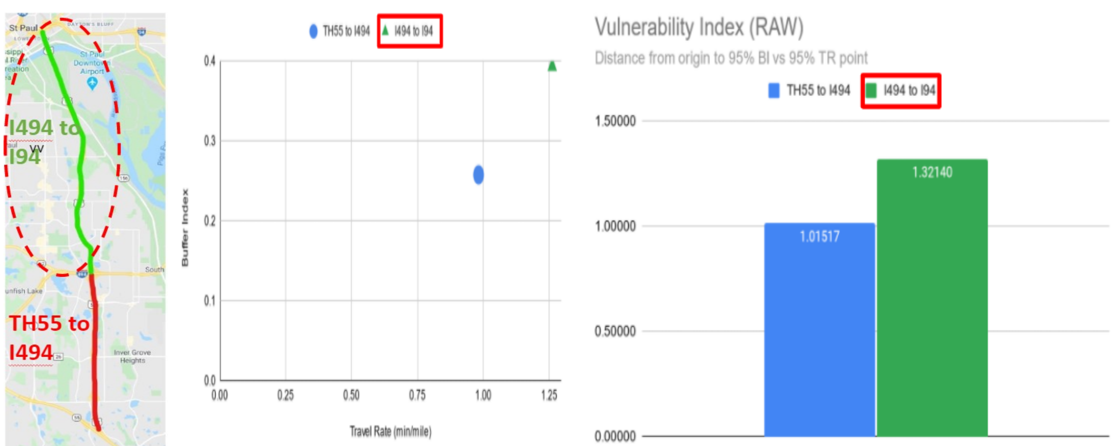


**Figure 4.28: Identification of Bottleneck Sections (TH52 NB)**

### 4.3.11 TH36 EB Afternoon ⇒ *I35W to I35E*

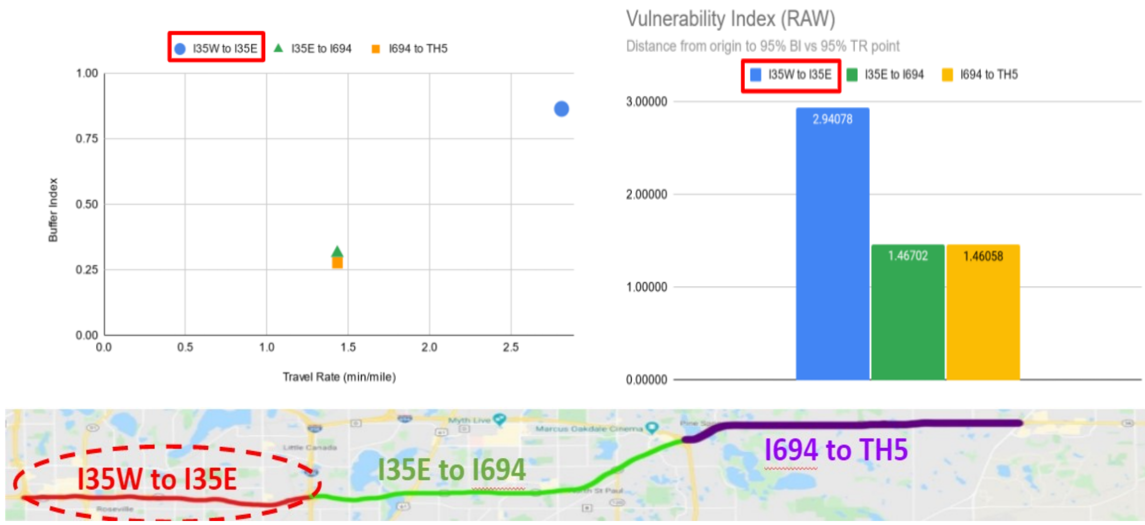


Figure 4.29: Identification of Bottleneck Sections (TH36 EB)

### 4.3.12 TH36 WB Morning ⇒ *I35E to I35W*

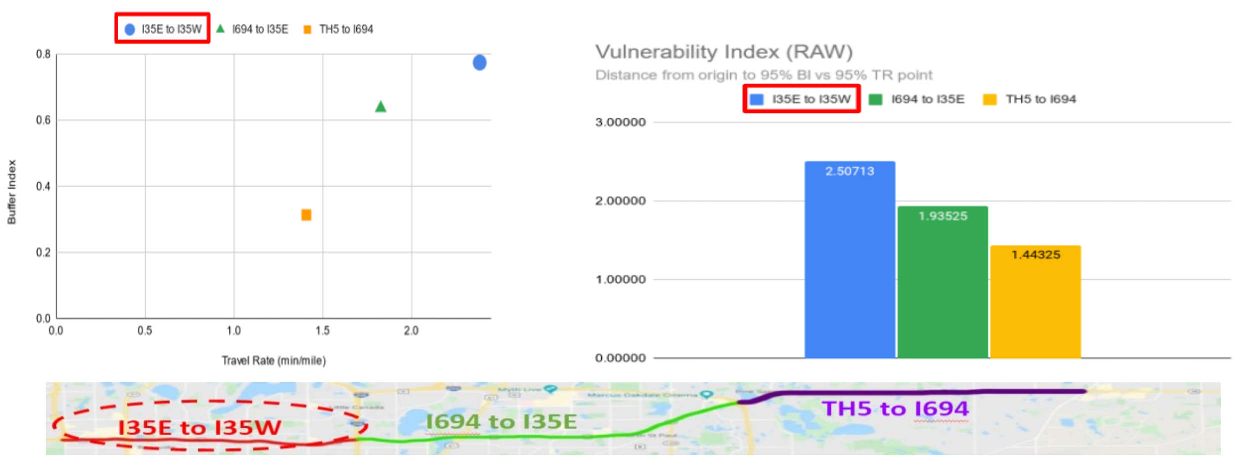


Figure 4.30: Identification of Bottleneck Sections (TH36 WB)

### 4.3.13 I-494 (TH212 to I35E) EB Afternoon ⇒ *MN100 to I35W*


Figure 4.31: Identification of Bottleneck Sections (I-494 S1 EB)

### 4.3.14 I-494 (I35E to TH212) WB Morning ⇒ *I35W to MN100*


Figure 4.32: Identification of Bottleneck Sections (I-494 S1 WB)

## 4.3.15 I-494 (I35E to I94) EB Afternoon ⇒ *I35E to MN52*

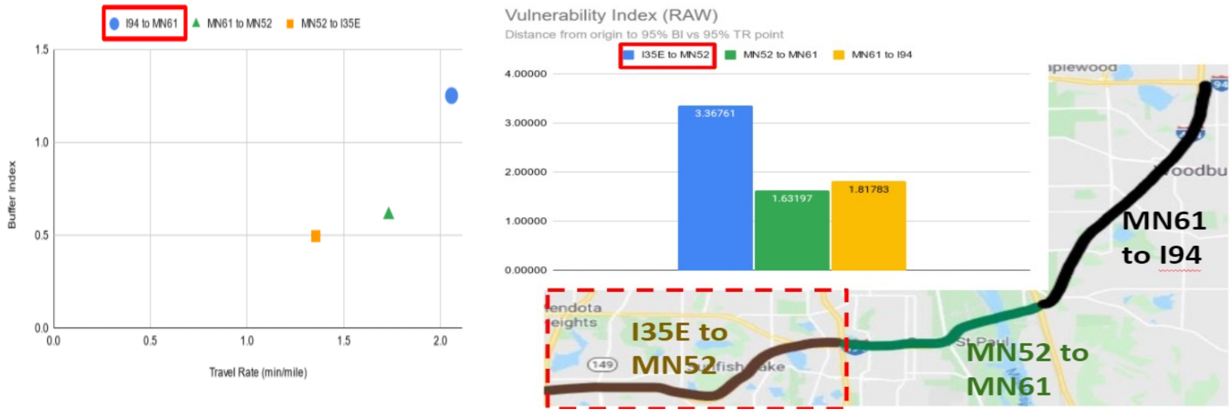


Figure 4.33: Identification of Bottleneck Sections (I-494 S2 EB)

## 4.3.16 I-494 (I94 to I35E) WB Morning ⇒ *I94 to MN61*

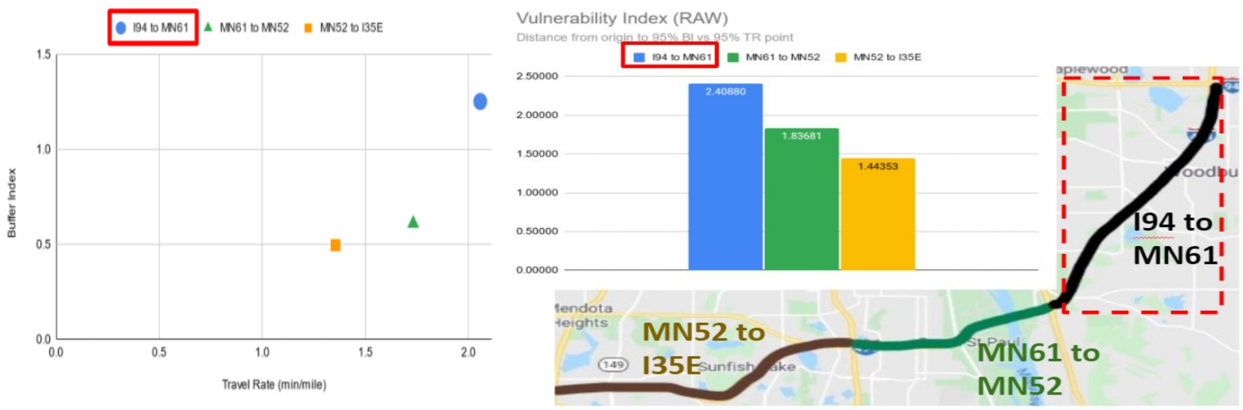


Figure 4.34: Identification of Bottleneck Sections (I-494 S2 WB)

### 4.3.17 I-494 (TH212 to I694) NB Afternoon ⇒ *US169 to I394*

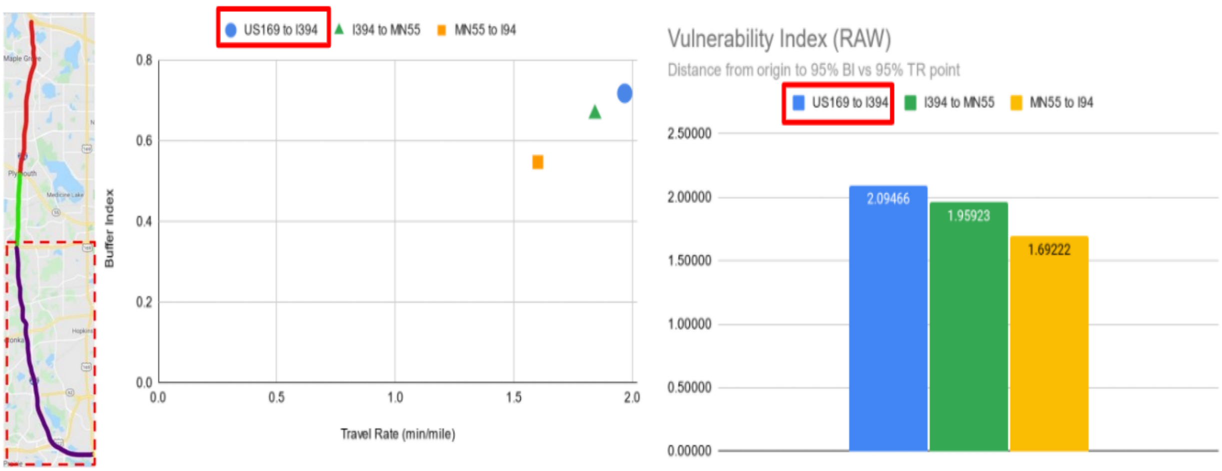


Figure 4.35: Identification of Bottleneck Sections (I-494 S3 NB)

### 4.3.18 I-494 (I694 to TH212) SB Morning ⇒ *MN55 to I394*


Figure 4.36: Identification of Bottleneck Sections (I-494 S3 SB)

### 4.3.19 I-394 EB Morning ⇒ *TH100 to MPLS*

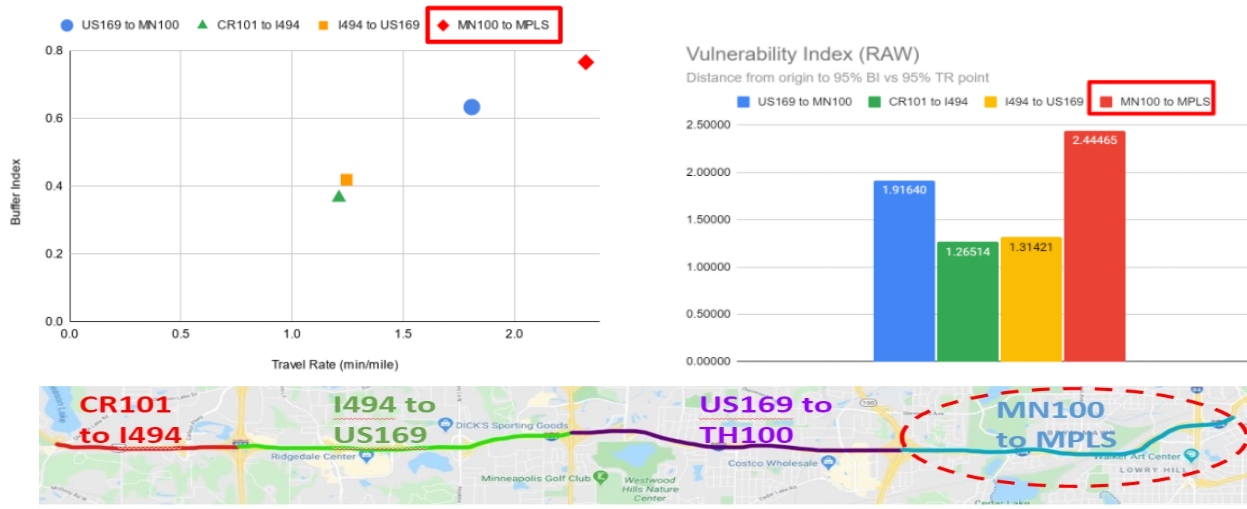


Figure 4.37: Identification of Bottleneck Sections (I-394 S1 EB)

### 4.3.20 I-394 WB Afternoon ⇒ *MPLS to MN100*

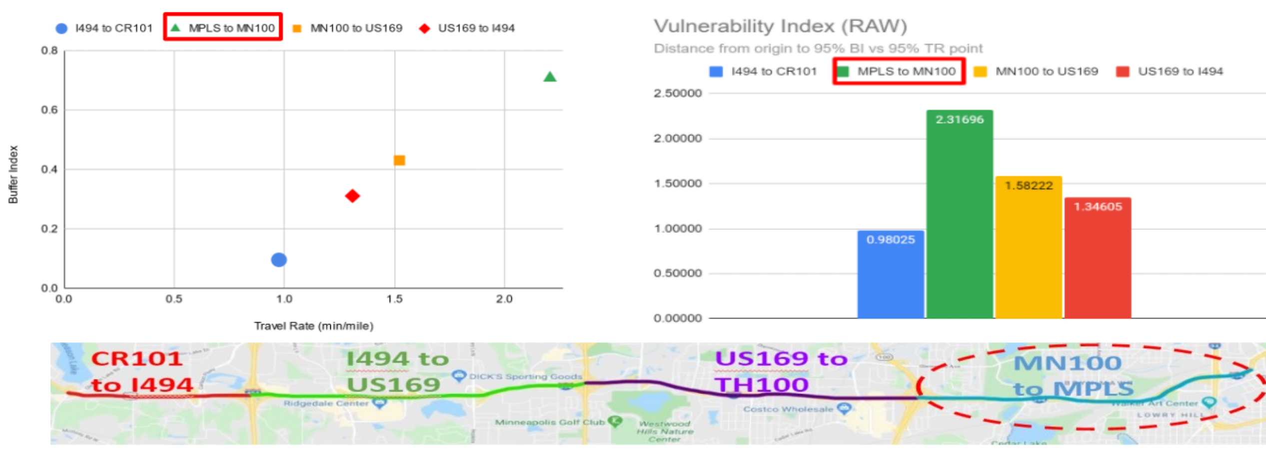


Figure 4.38: Identification of Bottleneck Sections (I-394 S1 WB)

### 4.3.21 I-94 (I494 to MPLS) EB Morning ⇒ *TH252 to I394*

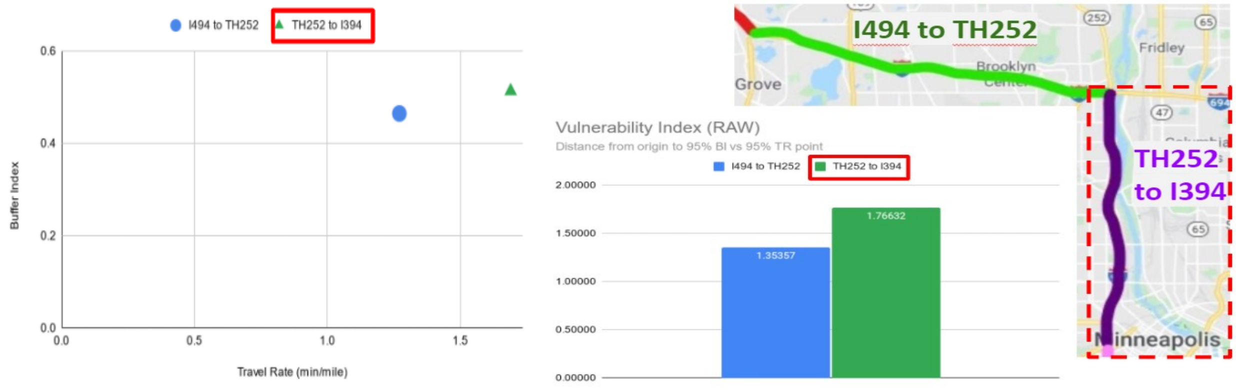


**Figure 4.39: Identification of Bottleneck Sections (I-94 S1 EB)**

### 4.3.22 I-94 (MPLS to I494) WB Afternoon ⇒ *I394 to TH252*

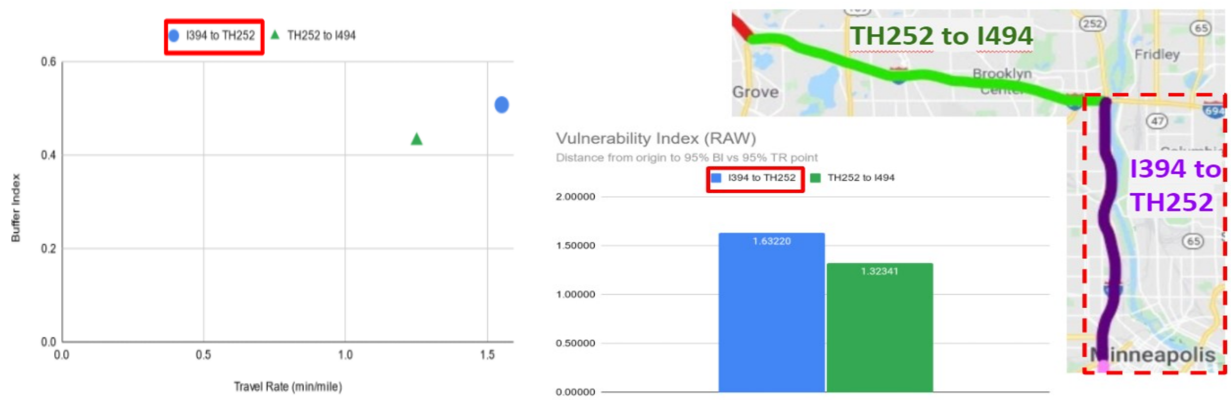


**Figure 4.40: Identification of Bottleneck Sections (I-94 S1 WB)**

### 4.3.23 I-94 (MPLS to STPL) EB Afternoon ⇒ *I394 to I35W*


Figure 4.41: Identification of Bottleneck Sections (I-94 S1 EB)

### 4.3.24 I-94 (STPL to MPLS) WB Afternoon ⇒ *I35E to I35W*

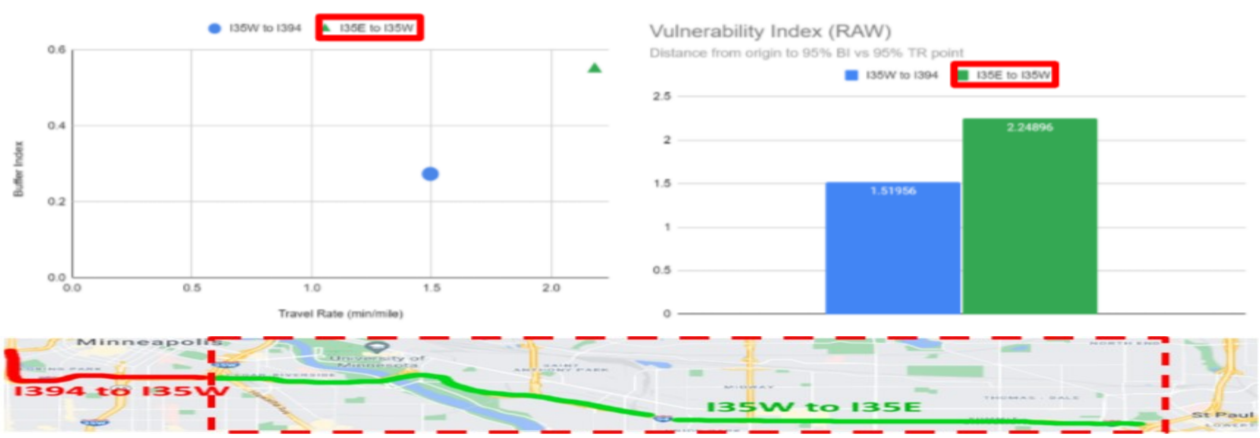


Figure 4.42: Identification of Bottleneck Sections (I-94 S2 WB)

## 4.3.25 I-94 (MPLS to STPL) EB Morning ⇒ *I394 to I35W*


Figure 4.43: Identification of Bottleneck Sections (I-94 S3 EB)

## 4.3.26 I-94 (STPL to MPLS) WB Morning ⇒ *I35E to I35W*


Figure 4.44: Identification of Bottleneck Sections (I-94 S3 WB)

## 4.3.27 I-94 (STPL to WISC) EB Afternoon ⇒ *I35E to I694*

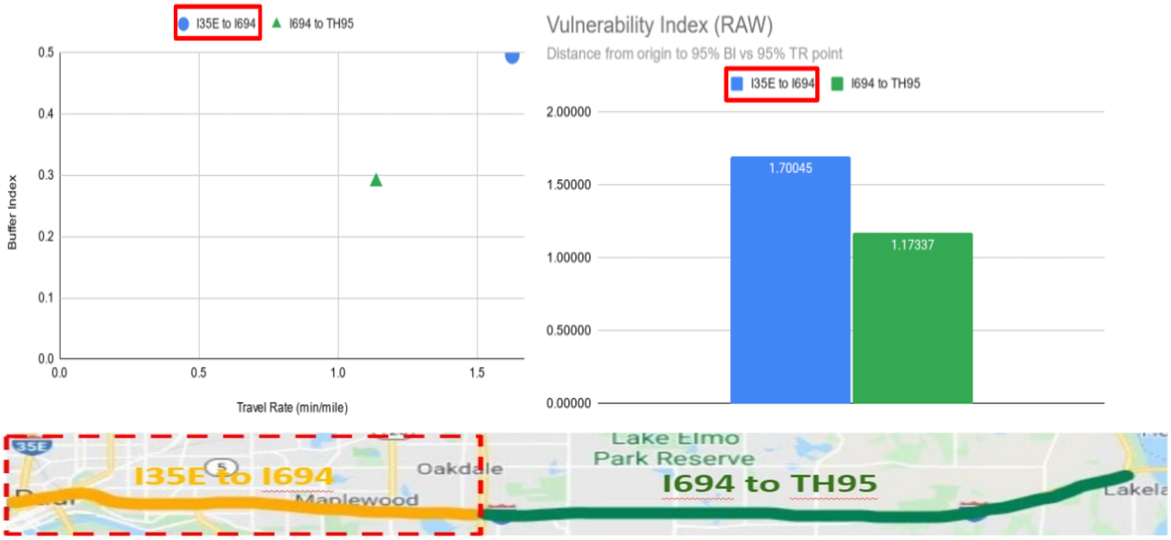


Figure 4.45: Identification of Bottleneck Sections (I-94 S4 EB)

## 4.3.28 I-94 (WISC to STPL) WB Morning ⇒ *I694 to I35E*

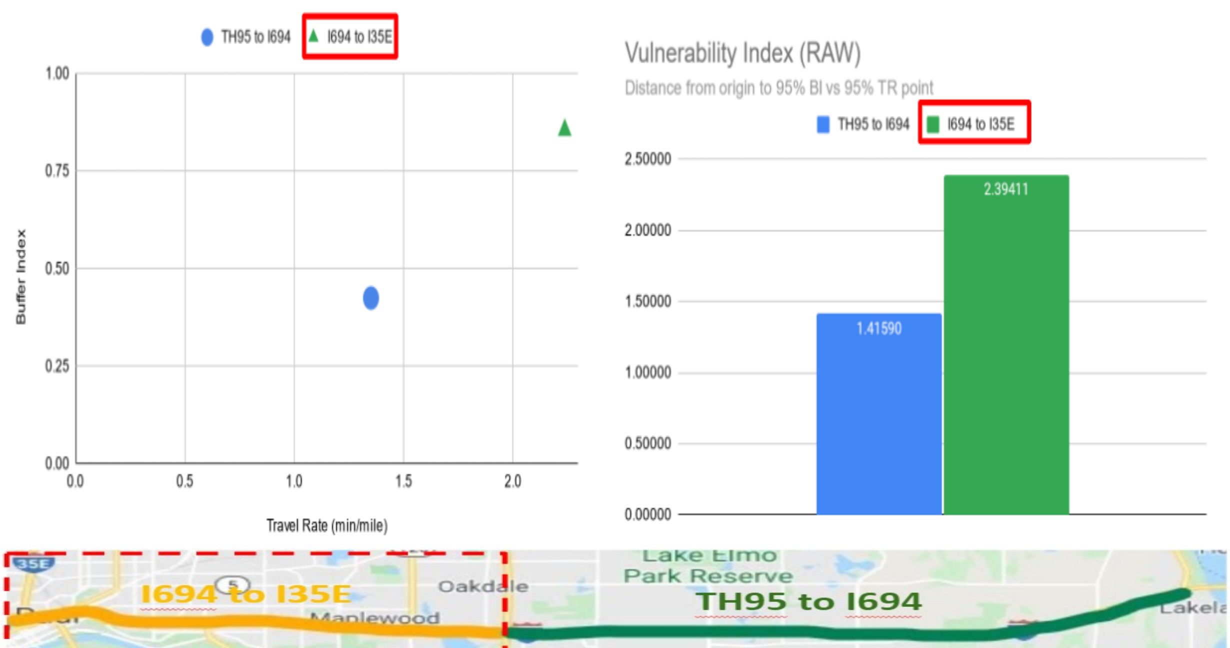


Figure 4.46: Identification of Bottleneck Sections (I-94 S4 WB)

## 4.3.29 I-35W (SS to MPLS) NB Morning ⇒ *I35E to River Bridge*

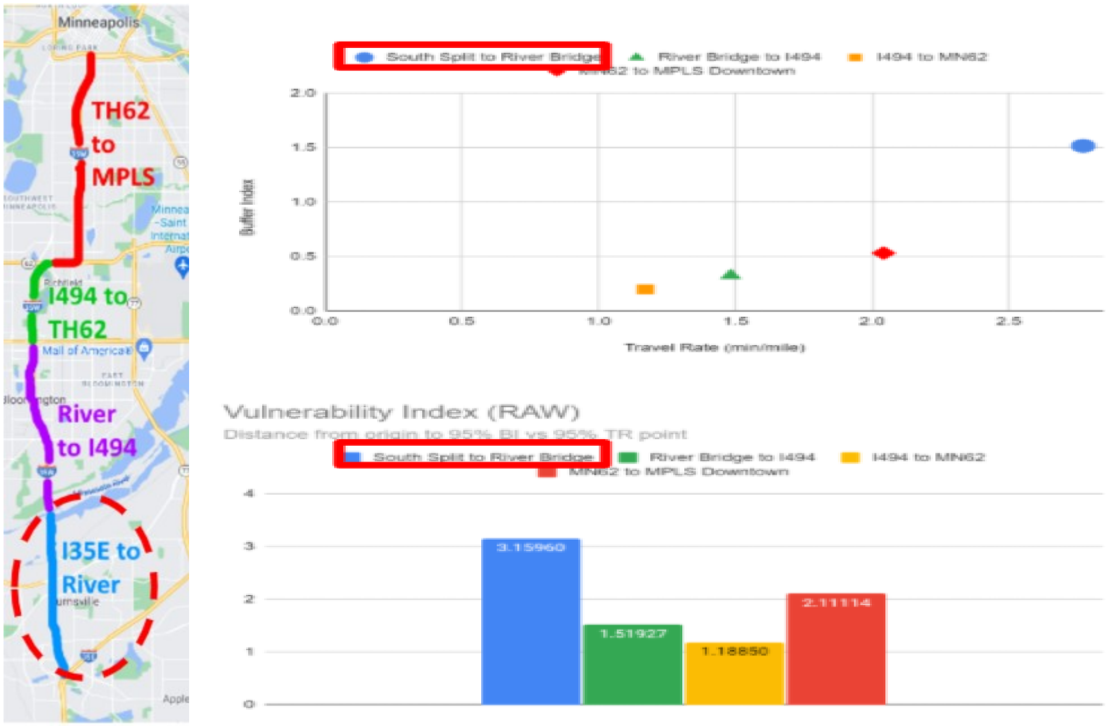


Figure 4.47: Identification of Bottleneck Sections (I-35W S1 NB)

### 4.3.30 I-35W (MPLS to SS) SB Afternoon ⇒ *I494 to River Bridge*


Figure 4.48: Identification of Bottleneck Sections (I-35W S1 SB)

### 4.3.31 I-35W (MPLS to NS) NB Afternoon ⇒ *MPLS to I694*

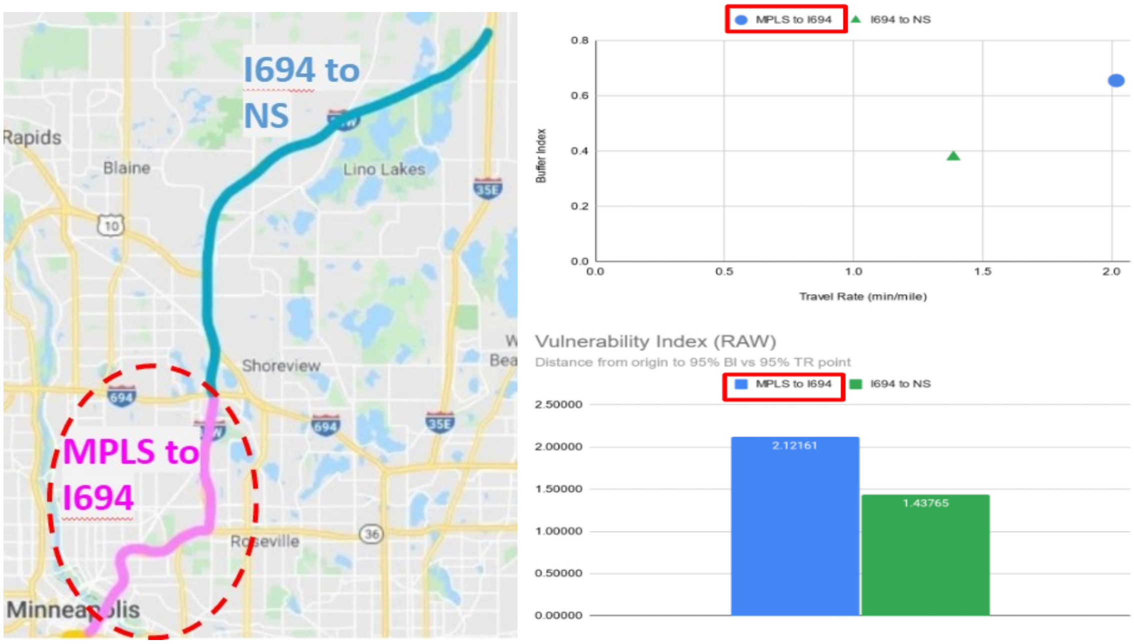


**Figure 4.49: Identification of Bottleneck Sections (I-35W S2 NB)**

## 4.3.32 I-35W (NS to MPLS) SB Morning ⇒ *NS to I694*

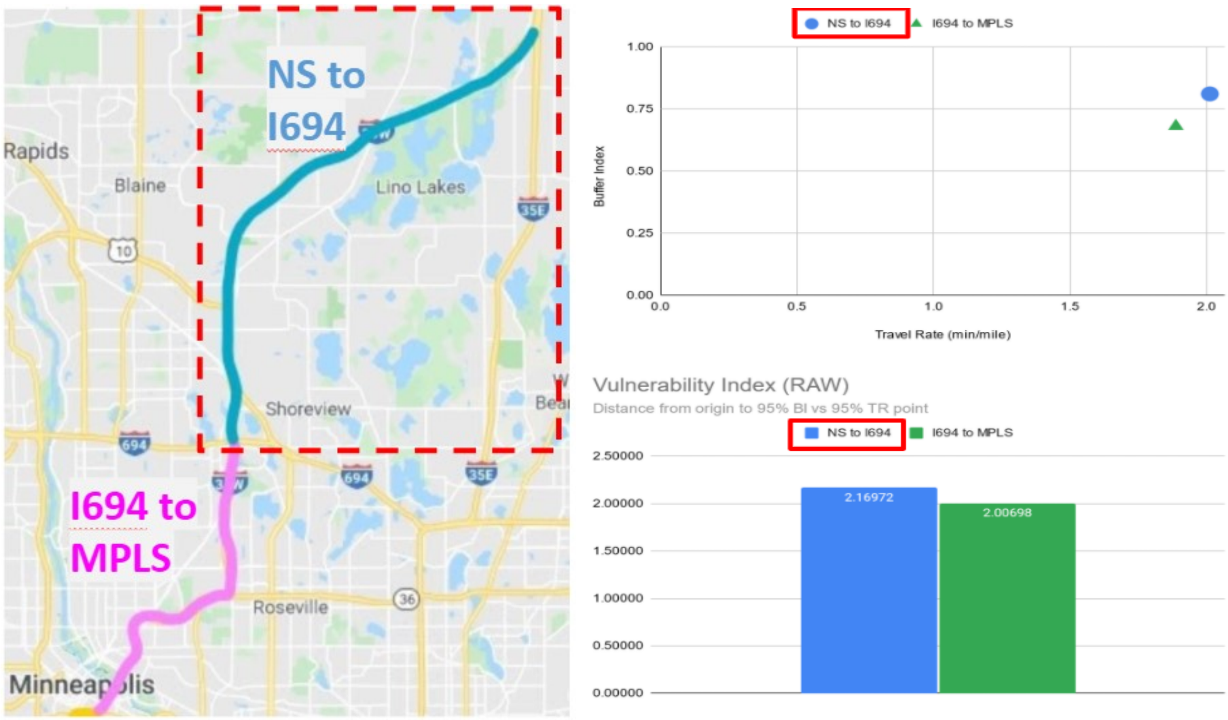


Figure 4.50: Identification of Bottleneck Sections (I-35W S2 SB)

## 4.3.33 I-35E (SS to STPL) NB Morning ⇒ *I494 to Ayd Mill Rd*

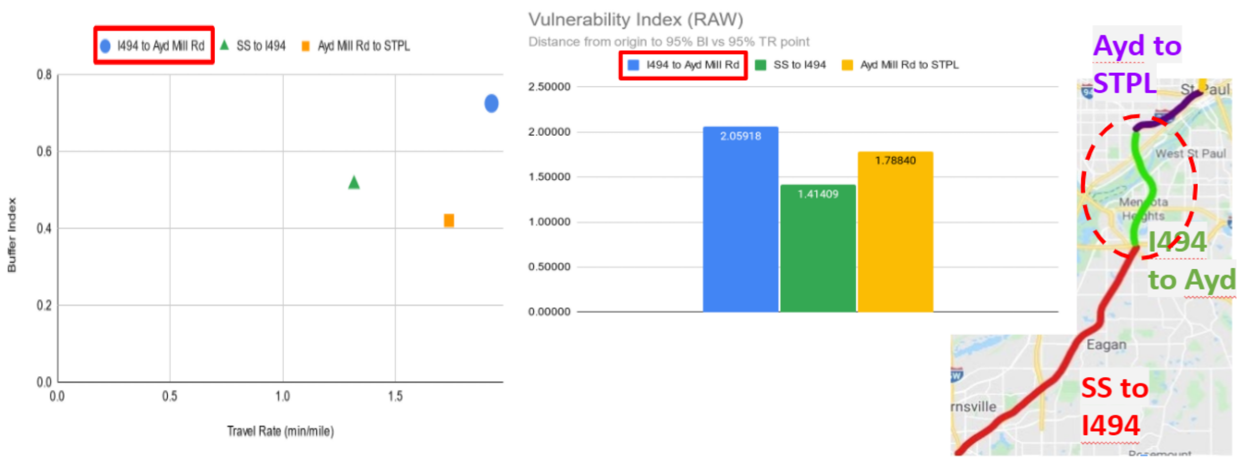


Figure 4.51: Identification of Bottleneck Sections (I-35E S1 NB)

### 4.3.34 I-35E (STPL to SS) SB Afternoon ⇒ *STPL to Ayd Mill Rd*

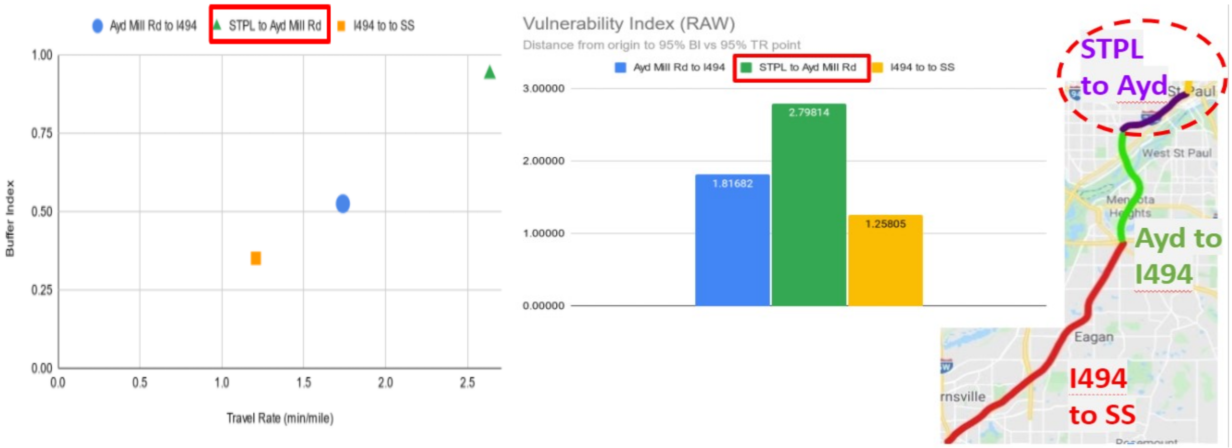


Figure 4.52: Identification of Bottleneck Sections (I-35E S1 SB)

### 4.3.35 I-35E (STPL to NS) NB Afternoon ⇒ *STPL to MN36*

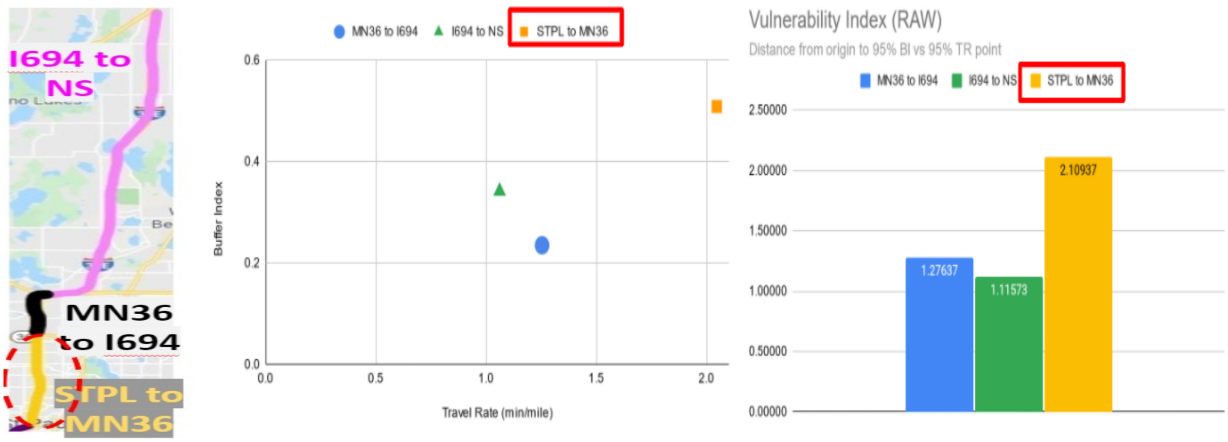


Figure 4.53: Identification of Bottleneck Sections (I-35E S2 NB)

### 4.3.36 I-35E (NS to STPL) SB Morning ⇒ *I694 to MN36*

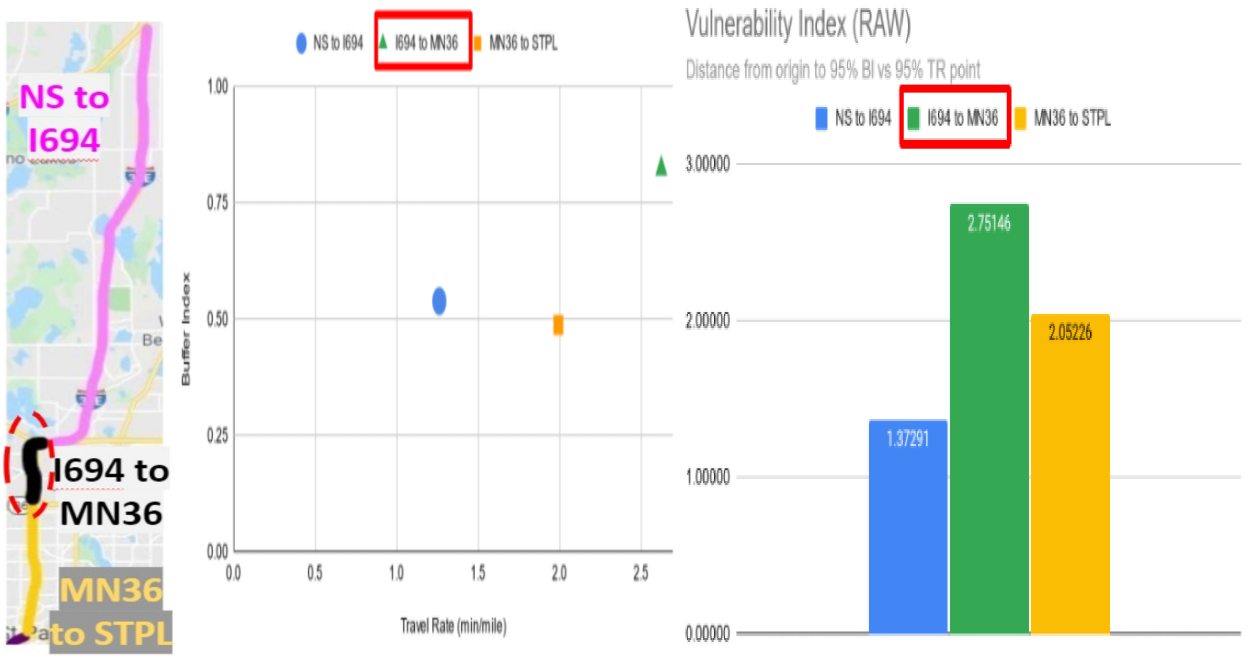


Figure 4.54: Identification of Bottleneck Sections (I-35E S2 SB)

### 4.3.37 I-694 (I94 to I35E) WB Morning ⇒ *TH36 to I35E*

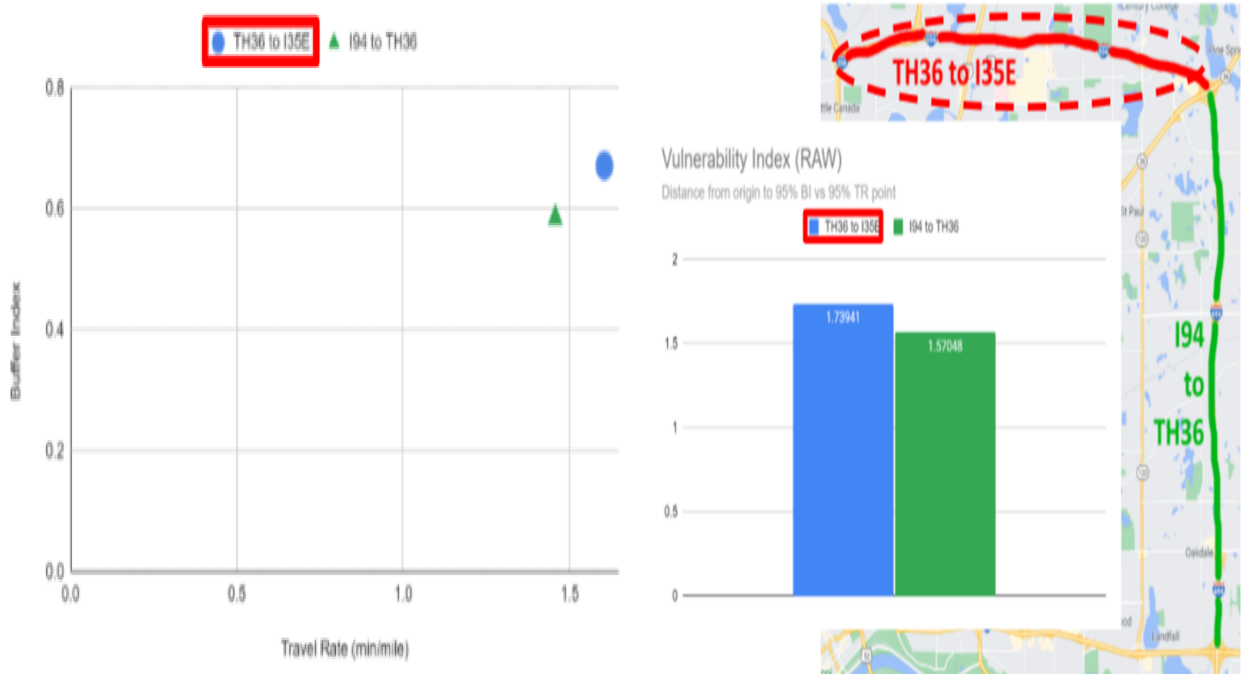


Figure 4.55: Identification of Bottleneck Sections (I-694 S1 WB)

### 4.3.38 I-694 (I-35E to I-94) EB Afternoon ⇒ *I35E to TH36*


Figure 4.56: Identification of Bottleneck Sections (I-694 S1 EB)

## 4.3.39 I-694 (I35E to TH252) WB Morning ⇒ *I35W to MN65*


Figure 4.57: Identification of Bottleneck Sections (I-694 S2 WB)

## 4.3.40 I-694 (TH252 to I35E) EB Afternoon ⇒ *MN65 to I35W*

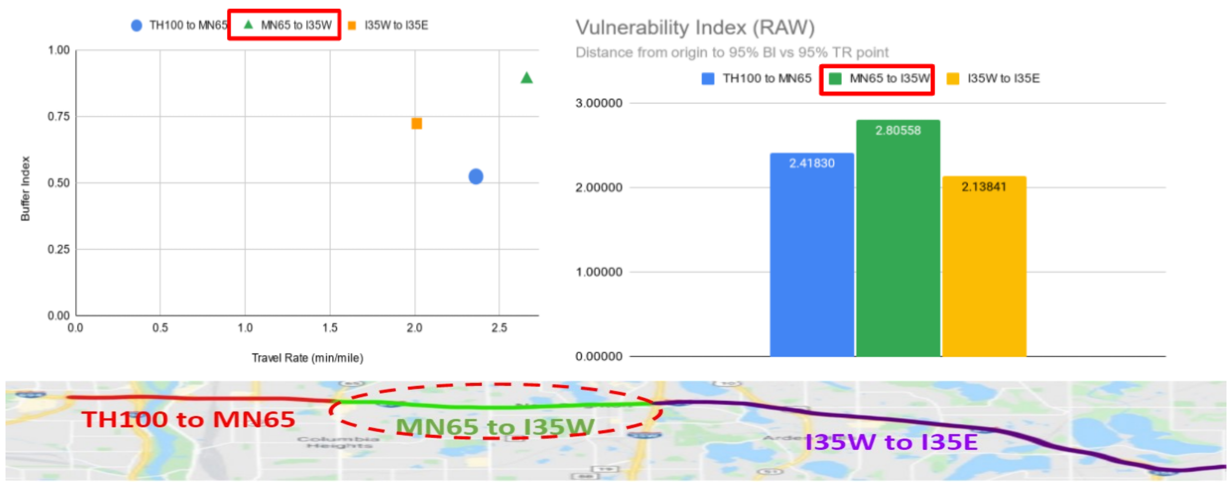


Figure 4.58: Identification of Bottleneck Sections (I-694 S2 EB)

## 4.4 SUMMARY

This chapter summarized the analysis results for the travel-time reliability trends of a total of 23 corridors (48 directional routes) in the metro freeway network for the period of 2016 to 2020. First, a set of the travel-time reliability and traffic-flow measures were estimated using TeTRES with the monthly and yearly data collected in the previous chapter. Further, a new vulnerability index combining the 95$^{th}$ percentile buffer index and the 95$^{th}$ percentile travel rate was used to assess the overall reliability status and variation trends of each route from 2016 to 2020 under all conditions. The resulting vulnerability index value for each route was also applied to identify the most vulnerable routes from 2016 to 2020 for both morning and afternoon peak periods. The yearly vulnerability values of individual directional routes in the metro freeway network indicate an improving trend from 2016 through 2018, while the increased construction activities in 2019 made reliability indices of most routes worse than those in 2018. These trends were also noted in the traffic-flow measures, i.e., the total vehicle-miles-traveled of all the directional routes were decreased in 2019 from 2018, while the total delayed-vehicle-hours were increased in 2019 for both morning and afternoon routes. The travel-time reliability estimates under different operating conditions indicate that the weather, in particular, snow is the most important factor affecting the travel-time reliability, while the quantified effects of snow on specific reliability measures can vary depending on the amount and frequency of precipitation on a given route. Finally, a set of potential bottleneck sections were identified for each directional route by examining the normal weekday congestion patterns and the specific geometry conditions of a given route. For each potential bottleneck section of a directional route, the vulnerability index was estimated with the 2019 data under all conditions and the bottleneck section with the highest vulnerability index was identified as the priority bottleneck section for a given route. Future research can extend the current work by normalizing the vulnerability indices of the bottleneck sections in each route and determine the network-wide priorities of the existing bottleneck sections of all directional routes.

# CHAPTER 5: PRELIMINARY EVALUATION OF FREEWAY CORRIDOR OPERATIONAL RESILIENCE

## 5.1 INTRODUCTION

A reliable and resilient freeway network, which can absorb, recover and adapt to various operating conditions, is of critical importance in sustaining the way of life and economic vitality of the Twin Cities metro area. While substantial progress has been made in estimating travel-time reliability on transportation networks, quantifying operational resiliency on a corridor level is still in its infancy.

To be sure, most research efforts to date on the resilience of transportation systems have focused on estimating the capability of a given transportation network in dealing with extreme events, such as natural disasters or large-scale incidents. In the early work by Murray-Tuite [3], a set of multiple metrics were estimated using simulation to quantify the resilience of a transportation network in four dimensions, i.e., adaptability, mobility, safety and recovery. Specifically, DYNASMART-P was used to estimate the effects of user equilibrium and system optimum traffic assignments on each of those four areas in a test network. Cimellro et al. [4] presented an approach to define the resilience of a transportation system as a time-variant functionality of a given system during adverse conditions. A conceptually similar approach was also proposed by Devannadham et al. [5], who defined the resilience of a transportation system as the ratio of the system's recovery at a given time to the loss that system suffered because of the adverse condition in subject. The use of graph theory to quantify the network-wide resilience was proposed by Leu et al. [6], and also by Berche et al. [7]. In both approaches, the structural deficiencies of a given network, e.g., network-connectivity and spatial distributions, were modeled with a graph theory, and applied to quantify the network-wide resilience. The incorporation of traffic-flow theory in formulating resilience has been tried by Kim et al. [8], who defined the resilience of a given traffic network as the sum of the areas between the network-wide fundamental diagrams under normal and emergence operations. The application of a network simulation model was also proposed by Dorbritz [9], who simulated node removals and estimated their operational impacts in measuring the resilience of a given network. A recent study by Calvert and Snelder [10] proposed a Link Performance Index for Resilience based on assumed values of the capacity and critical density for individual links. A similar effort to quantify the resilience of individual roadway sections was also presented by Khaghani [11], who proposed a resilience score for an individual section as a weighted average of multiple-dimensional measures on the speed-variation patterns, such as loss, recovery rates and event duration time.

As noted above, most existing research efforts regarding resiliency have tried to quantify network or community-wide resilience by integrating the individual metrics in multiple dimensions, i.e., organizational, and social aspects of resilience with financial and technical ones. While these approaches tried to capture multi-dimensional aspects of resilience and their complex interactions, the major difficulties of such approaches include the quality and availability of the data required for estimating proposed resilience measures. As a result, no-widely accepted measure of resilience is currently available for transportation systems. Recently some researchers tried to quantify the operational resilience of roadways using traffic data, their efforts to date have been limited to individual roadway sections and the development of a corridor-wide resilience measure reflecting the interactions of various bottleneck types has not been addressed in their work.

Developing corridor-specific resilience measures that can be estimated with the field data available from the current detection system is of critical importance for an effective allocation of limited resources to competing corridors, thus for improving the resilience of a given roadway network. In this chapter, a preliminary study to formulate and estimate operational resilience of a freeway corridor is conducted using 3 corridors in the metro freeway network as the sample corridors. The proposed corridor-wide operational resilience index (CORI) from this study is designed to capture the capability of a given directional corridor, i.e., route, in coping with the common traffic disturbances on a day-to-day operation, such as incidents and demand variations. The rest of the chapter summarizes the collected data, formulation, and estimation of the corridor-wide operational resilience measures with the traffic and geometry data from the sample corridors.

## 5.2 MODELING AND ESTIMATION OF OPERATIONAL RESILIENCE OF SAMPLE CORRIDORS

### 5.2.1 Sample Corridors and Data Collection

Figure 5.1 shows the locations of the 3 sample freeway corridors, i.e., I-494 Northbound/Southbound (NB/SB), TH 100 (NB/SB) and US 169 (NB/SB), used in this study to formulate and estimate the operational resilience of each corridor. As can be seen from the figure, these 3 corridors were in parallel and each of them could be used as an alternative to others. It needs to be noted that the corridor-wide operational resilience measure to be developed in this study is focusing on the capability of each individual corridor in dealing with the traffic disturbances on its own roadway, while the effects of the potential interaction among adjacent corridors can be reflected on the traffic demand entering/exiting to/from each corridor.

First, the peak-period, traffic-flow data for each directional route of those 3 corridors, i.e., two routes per corridor, were collected by using TICAS, Traffic Information Condition Analysis System developed at University of Minnesota Duluth, for the weekdays, i.e., Tuesdays, Wednesdays, and Thursdays, of a two-month period from September to October 2019. They include route-wide total entering volume ($V_{E,t}$) and delayed-vehicle-hours ($DVH_t$) for every 5-minute interval. Figure 5.1 also shows the locations of the three sample corridors used in this study along with the detector stations on the northbound directional route on each corridor. Further, all the accident data during the same periods were also collected in cooperation with the Regional Transportation Management Center, MnDOT. Figure 5.2.2 shows a screenshot of an example incident data extracted from the MnDOT incident database for the sample corridors. As shown in Figure 5.2, the collected data includes incident location, type and time duration for each incident on each corridor. In addition, the weather data for the study period were also extracted from the TeTRES, Travel Time Reliability Estimation System, database for the sample corridors. In this study, only the traffic data under dry-weather condition were used for formulating the operational resilience of each directional route.

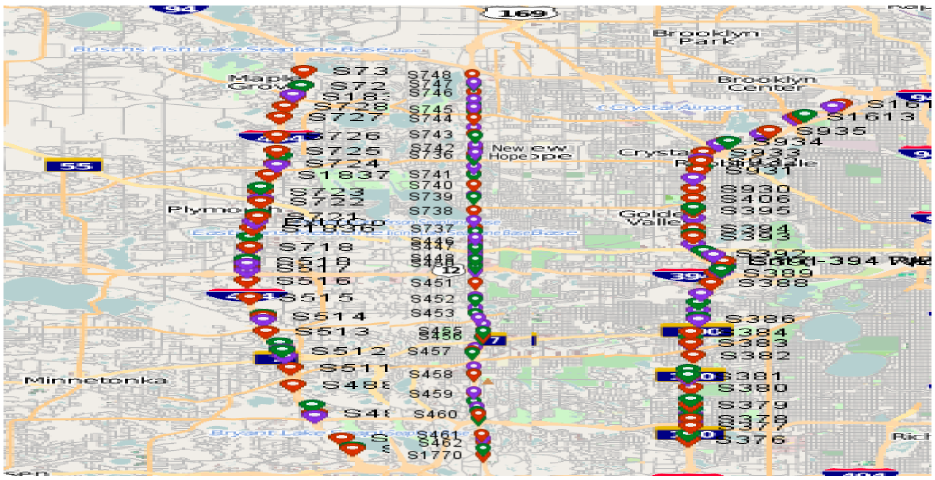


**Figure 5.1: Locations of Sample Freeway Corridors and Detector Stations on Northbound Routes**

| Cdts | Udts | Xdts | Number of Lan | Event Type | Sub Event Type | Classification | XStreet1 | XStreet2 |
|---|---|---|---|---|---|---|---|---|
| 2019-09-03 15:3 | 2019-09-03 16:0 | 2019-09-03 16:0 | 0 | TRAFFIC MGMT | OCCUPIED STA | STALL | NB 100 HWY N | W 50TH ST |
| 2019-09-03 16:2 | 2019-09-03 16:2 | 2019-09-03 17:1 | 0 | PROPERTY DA | HIT AND RUN | CRASH | EB 494 I E | NB 100 HWY N |
| 2019-09-04 16:2 | 2019-09-04 16:2 | 2019-09-04 17:1 | 0 | PROPERTY DAMAGE CRASH | | CRASH | NB 100 HWY N | CEDAR LAKE RD S |
| 2019-09-04 17:0 | 2019-09-04 17:0 | 2019-09-04 18:3 | 0 | TRAFFIC MGMT | UNOCCUPIED S | STALL | NB 100 HWY N | 394 HOV I |
| 2019-09-05 18:1 | 2019-09-05 18:1 | 2019-09-05 19:1 | 0 | PROPERTY DAMAGE CRASH | | CRASH | NB 100 HWY N | 394 HOV I |
| 2019-09-11 06:0 | 2019-09-11 06:0 | 2019-09-11 19:3 | 0 | TRAFFIC MGMT | UNOCCUPIED S | STALL | SB 81 CR | NB 100 HWY N TO SB 81 CR RMP |
| 2019-09-11 17:1 | 2019-09-11 17:1 | 2019-09-11 17:5 | 0 | TRAFFIC MGMT | UNOCCUPIED S | STALL | DULUTH ST TO | DULUTH ST |
| 2019-09-11 17:2 | 2019-09-11 17:3 | 2019-09-11 18:4 | 0 | TRAFFIC MGMT | OCCUPIED STA | STALL | NB 100 HWY N | MINNETONKA BLVD |
| 2019-09-12 15:1 | 2019-09-12 15:1 | 2019-09-12 15:5 | 0 | PROPERTY DAMAGE CRASH | | CRASH | NB 100 HWY N | 10 CR |
| 2019-09-17 17:4 | 2019-09-17 17:4 | 2019-09-17 19:3 | 0 | PERSONAL INJURY CRASH | | CRASH | NB 100 HWY N | MINNETONKA BLVD |
| 2019-09-19 15:3 | 2019-09-19 15:3 | 2019-09-19 18:2 | 0 | TRAFFIC MGMT | OCCUPIED STA | STALL | NB 100 HWY T | 36TH AVE N TO NB 100 RMP |
| 2019-09-25 15:2 | 2019-09-25 15:2 | 2019-09-25 17:1 | 0 | STALLED VEHICLE- BLOCKING | | STALL | NB 100 HWY N | MINNETONKA BLVD |
| 2019-09-25 16:1 | 2019-09-25 16:1 | 2019-09-25 17:3 | 0 | PROPERTY DAMAGE CRASH | | CRASH | NB 100 HWY N | 394 HOV I |
| 2019-09-25 17:2 | 2019-09-25 17:2 | 2019-09-25 18:1 | 0 | STALLED VEHICLE NOT BLOCK | | STALL | NB 100 HWY N | DULUTH ST |
| 2019-09-25 18:1 | 2019-09-25 18:1 | 2019-09-26 12:1 | 0 | STALLED VEHICLE NOT BLOCK | | STALL | NB 100 HWY N | 394 HOV I |
| 2019-10-01 13:4 | 2019-10-01 13:4 | 2019-10-03 09:0 | 0 | TRAFFIC MGMT | UNOCCUPIED S | STALL | NB 100 HWY N | BROOKLYN BLVD TO NB 100 HWY RMP |
| 2019-10-01 17:4 | 2019-10-01 18:2 | 2019-10-01 18:2 | 0 | TRAFFIC MGMT | LAW ENFORCE | LAW ENFORCE | NB 100 HWY N | W 50TH ST |
| 2019-10-08 17:2 | 2019-10-08 17:2 | 2019-10-08 18:1 | 0 | PROPERTY DAMAGE CRASH | | CRASH | NB 100 HWY N | EB 7 HWY |
| 2019-10-09 14:2 | 2019-10-09 14:2 | 2019-10-09 15:3 | 0 | NON-MOTORIZED VEHICLE ON | | PEDESTRIAN | NB 100 HWY N | BROOKLYN BLVD |
| 2019-10-09 14:5 | 2019-10-09 14:5 | 2019-10-09 15:3 | 0 | PEDESTRIAN ON FREEWAY | | PEDESTRIAN | NB 100 HWY N | W 77TH ST |
| 2019-10-15 15:4 | 2019-10-15 16:0 | 2019-10-15 17:1 | 0 | TRAFFIC MGMT | OCCUPIED STA | STALL | NB 100 HWY N | 10 CR |
| 2019-10-16 15:4 | 2019-10-16 15:4 | 2019-10-16 15:5 | 0 | MOTORIST ASSIST | | STALL | LILAC DR N | EB 55 HWY TO NB 100 HWY RMP |
| 2019-10-16 15:4 | 2019-10-16 15:4 | 2019-10-16 16:5 | 0 | TRAFFIC MGMT | OCCUPIED STA | STALL | NB 100 HWY N | 55 HWY |
| 2019-10-23 17:4 | 2019-10-23 17:5 | 2019-10-23 18:2 | 0 | TOW ASSIST | | STALL | NB 100 HWY N | 394 HOV I |
| 2019-10-24 10:5 | 2019-10-24 10:5 | 2019-10-25 07:5 | 0 | STALLED VEHICLE NOT BLOCK | | STALL | NB 100 HWY N | LAKE BREEZE AVE |
| 2019-10-29 14:1 | 2019-10-29 14:1 | 2019-10-29 17:1 | 0 | TRAFFIC MGMT | OCCUPIED STA | STALL | W BROADWAY | 42ND AVE N |
| 2019-10-30 17:1 | 2019-10-30 17:1 | 2019-10-30 18:2 | 0 | PROPERTY DA | HIT AND RUN | CRASH | WB 62 HWY | NB 100 HWY N |

**Figure 5.2: Sample Incident Data**

### 5.2.2 Collection of Geometry Data for Each Directional Route

A set of the geometry data for each directional route was also collected in this task to study the potential relationship between the operational resilience and the geometry of each corridor. The selected data for each directional route includes the followings:

- *Route length (Linear distance between upstream and downstream boundary stations)*
- *Number of exit and entrance ramps on each route*
- *Lengths of weaving sections on each route*
    - *The length of each weaving section is measured from the Google Earth map as the distance from the merge to diverge gore points, i.e., pavement markings.*
- *Length of each mainline section with same number of through lanes*
    - *Auxiliary lanes are not considered as through lanes.*

Table 5.1 shows the raw geometric data collected for each directional route of the sample corridors.

**Table 5.1: Geometric data of Directional Routes**

| | Length (mi) | Miles of Weaving Sections (number of) | # of Exit Ramps | # of Entrance Ramps |
|---|---|---|---|---|
| I494 NB A | 14.4 | 0.17 (2) | 11 | 12 |
| I494 SB M | 15 | 0.12 (2) | 12 | 11 |
| US169 NB A | 14.5 | 1.91 (14) | 24 | 26 |
| US169 SB M | 14 | 1.82 (12) | 24 | 24 |
| TH100 NB A | 13.7 | 0.97 (6) | 18 | 19 |
| TH100 SB M | 14.4 | 0.95 (6) | 20 | 22 |

### 5.2.3 Formulation and Estimation of Operational Resilience for Selected Corridors with Traffic-Flow Data

Figures 5.3 and 5.4 show the Delayed-Vehicle-Hours ($DVH_t$) through time for each directional route of the sample corridors during the weekday peak periods. The values of $DVH_t$ are estimated every 5-minute for an entire route with the traffic data from each route using the following formula:

$$DVH_t = \Sigma\ [(TT_{i,t} - FF\_TT_i) * K_{i,t} * L_i] \text{ for all segment i in a given route,}$$

*where,* $DVH_t$ *= Total Delayed-vehicle-hours during t for a given route,*

$TT_{i,t}$ *= Estimated travel time of segment i during t,*

$FF\_TT_i$ *= Free-Flow travel time of segment i*

$K_{i,t}$ *= Traffic density of segment i during t,*

$L_i$ *= Length of segment i.*

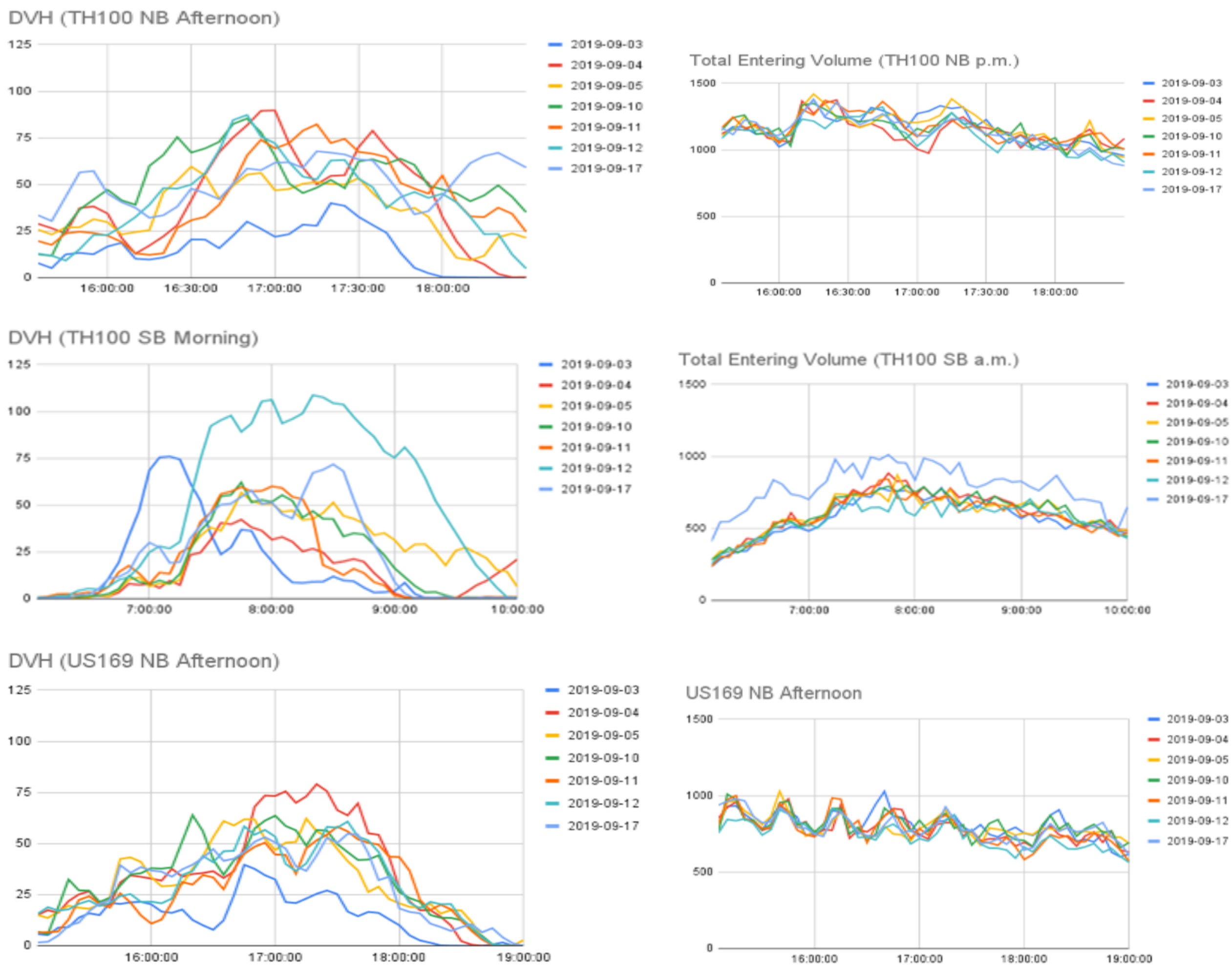


**Figure 5.3: Delayed-Vehicle-Hour (DVHt) and Total Entering Volume (VE,t) Variations through Time**

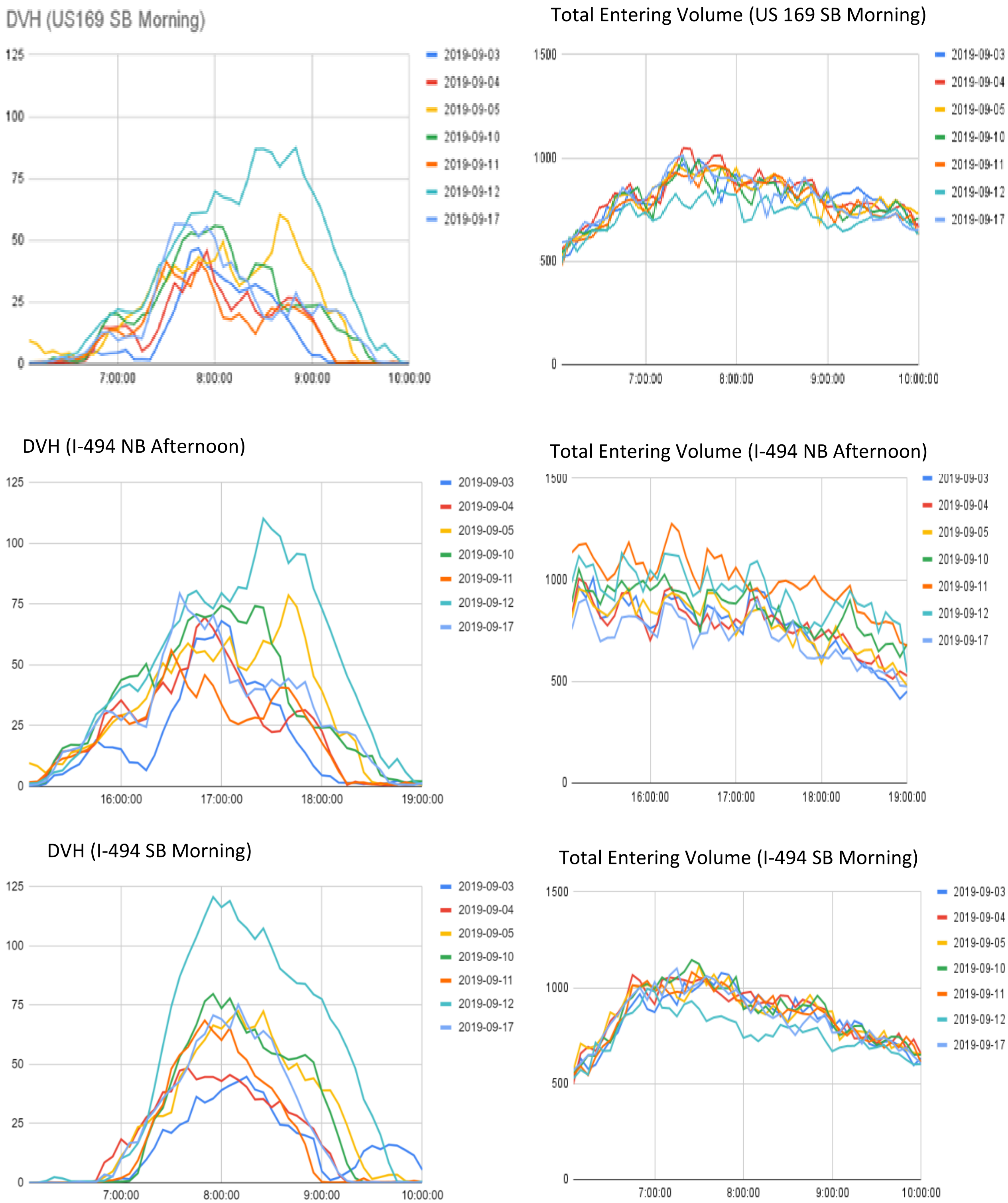


**Figure 5.4: Delayed-Vehicle-Hour (DVHt) and Total Entering Volume (VE,t) Variations through Time**

As implied in the above definition, $DVH_t$ indicates the amount of congestion during t interval and the $DVH_t$ – time variation pattern directly reflects the congestion start-expansion-recovery process of a given route in responding to the various types/levels of traffic disturbances, e.g., changes in traffic demand and incidents. Figure 5.3 also includes the variations of the total route-wide entering volume, $V_{E,t}$, through time for each directional route during the weekday peak periods. The values of $V_{E,t}$ are calculated every 5 minutes with the traffic-volume data from the detector stations on each route as follows:

$$V_{E,t} = (\text{Upstream Boundary Station Volume})_t + \Sigma\,(\text{All Entrance Ramp Volumes})_t$$

The analysis of the $DVH_t$ variation patterns of the sample directional routes indicates:

- *The $DVH_{t,max}$, i.e., the maximum value of $DVH_t$ during a peak period, and the time duration to reach $DVH_{t,max}$, reflect the 'Resistance' and 'Adaptation' capabilities of a given route in coping with the congestion caused by the traffic disturbances, i.e., incidents, weather or traffic demand changes.*
- *The congestion 'Recovery' patterns, i.e., the slope of the '$DVH_t$ Recovery' lines, i.e., the lines from $DVH_{t,max}$ to Zero DVH in the $DVH_t$-time graphs, exhibit remarkable similarities for a same route, while the slopes of those recovery lines vary from route to route. This could imply each route has its own 'Recovery' capability from congestion.*

Figure 5.5 illustrates the above observations with the DVH variations on multiple days at the I-494 Northbound routes. As shown in this figure, the DVH recovery lines on different days indicate similar slopes, while the time duration and pattern to reach the maximum DVH value on each day varies depending on the demand and incident patterns.

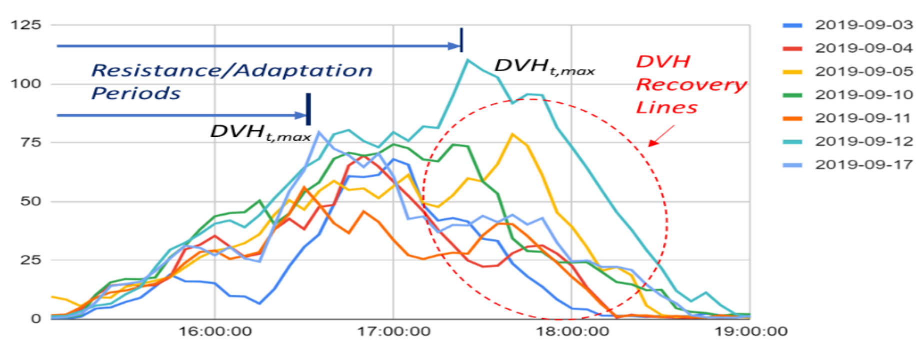


**Figure 5.5: I-494 Northbound DVH Variation Patterns**

Based on the above observations, in this study, the ***Operational Resilience of a freeway corridor*** is defined as "***the capability of a freeway corridor traffic system to absorb and adapt to various levels of***

***traffic disturbances and recover from congestion with maximum efficiency under given operating conditions***." Figure 5.6 shows the schematic diagram, where the congestion duration/scope of a freeway corridor is the direct output from the operational resilience, which is the core capability of a given corridor in resisting and recovering from congestion caused by various external factors.

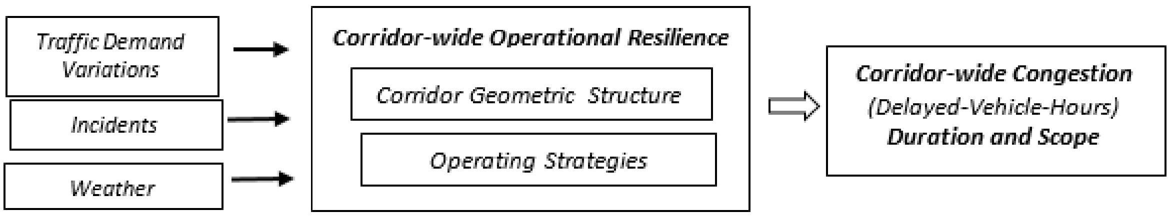


**Figure 5.6: Conceptual Relationship between Operational Resilience and External Factors**

The conceptual relationship shown in Figure 5.6 implies that each corridor has its own operational resilience level, which can be directly reflected by the corridor-wide delay measures. Further, the resilience level of each corridor depends on the geometric structure and operating strategies of a given corridor. In this study, a Corridor-wide Operational Resilience Index (CORI) is formulated and estimated for each directional route with the traffic-flow data available from the current detection system on freeways as follows:

$$CORI_i = \frac{\sum_t (DVH_t * A_t)}{(\sum_t V_{E,t}) * \sigma}$$

where,

*$CORI_i$ = Operational Resilience Index of Corridor i*

*$DVH_t$ = Corridor-wide delayed-vehicle-hours during t,*

*$A_t$ = Proportion of weighted average number of lanes during t,*

*$V_{E,t}$ = Corridor-wide total entering volume during t,*

*$\sigma$ = Standard deviation of $V_{E,t}$ during a peak period.*

As noted from the above formulation, the proposed CORI tries to quantify the capability of a given directional corridor in minimizing the traffic delay under given variations in corridor-wide traffic demand and geometric conditions, i.e., number of available through lanes through time. Therefore, a smaller CORI index indicates a stronger resilience level of a given corridor. It needs to be noted that, in the proposed formulation of CORI, the effects of incidents on the traffic flow are reflected in $A_t$, the proportion of the corridor-wide available lanes during t, which is determined as follows:

$$A_t = \frac{Average\ Weighted\ Number\ of\ Through\ Lanes\ -\ (Number\ of\ Lanes\ Blocked)_t}{Average\ Weighted\ \ Number\ of\ Through\ Lanes}$$

In the above formulation, the ‘number of blocked lanes’ during t depends on the type/scope of an individual incident, however, in the current incident database from MnDOT, very few incidents have the blocked-lane data, while the data regarding the type and duration of each incident are available. Since most incidents affect the speed of the traffic flow going through an incident location, in this study, due to the time limitation, the following values in Table 5.2 are assumed to be the number of the blocked lanes for each type of incident. It needs to be noted that these values should be refined with the field data in the future study.

**Table 5.2: Assumed Number of Blocked Lanes**

| Incident Classification | Number of Lanes Blocked |
|---|---|
| STALL | 0.3 |
| PEDESTRIAN | 0.6 |
| CRASH | 0.9 |
| SPINOUT | 0.6 |
| DEBRIS | 0.6 |
| WRONG WAY DRIVER | 1.2 |
| JUMPER | 0.6 |
| LAW ENFORCEMENT | 0.6 |
| MAINTENANCE | 0.6 |
| FIRE | 1.2 |
| ANIMAL | 0.6 |
| MEDICAL | 1.2 |
| SLUMPER | 0.9 |
| MNPASS MAINTENANCE | 0.6 |
| CLASSIFICATION NOT LISTED | 0.3 |

In addition, the ‘Average weighted number of through lanes’ of a given corridor, a surrogate measure of the corridor-wide through capacity, is determined as shown in Figure 5.7:

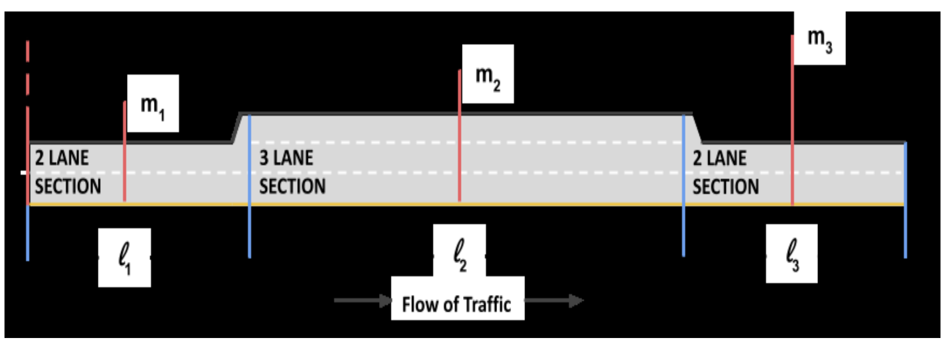


$$Avg.Weighted\ \#\ of\ Through\ Lanes\ = \frac{(m_1 \times 2\ lanes) + (m_2 \times 3\ lanes) + (m_3 \times 2\ lanes)}{m_1 + m_2 + m_3}$$

$$= \frac{\left[\frac{l_1}{2} \times 2\ lanes\right] + \left[\left(l_1 + \frac{l_2}{2}\right) \times 3\ lanes\right] + \left[\left(l_1 + l_2 + \frac{l_3}{2}\right) \times 2\ lanes\right]}{\frac{5}{2}l_1 + \frac{3}{2}l_2 + \frac{1}{2}l_3}$$

**Figure 5.7: Process to Determine Average Number of Through Lanes**

In the above formulation, the roadway sections located downstream have larger weights than those upstream, therefore, the effects of downstream bottleneck sections on the corridor-wide through traffic can be captured more effectively. It also needs to be noted that the auxiliary or acceleration/deceleration lanes are not considered as through lanes in this formulation.

#### 5.2.3.1 Estimation of Corridor-wide Operational Resilience for Sample Directional Routes

The above definition of the corridor-wide operational resilience is applied to the sample corridors and the daily CORI values of each directional route is calculated with the traffic data from a two-month period, September – October 2019. In this preliminary study, the specific effects of weather are not directly addressed, i.e., the traffic data from only dry weather conditions were used to estimate the daily CORI values of the sample directional routes. Figure 5.2.7 includes the daily estimates of CORI for each directional route under the dry weather conditions, i.e., no precipitation, during September – October 2019. It needs to be noted that, according to the NOAA weather data, there were rains in the mornings of Sept 11 and Oct 22, while no rain was reported in the afternoons of those two days. Therefore, the CORI values of all the southbound routes with morning peak periods are not determined for those two days. Table 5.2.3 includes the average and standard deviation values of the daily CORI during the test period and Figure 5.2.8 shows the graphical comparison of the average CORI for each sample route.

As noted in Figures 5.8 and 5.9, the CORI estimates of those routes with the morning-peak periods show relatively stable day-to-day variations, while the afternoon peak-period routes show more fluctuations than those from the morning-peak routes. The t-test results indicate that the CORI values of the sample routes are significantly different at 95% confidence level. While the further study needs to address these differences in CORI between the northbound and the southbound routes, the initial assessments indicate the northbound routes appear to have more favorable geometric structures, as discussed in the following section with the geometric friction modeling, compared to the southbound routes. Furthermore, the afternoon traffic-demand patterns also show more variations than those with the morning periods. It can also be noted that more accurate incident data regarding the blocked number of lanes and time durations for each incident will improve the accuracy of the estimation results.

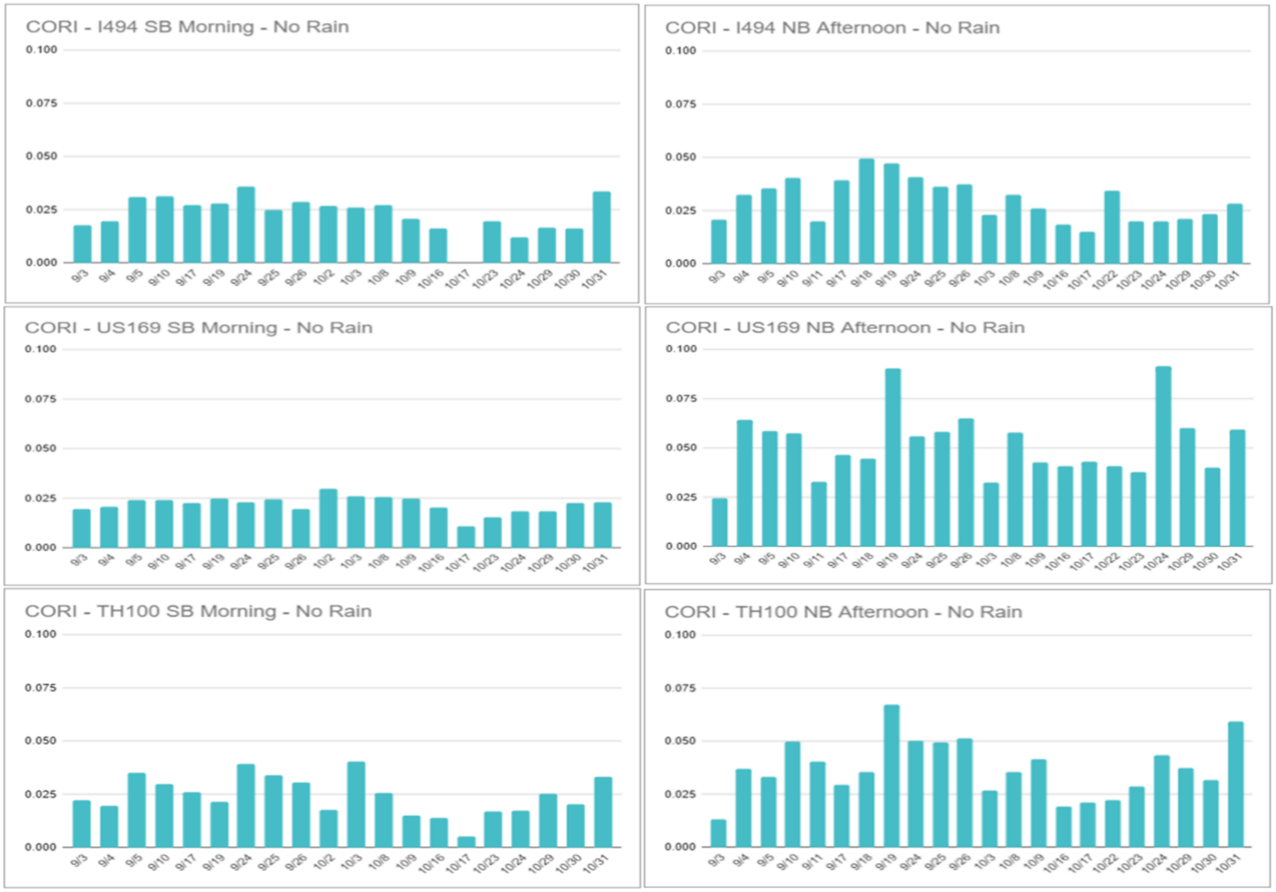


**Figure 5.8: Daily Estimates of CORI for the Sample Directional Routes**

**Table 5.3: Average CORI for Each Route**

| Route | I494 NB A | I494 SB M | US169 NB A | US169 SB M | TH100 NB A | TH100 SB M |
|---|---|---|---|---|---|---|
| CORI | 0.0302 | 0.0244 | 0.0486 | 0.0220 | 0.0375 | 0.0261 |
| Standard Dev. | 0.0095 | 0.0067 | 0.0197 | 0.0042 | 0.0139 | 0.0092 |

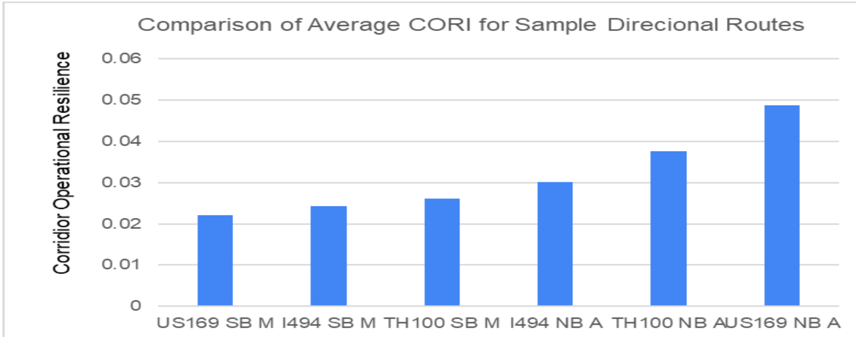


**Figure 5.9: Comparison of Sample Route Operational Resilience**

## 5.3 EFFECTS OF CORRIDOR-WIDE GEOMETRIC FEATURES ON OPERATIONAL RESILIENCE

Finally, the potential relationship between the corridor-wide operational resilience and the geometric structure of each corridor is studied in this task. In this study, the 'strength' of the corridor-wide geometric structure in terms of handling the traffic flows going through a given corridor is quantified with the following geometry-based parameters:

- Number of Exit Ramps per mile (G1),
- Number of Entrance Ramps per mile (G2),
- Proportion of the total non-weaving section length (G3) = 1 – [Σ (lengths of all weaving sections) / route length],
- Average number of through lanes weighted with the distance from upstream boundary (G4) as defined before.

Using the above parameters, the 'strength' of the geometric structure of a given corridor in terms of facilitating through traffic movements, G, is formulated as follows:

$$\mathrm{G} = \frac{G1 * G3 * G4}{G2}$$

In the above formula, the numerator reflects the combined effects of the geometric features facilitating the through movements within a given corridor, while the denominator quantifies the potential frictions caused by the entrance volumes to the through traffic in a given corridor. In this study, the G factor is named as the geometric-friction factor, i.e., the higher G value, the less geometric friction in a given directional route. Table 5.4 includes the values of each parameter and the resulting G values for all the sample directional routes. As shown in this table, the southbound routes show a higher G value, i.e., less geometric friction, than the northbound route in a same corridor. Figure 5.10 shows the relationship between the CORI, corridor-wide operational resilience index, and the geometric-friction parameter, G, of each route. As expected, the routes with the higher G values, i.e., less geometric friction, generally show stronger operational resilience.

Table 5.4: Geometric Friction Parameters and Estimation Results

| | I494 NB | I494 SB | US169 NB | US169 SB | TH100 NB | TH100 SB |
|---|---|---|---|---|---|---|
| Total Route Length (mi) | 14.4 | 15 | 14.5 | 14 | 13.7 | 14.4 |
| G1 (Exit ramps/mi) | 0.764 | 0.800 | 1.655 | 1.714 | 1.314 | 1.389 |
| G2 (Entrance ramps/mi) | 0.833 | 0.733 | 1.793 | 1.714 | 1.387 | 1.528 |
| G3c (Proportion of non-weaving length) | 0.988 | 0.992 | 0.868 | 0.870 | 0.929 | 0.934 |
| G4 (Avg weighted # of through lanes) | 3.426 | 3.411 | 2.520 | 2.476 | 3.033 | 3.344 |
| **G** | **3.104** | **3.691** | **2.020** | **2.155** | **2.669** | **2.840** |

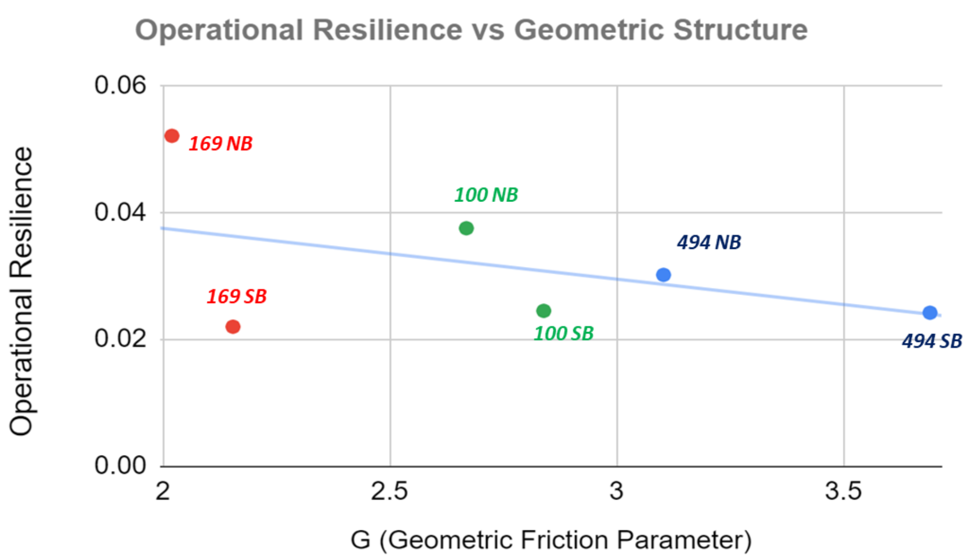


Figure 5.10: Operational Resilience vs Geometric Friction

## 5.4 SUMMARY

This chapter summarized the results from the preliminary study to quantify the operational resilience of a freeway corridor.  A total of 6 directional routes in 3 corridors were selected as the sample routes and, for each route, a set of the detailed geometric and traffic-flow data, including incidents and weather information, were collected for a two-month period from September to October in 2019.  Using the collected traffic and incident data, the congestion start/recovery process of each route were analyzed and a model to quantify the corridor-wide operational resilience, CORI, of a given corridor was formulated and applied to the sample directional routes for the weekday peak periods under dry weather condition. The resulting CORI estimates of the sample directional routes indicate that the southbound routes show consistently stronger resilience with stable day-to-day variations than the northbound route in a same corridor. Further, the average resilience values of all the sample routes are significant different at 95% confidence level.  Finally, the potential relationship between the operational resilience and the geometric structure of each sample route was analyzed by quantifying the geometric friction of each directional route in facilitating corridor-wide through traffic flows. The quantification of the geometric friction is based on the geometry data easily measurable from the field. The resulting geometric friction parameters of the sample routes show clear correlation with the operational resilience of each route, i.e., for the sample routes selected in this study, the southbound route in a given corridor has less geometric friction with stronger operational resilience than the northbound route in a same corridor.

The corridor-wide operational resilience and geometric friction measures developed and tested in this study shows the possibility of applying the proposed measures for prioritizing freeway corridors with accurate understanding of the main sources of traffic congestion and travel-time reliability issues. Future study needs include the expanded testing of the proposed resilience and geometric-friction models to other corridors in the metro network with the detailed information on the blocked lanes during incidents.

# CHAPTER 6: CONCLUSIONS – RESEARCH BENEFITS/IMPLEMENTATION/FUTURE STUDY NEEDS

## 6.1 RESEARCH BENEFITS

### 6.1.1 Decrease Engineering/Administration Costs

The enhanced TeTRES and its newly expanded database, populated with the historical data from the metro freeway network, can significantly reduce the time and effort of MnDOT staff in preparing data, calculating reliability measures and analyzing estimation results. The detailed quantification of time and cost savings in MnDOT through TeTRES would depend on the types and/or scopes of potential MnDOT projects and their specific needs for estimating travel-time reliability and traffic-flow measures.

### 6.1.2 Operation and Maintenance Savings

As described in this report, the enhanced TeTRES with the additional traffic-flow MOE module can estimate both travel-time reliability and traffic-flow measures under different operating conditions for given corridors and periods. This indicates TeTRES can be applicable for an efficient identification of the major factors affecting the performance of various operational strategies for selected corridors. Such a capability can lead to the development of effective operation and maintenance strategies for each corridor, i.e., tailored strategies addressing the specific issues of given corridors, thus saving the operational and maintenance costs for the metro freeway network.

### 6.1.3 Reduce Risk

The identification of the vulnerable bottleneck sections in the major freeway corridors, which resulted from this study, can be used as the basis for developing optimal resource-allocation plans, which could maximize the cost-effectiveness of improving the metro freeway network, thus minimizing risks.

### 6.1.4 Reduce Road-User Cost

The identification of vulnerable freeway sections can also contribute to the improvement of the daily operations of freeway traffic systems, e.g., effective routing of FIRST trucks during peak periods and advanced driver guidance with time-of-day reliability information for pre-defined corridors. Such improved operations of freeway systems could decrease the unpredictability in corridor travel times, and, thus, reduce road-user cost in the metro freeway network.

## 6.2 IMPLEMENTATION STEPS

To facilitate the realization of the benefits that resulted from this study, the following steps are recommended to be taken in cooperation with the Regional Traffic Management Center (RTMC), MnDOT:

- Technical assistance in installing the final version of TeTRES at the RTMC, MnDOT, and conducting customized workshops for MnDOT staff to facilitate the adaptation of TeTRES for each office operations.
- Technical assistance to MnDOT offices in estimating and applying reliability and traffic-flow measures with TeTRES for selected corridors.
- Technical assistance to MnDOT offices in applying TeTRES for formulating and conducting before/after studies to quantify the changes in traffic-system performances in terms of travel-time reliability and traffic-flow measures of effectiveness.

## 6.3 FUTURE STUDY NEEDS

Developing a reliable and resilient freeway network requires the continuous assessment of the corridor-wide reliability trends and operational resilience on an ongoing basis. Future research needs include 1) continuous population of the TeTRES database with detailed data on incident and work-zone information, including the lane status affected by each incident and work zone, 2) analysis of the integrated effects of operational and geometric-changes at selected corridors on travel-time reliability and traffic-flow measures, 3) refinements of the corridor-wide operational-resilience and the geometric-friction indices, developed in this study, with data from additional corridors with diverse geometric features. Finally, an institutional support for ongoing system enhancements needs to be explored to continuously improve the operations and maintenance of the TeTRES software and the databases associated with TeTRES.

# REFERENCES


[1]. Kwon, E., & Park, C. (2018)., *Development of Travel-Time Reliability Measurement System, (MN/RC 2018-28*, Final Report). St. Paul, MN: Minnesota Department of Transportation.

[2]. Metro District, MnDOT (2016)., *Snow and Ice Event/Bare Lane Training 2016-2017.* St. Paul, MN: MnDOT.

[3]. Murray-Tuite, P. (2006-December)., *A comparison of transportation network resilience under simulated system optimum and user equilibrium conditions*. Paper presented at the 2006 Winter Simulation Conference, Monterey, Canada.

[4]. Cimellro, G.P., Reinhorn, A.M., & Bruneau, M. (2010)., *Framework for analytical quantification of disaster resilience*., Engineering Structure, 32(11), 3639-3649.

[5]. Devannadham, H., & Ramirez-Marquez, J.E. (2012), *Generic metrics and quantitative approaches for system resilience as a function of time*., Reliability Engineering and System Safety, 99, 114-122.

[6]. Kim, S., & Yeo, H. (2016)., *A Flow-based vulnerability measures for the resilience of urban road network*., 11th -International conference of the International Institute for Infrastructure Resilience and Reconstruction, Procedia-Social and Behavioral Sciences 218, 12-23.

[7]. Leu, L., Abbass, H., & Curtis, N. (2010)., *Resilience of ground transportation networks: A case study on Melbourne*., Paper presented at the 33rd Australasian Transport Research Forum Conference, Canberra, Australia, September 29-October 1.

[8]. Berche, B., von Ferber, C., Holovatch, T., & Holovatch, Y. (2009)., *Resilience of public transport networks against attacks*., European Physical Journal B., 7191, 125-137.

[9]. Dorbritz, R. (2011)., *Assessing the resilience of transportation systems in case of large-scale disastrous events*., Paper presented at the 8th International Conference on Environmental Engineering, Vilnius, Lithuania, May.

[10] Calvert, S.C. & Snelder, M. (2018)., *A methodology for road traffic resilience analysis and review of Related Concepts.*, Transportmetrica A: Transport Science, 14, 2, 130-154., https://10.1080/23249935.2017.1363315.

[11]. Khaghani, F. (2020)., *Resilience-based Operational Analytics of Transportation Infrastructure: A Data- driven Approach for Smart Cities*., Doctoral Dissertation, Virginia Polytechnic Institute and State University, Blacksburg, VA.